The COM-Poisson distribution for modelling ionization statistics

Daniel Durnford
On behalf of the NEWS-G Collaboration

PHYSTAT DM Conference
August 1st 2019

UNIVERSITY OF ALBERTA

CFI | FCI

Outline

Modelling ionization statistics

Candidate distributions

The COM-Poisson distribution

Empirical support with ^{37}Ar data

The impact of F on sensitivity to low-mass dark matter

The statistics of ionization

$$F = \frac{\sigma^2}{\mu}$$

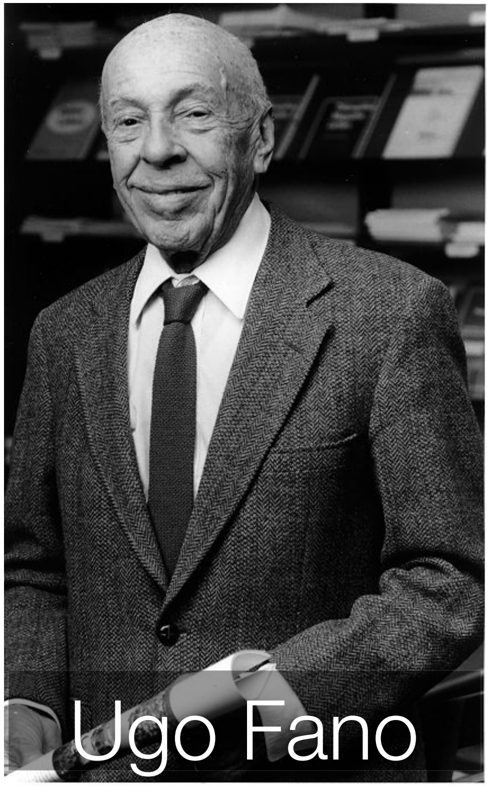

PHYSICAL REVIEW VOLUME 72, NUMBER 1 JULY 1, 1947

Ionization Yield of Radiations. II. The Fluctuations of the Number of Ions

U. Fano
X-Ray Section, National Bureau of Standards, Washington, D. C.
(Received March 7, 1947)

The ionization produced by individual fast charged particles is frequently used as a measure of their initial energy; fluctuation effects set a theoretical limit to the accuracy of this method. Formulas are derived here to estimate the statistical fluctuations of the number of ions produced by constant amounts of radiation energy. The variance of the number of ionizations is found to be two or three times smaller than if this number were governed by a Poisson distribution. An improved understanding is gained of the statistical treatment of fluctuation phenomena.

The Fano factor describes the dispersion of ionization processes

F ≠ 1: for a charged particle slowing down the probability of successive collisions is not independent, energy loss mechanisms other than ionization are possible

First explained by U. Fano in 1947, based on calculation with electron scattering cross sections [16]

The statistics of ionization

$$F = \frac{\sigma^2}{\mu}$$

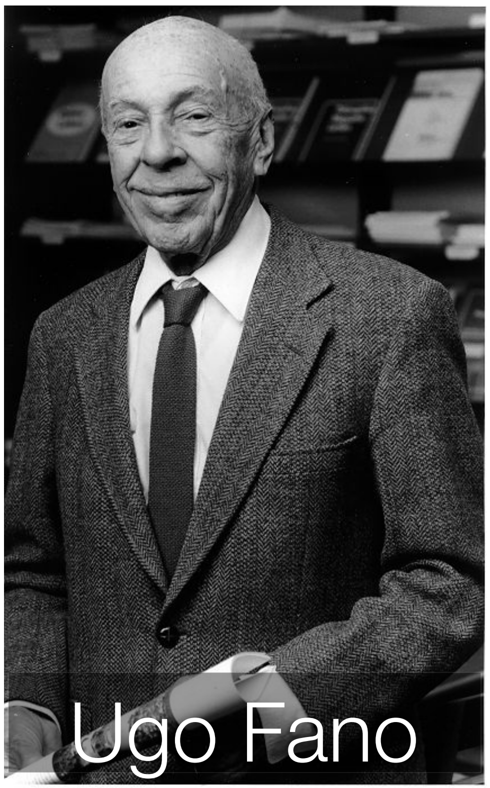

Since then, many measurements of F in different substances have been made:

$$F \lesssim 0.2$$

A. Hashiba et al., NIM A 227(2), 305–310 (1984).

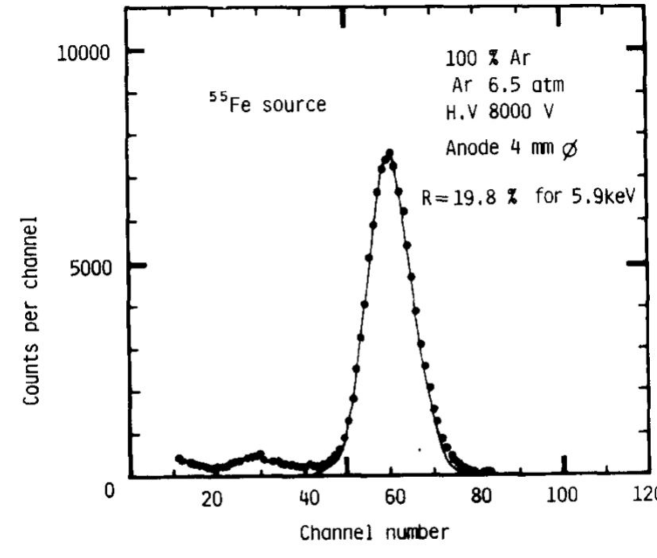

Fig 3 A typical pulse height spectrum of proportional scintillation produced by X-rays from a ^{55}Fe source in argon

Medium	F	Reference
Si	0.155 ± 0.002 (3 keV e^-)	[28]
	0.134 ± 0.003 (F-Kα)	[26]
Ar	0.23 ± 0.05 (^{55}Fe)	[21]
	0.20 ± 0.02 (5.3 MeV α)	[22]
Ar+0.8% CH4	0.19 (5.68 MeV α)	[3]
Xe (gas)	0.170 ± 0.007 (soft x-rays)	[30]
Xe (liquid)	0.033 ± 0.045	[31]
Ge	0.121 ± 0.001 (Al-Kα)	[26]

The issue of modelling ionization

At high energies, it is valid to fold ionization fluctuations in with resolution effects (i.e. baseline noise), to give an overall model with an effective F

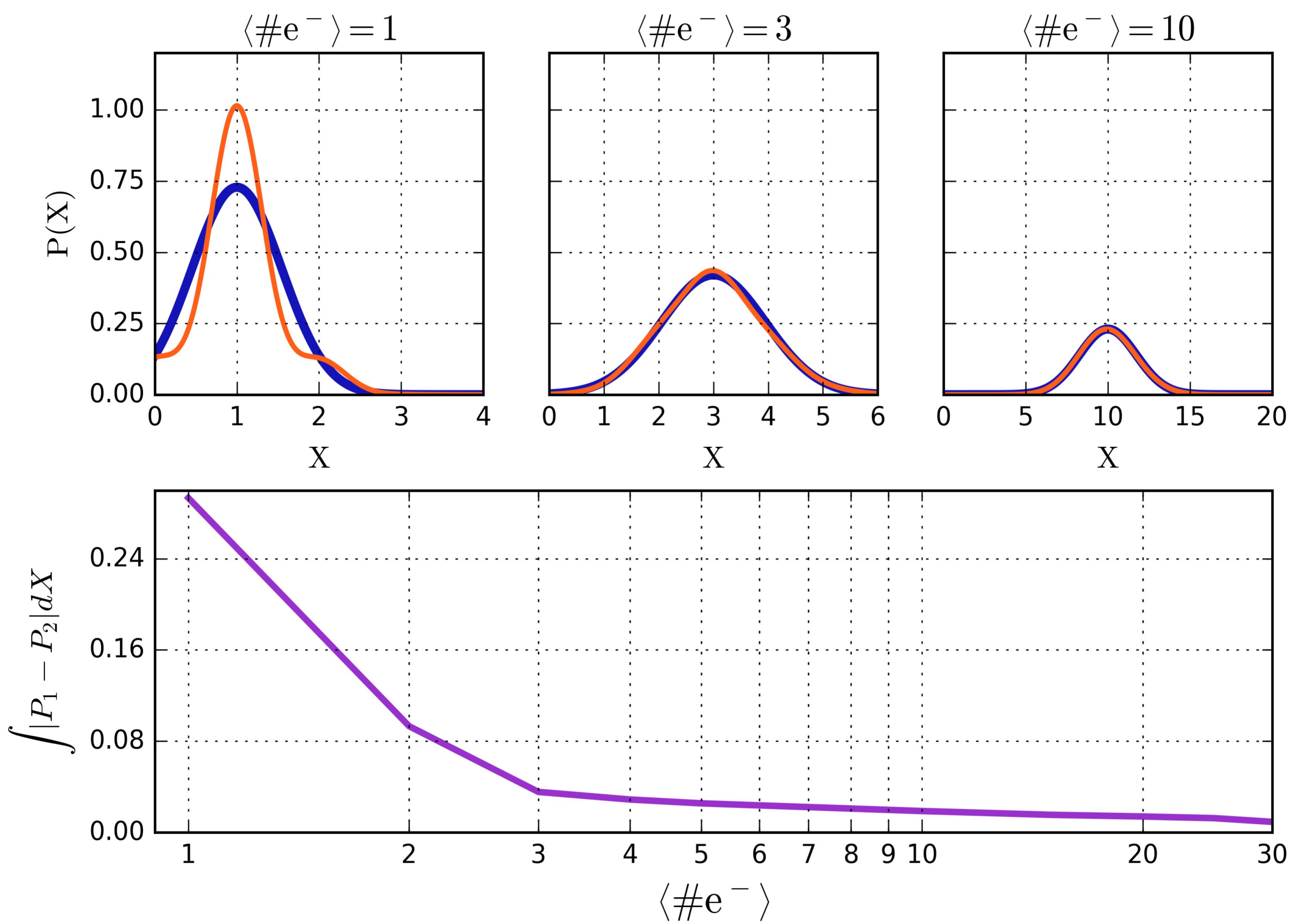

F = 0.2 for ionization + Gaussian noise with σ = 0.5

Gaussian with same "effective F"

At high energies, it is valid to fold ionization fluctuations in with resolution effects (i.e. baseline noise), to give an overall model with an effective F

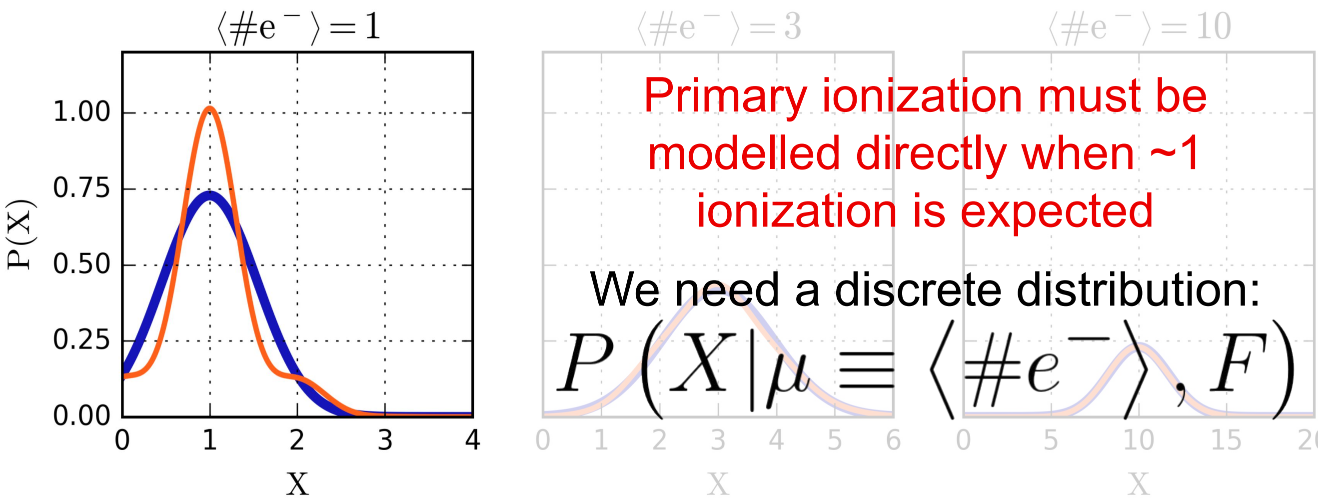

Primary ionization must be modelled directly when ~1 ionization is expected

We need a discrete distribution:

$$P\left(X|\mu \equiv \langle \#e^{-} \rangle, F\right)$$

F = 0.2 for ionization + Gaussian noise with σ = 0.5

Gaussian with same "effective F"

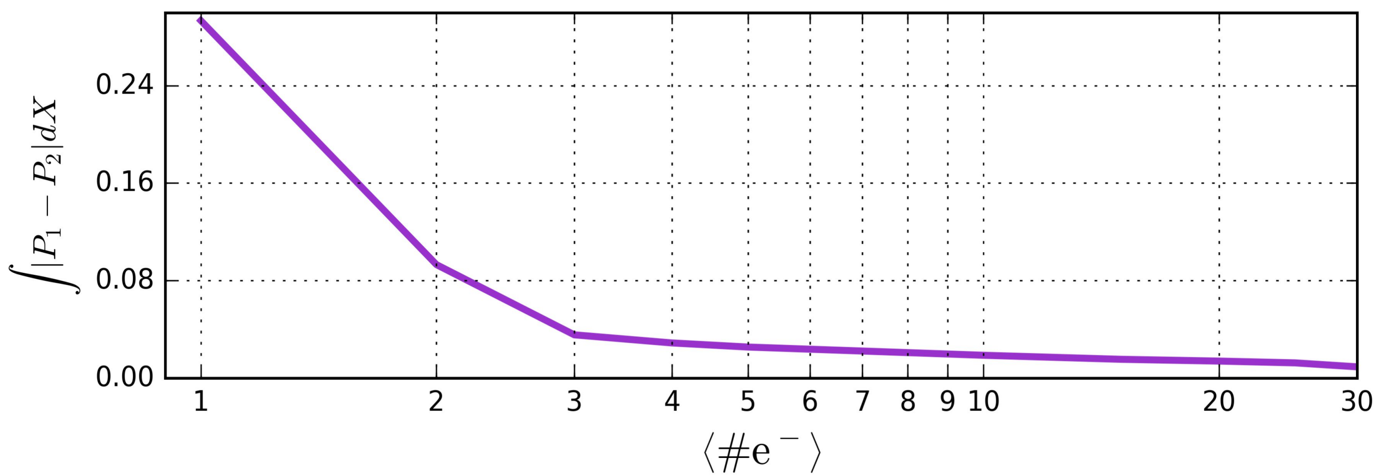

Who does this problem affect?

Any detector which measures ionization, operating in an energy regime too low to be modelled with Gaussian

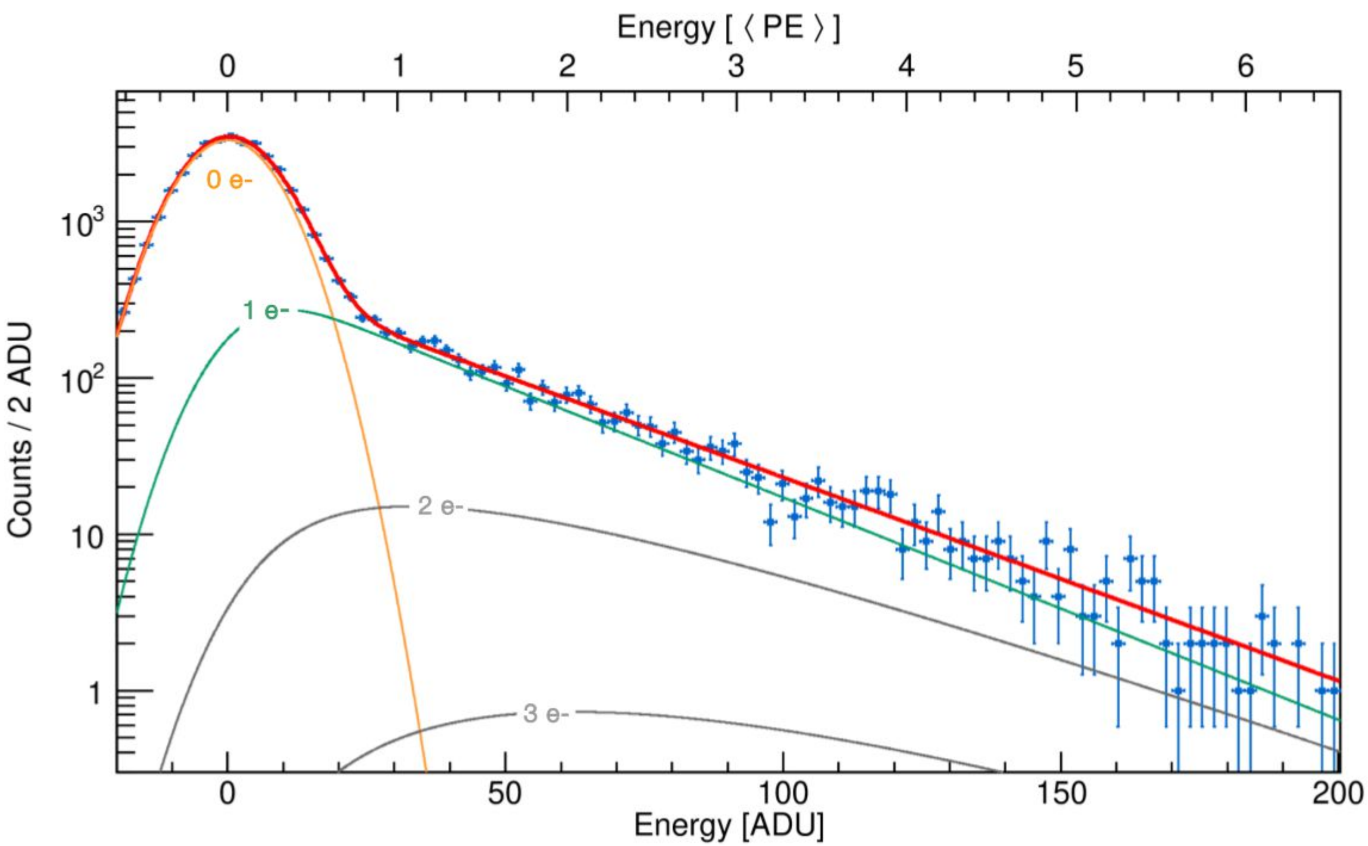

Q. Arnaud et al. (NEWS-G Collaboration), Phys. Rev. D 99, 102003 (2019)

NEWS-G [5]

SuperCDMS single charge device [2]

Edelweiss [4]

DAMIC [13]

SENSEI [34]

Darkside50 [1]

Who does this problem affect?

Any detector which measures ionization, operating in an energy regime too low to be modelled with Gaussian

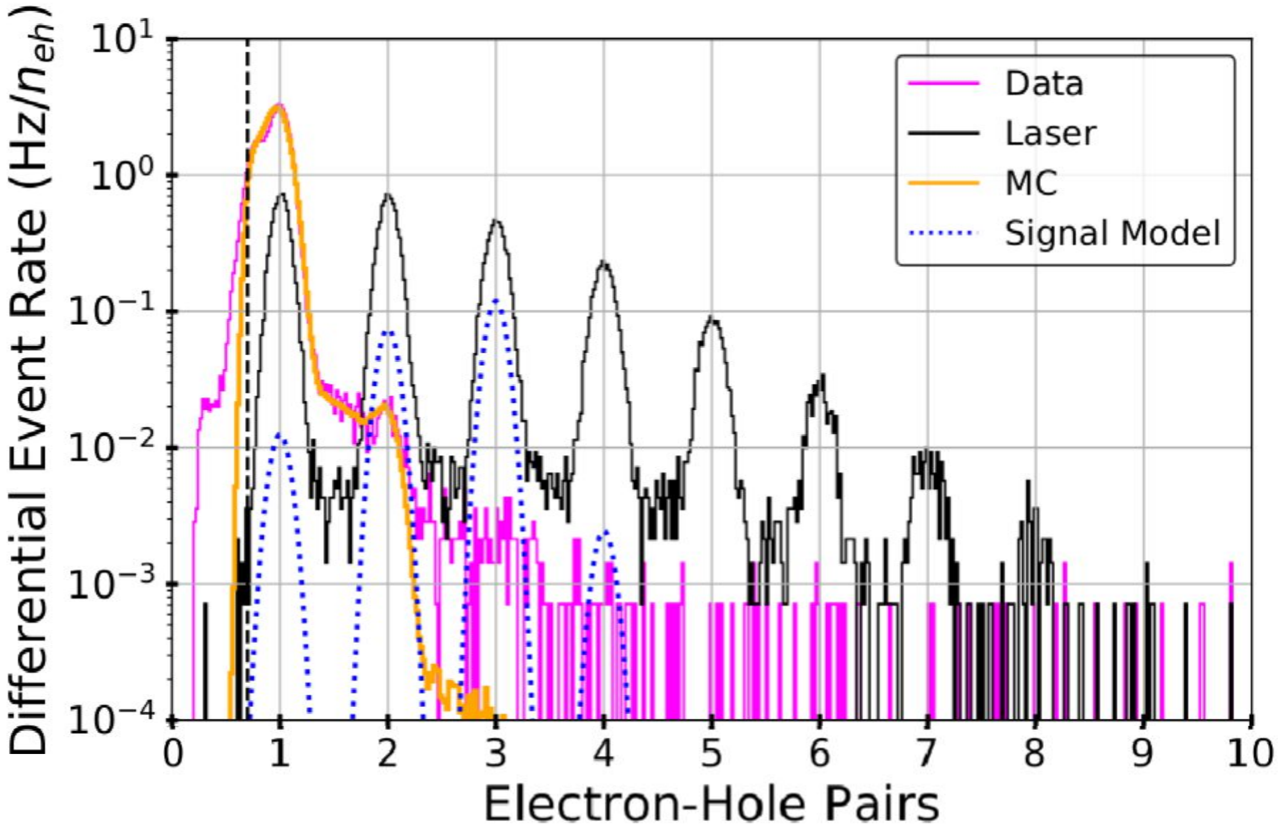

R. Agnese et al. (SuperCDMS Collaboration), Phys. Rev. Lett. 121, 051301 (2018)

- NEWS-G [5]
- SuperCDMS single charge device [2]
- Edelweiss [4]
- DAMIC [13]
- SENSEI [34]
- Darkside50 [1]

Who does this problem affect?

Any detector which measures ionization, operating in an energy regime too low to be modelled with Gaussian

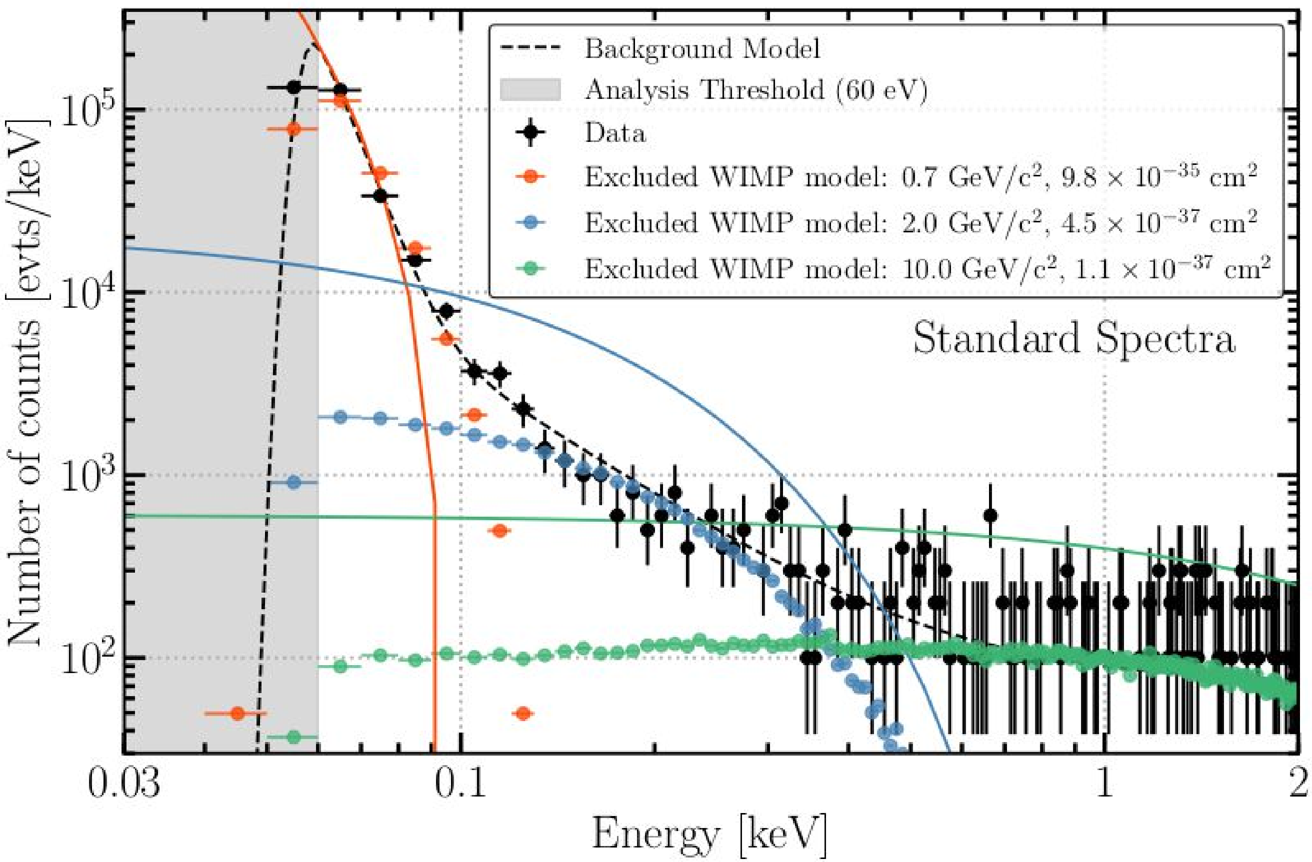

E. Armengaud et al. (EDELWEISS Collaboration), Phys. Rev. D 99, 082003 (2019)

NEWS-G [5]

SuperCDMS single charge device [2]

Edelweiss [4]

DAMIC [13]

SENSEI [34]

Darkside50 [1]

Who does this problem affect?

Any detector which measures ionization, operating in an energy regime too low to be modelled with Gaussian

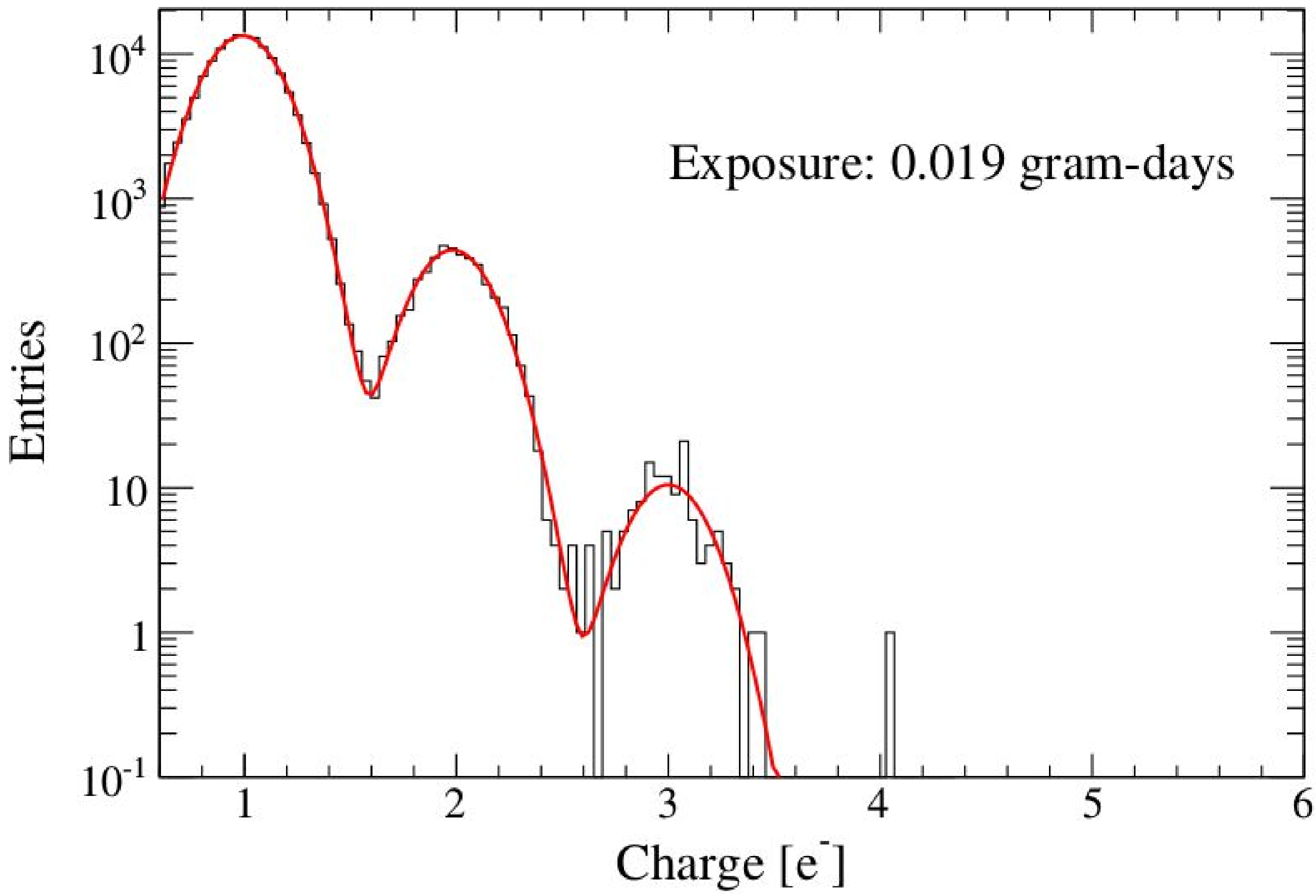

M. Crisler et al. (SENSEI Collaboration), Phys. Rev. Lett. 121, 061803 (2018)

NEWS-G [5]

SuperCDMS single charge device [2]

Edelweiss [4]

DAMIC [13]

SENSEI [34]

Darkside50 [1]

Who does this problem affect?

Any detector which measures ionization, operating in an energy regime too low to be modelled with Gaussian

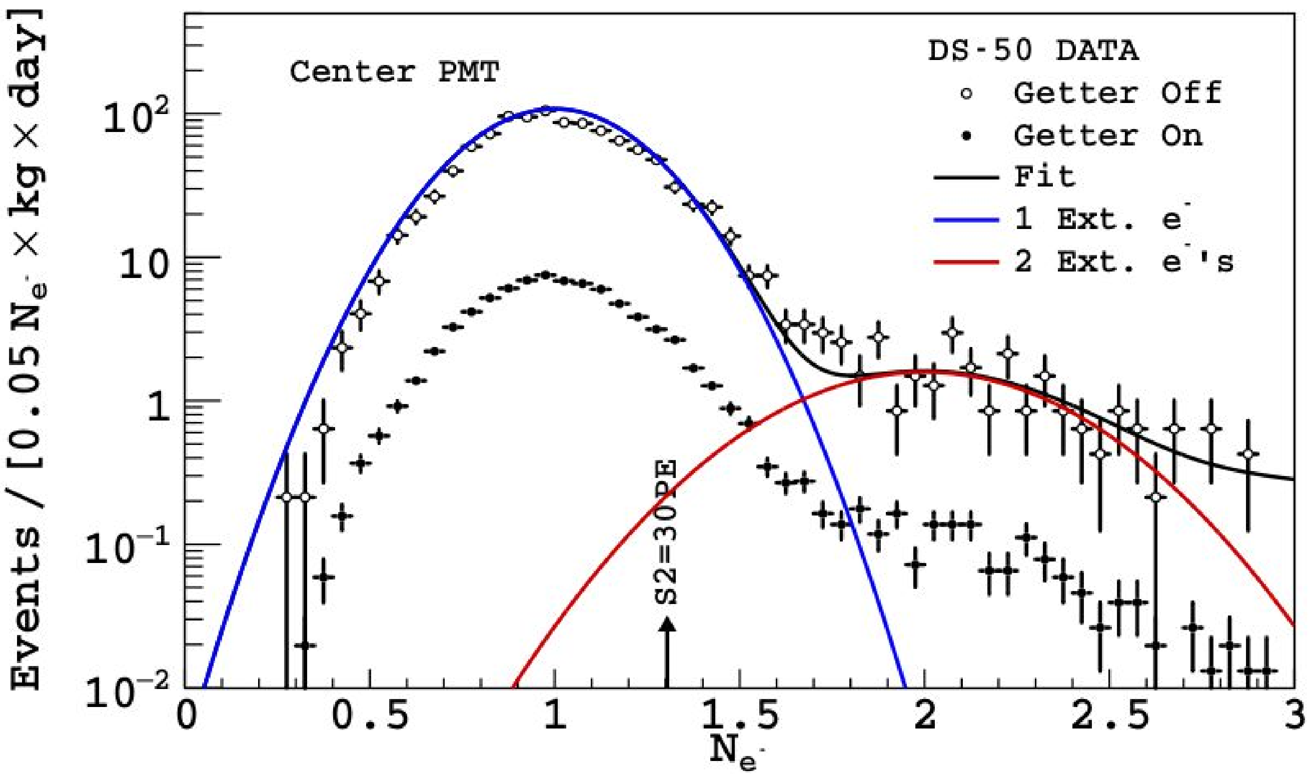

P. Agnes et al. (DarkSide Collaboration), Phys. Rev. Lett. 121, 081307 (2018)

NEWS-G [5]

SuperCDMS single charge device [2]

Edelweiss [4]

DAMIC [13]

SENSEI [34]

Darkside50 [1]

Theoretical expectations

Calculations based on electron scattering cross sections confirm that at high energy F approaches an asymptotic limit [3,19,20]

At low energies, F is expected to tend to 1

B. Grosswendt, J. Phys. B 17(7), 1391–1404 (1984).

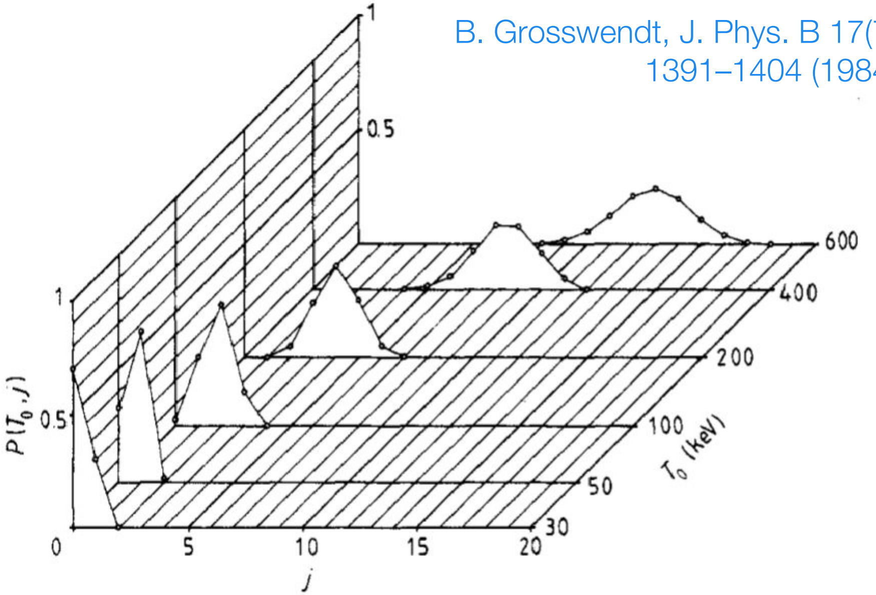

Figure 4. Three-dimensional plot of the probability $P(T_0, j)$ that exact-j ionisations are produced upon the complete slowing down of electrons of initial energy T_0 in He.

B. Grosswendt and E. Waibel, Radiation Protection Dosimetry 13(1–4), 95–102 (1985).

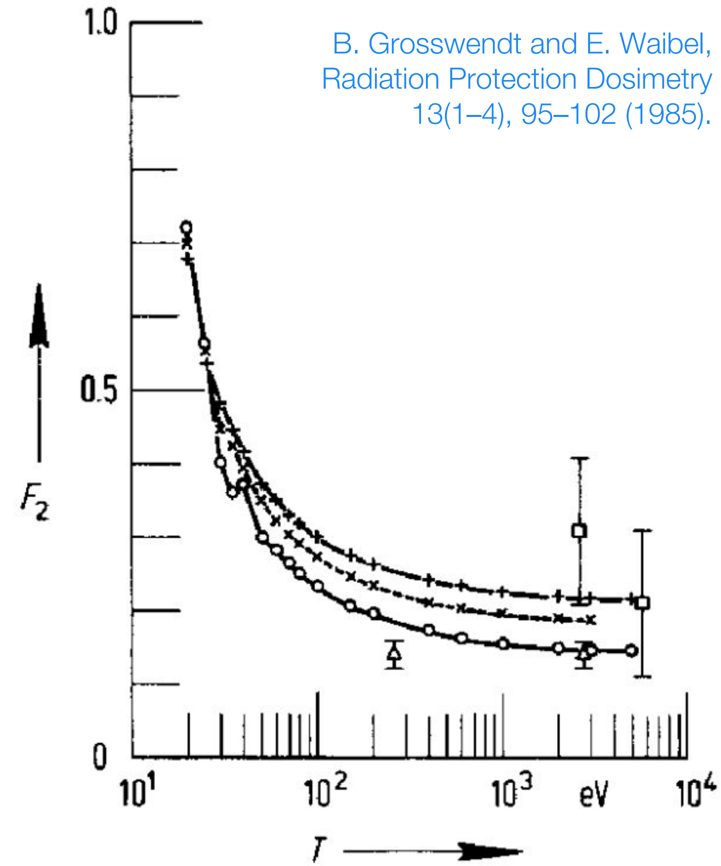

Figure 5. Dependence of Fano factor F_2 for electrons completely stopped in methane (+——+), argon[12] (○——○) and a gas mixture of 50% methane and 50% argon (×---×) on the electron energy T compared with experimental results for a gas mixture of 90% argon and 10% methane of Hurst *et al*[13] for 2.6 keV and 5.9 keV X rays (□) and of Neumann[14] for 0.26 keV and 2.82 keV electrons (△).

To treat F as a systematic, a modelling distribution defined at every point* in this parameter space is needed

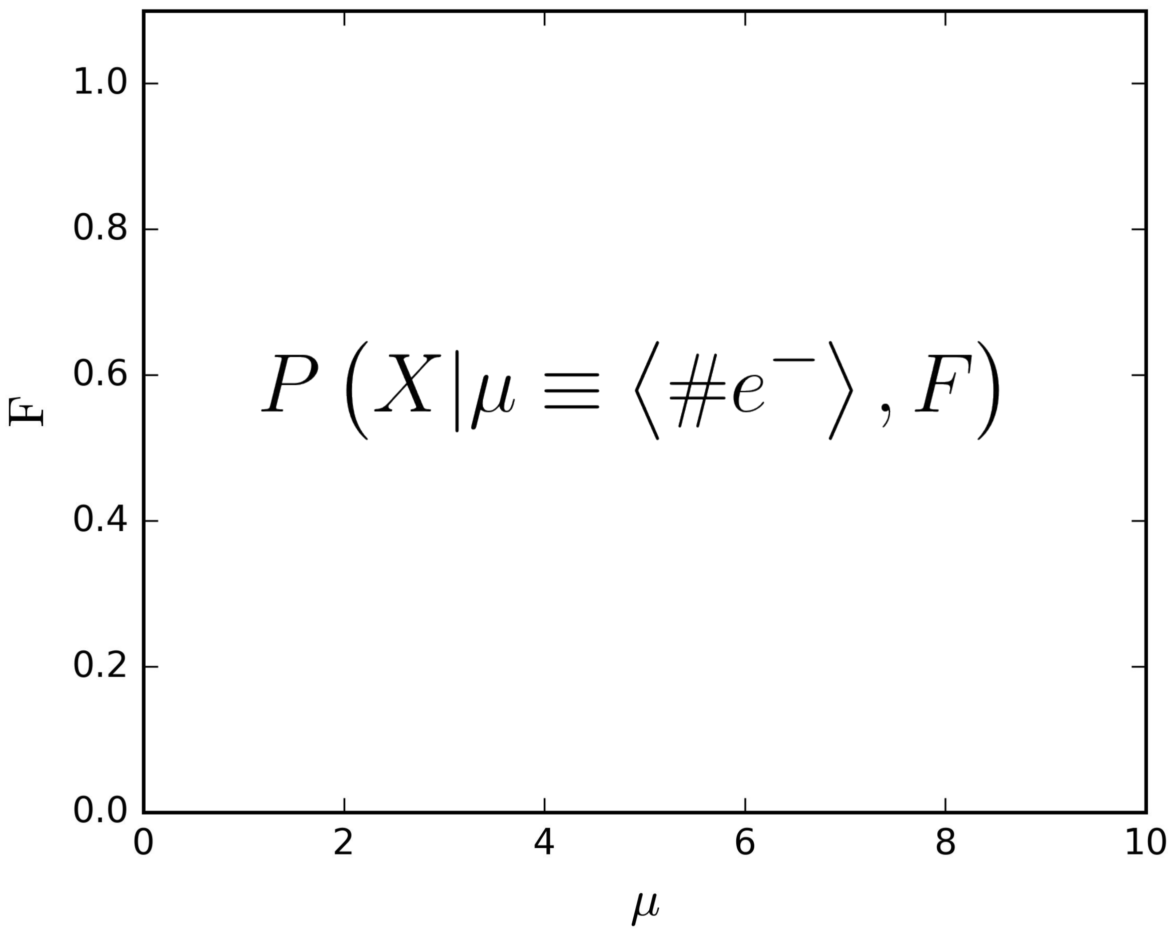

To treat F as a systematic, a modelling distribution defined at every point* in this parameter space is needed

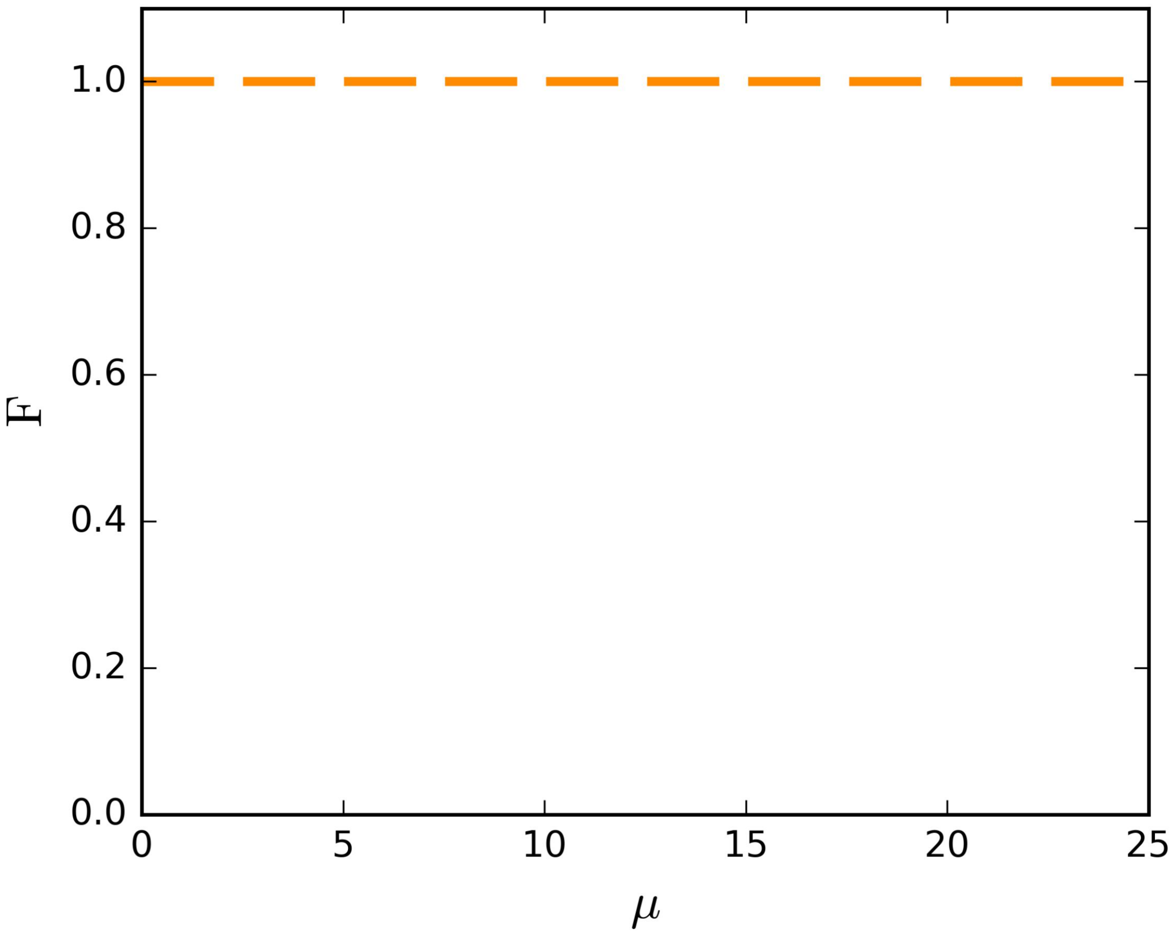

*Empirically we know that F < 1

To treat F as a systematic, a modelling distribution defined at every point* in this parameter space is needed

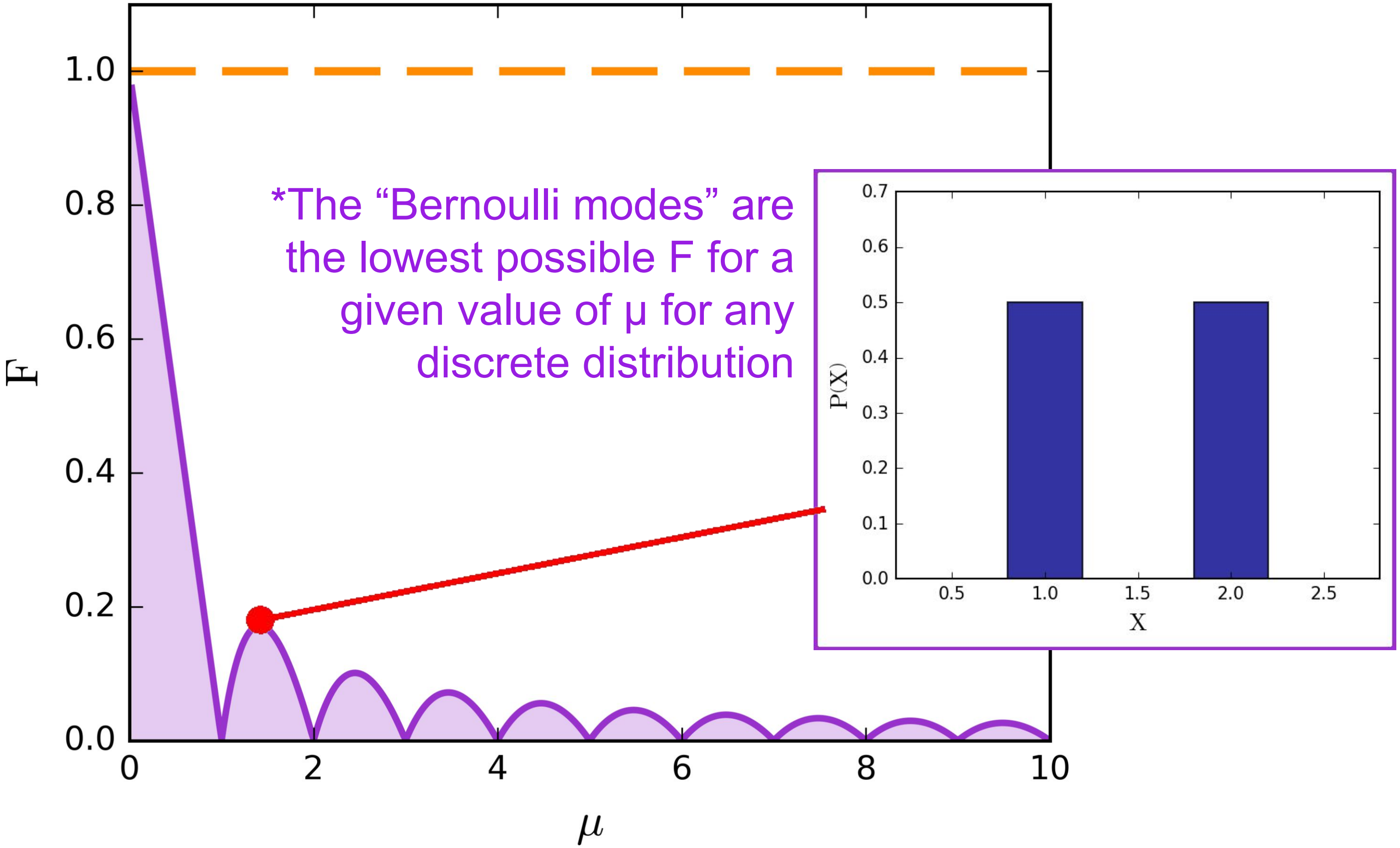

The Binomial distribution is an intuitive guess for a possible model

However it covers μ/F parameter space very sparsely at low μ and F

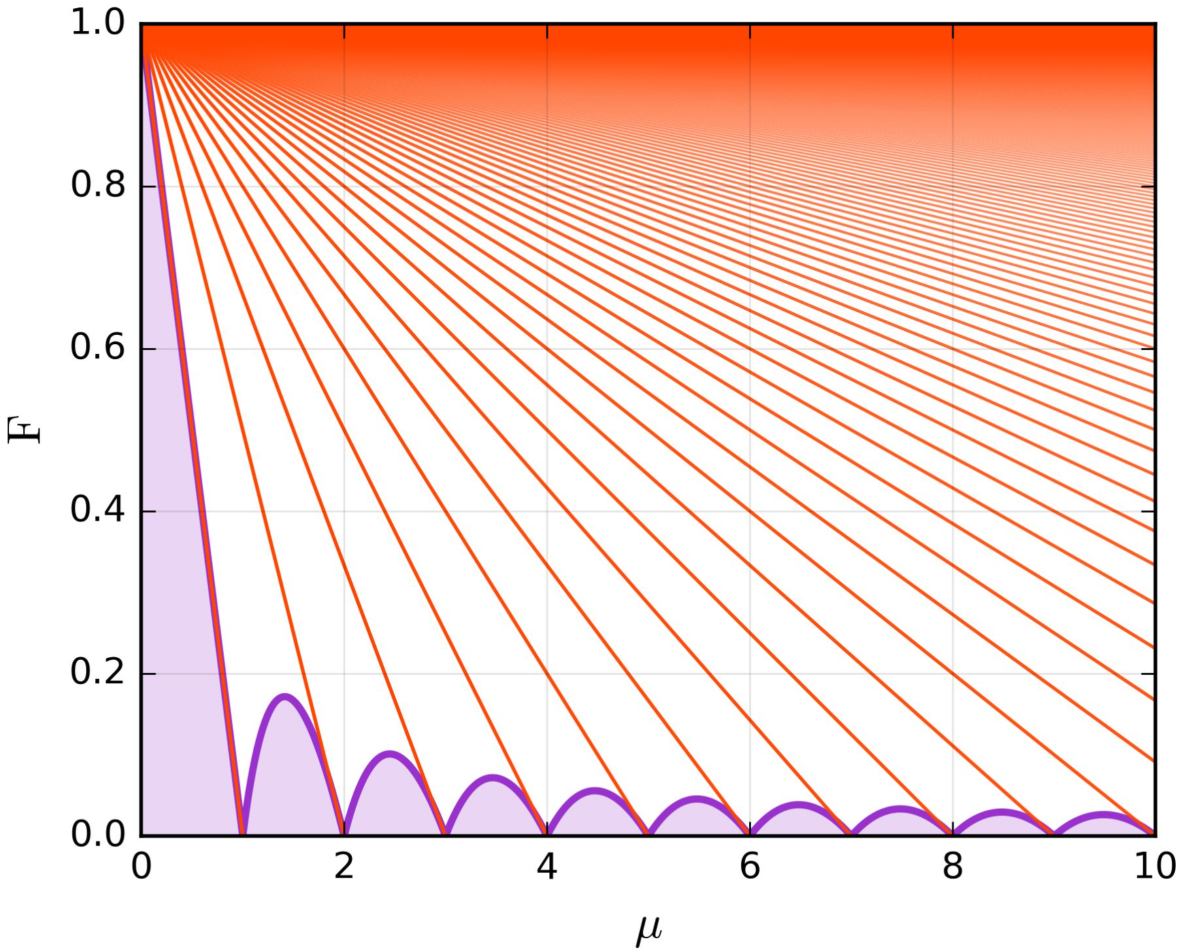

Binomial distributions (for n < 2000)

Bernoulli modes

$$P(X = k|n, p) = \binom{n}{k} p^k (1-p)^{n-k}$$

for $n \in \mathbb{N}_0, \quad k \leq n, \quad p \in [0, 1].$

$$\mu = np \qquad F = 1 - p = 1 - \frac{\mu}{n}$$

The Weighted Double Binomial (WDB) distribution [2] covers much more of μ/F space. However it still leaves gaps in a critical regime

$$n_l = \left\lfloor \frac{\mu}{1-F} \right\rfloor \quad P_l\left(x|\mu, F\right) = P_{\text{Binom}}\left(x|n_l, 1-F_l\right)$$

$$n_u = \left\lceil \frac{\mu}{1-F} \right\rceil \quad P_u\left(x|\mu, F\right) = P_{\text{Binom}}\left(x|n_u, 1-F_u\right)$$

$$\mathcal{P}\left(x|\mu, F\right) = (1-\Delta F)P_l\left(x|\mu, F\right) + (\Delta F)P_u\left(x|\mu, F\right)$$

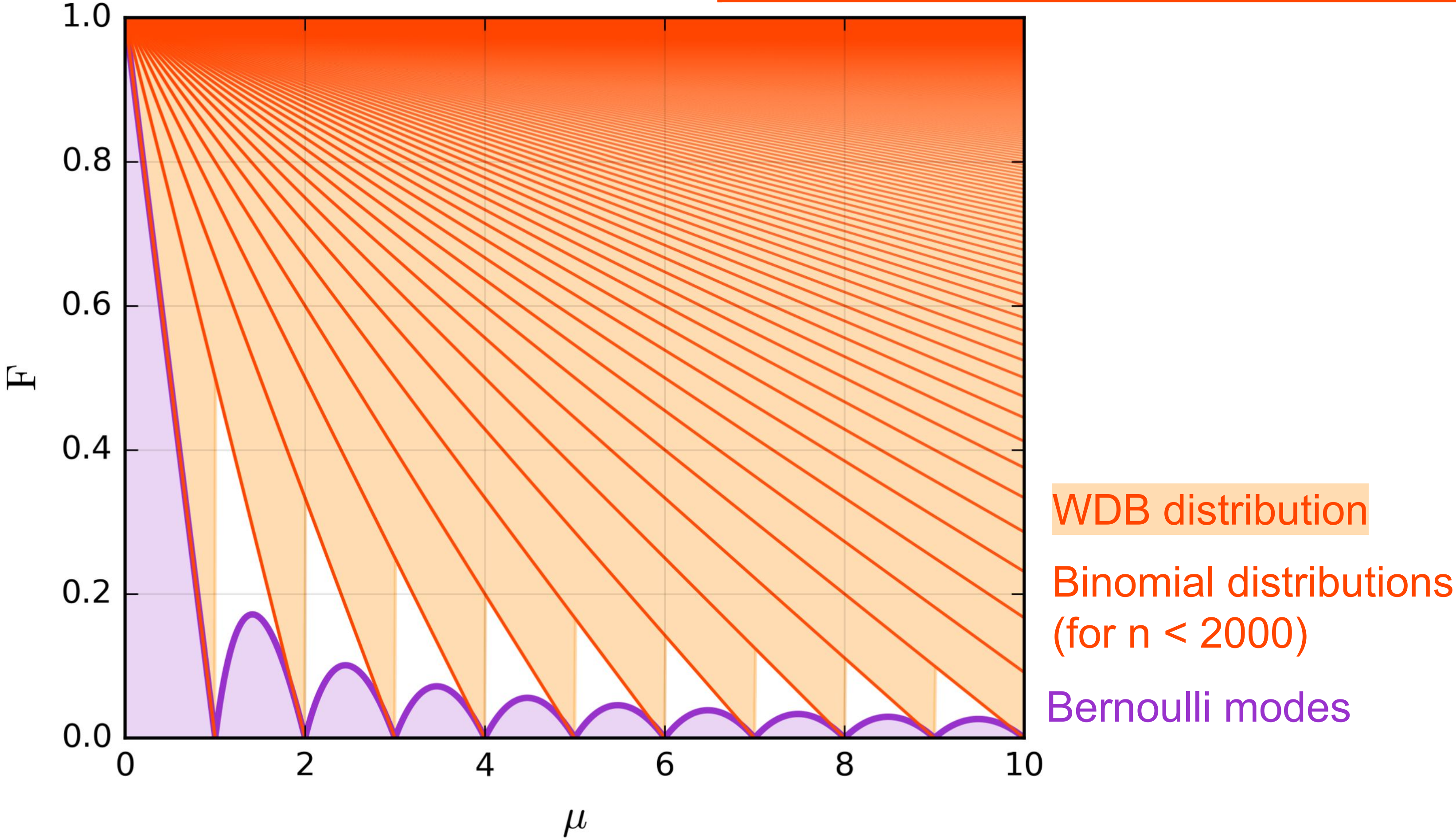

Possible models - WDB distribution

The Weighted Double Binomial (WDB) distribution [2] covers much more of μ/F space. However it still leaves gaps in a critical regime

$$n_l = \left\lfloor \frac{\mu}{1-F} \right\rfloor \qquad P_l\left(x|\mu,F\right) = P_{\mathrm{Binom}}\left(x|n_l, 1-F_l\right)$$

$$n_u = \left\lceil \frac{\mu}{1-F} \right\rceil \qquad P_u\left(x|\mu,F\right) = P_{\mathrm{Binom}}\left(x|n_u, 1-F_u\right)$$

$$\mathcal{P}\left(x|\mu,F\right) = (1-\Delta F)P_l\left(x|\mu,F\right) + (\Delta F)P_u\left(x|\mu,F\right)$$

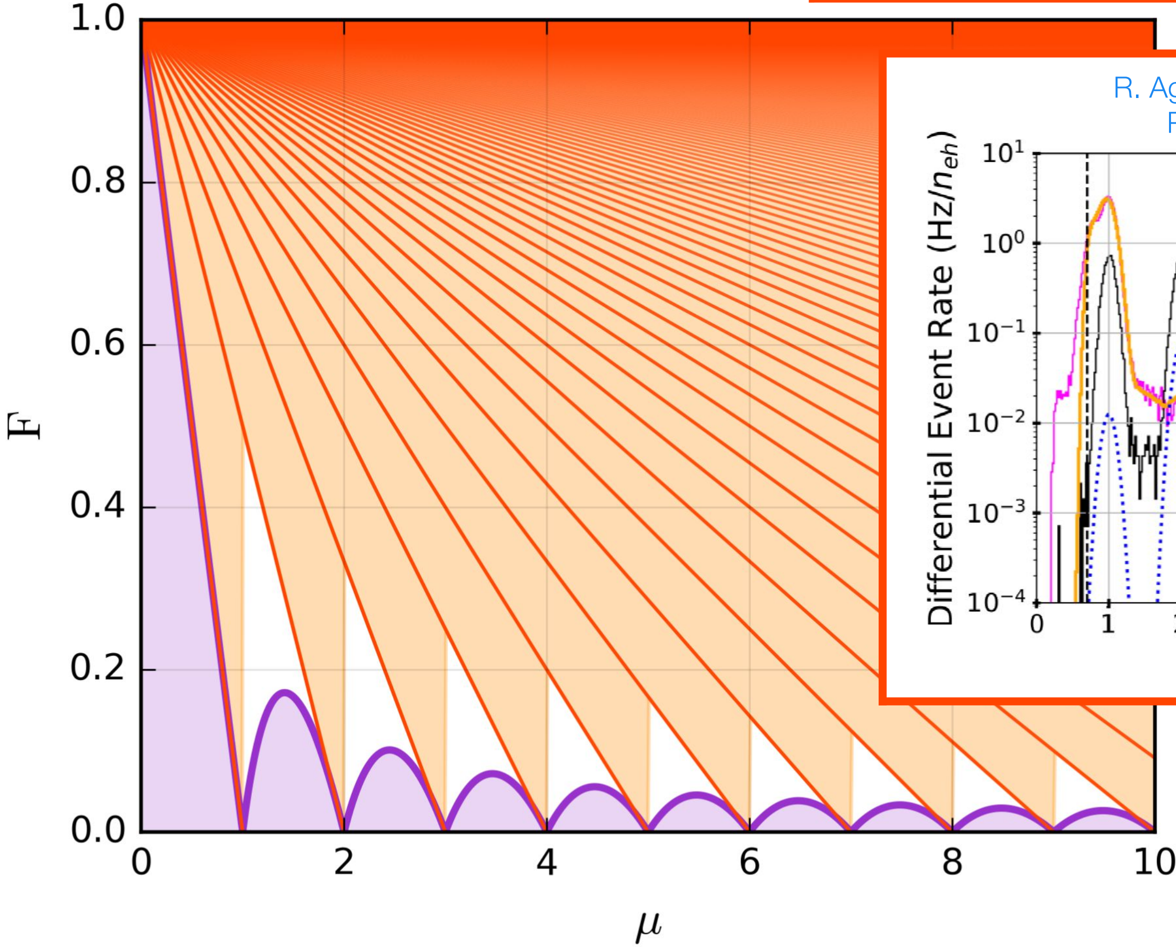

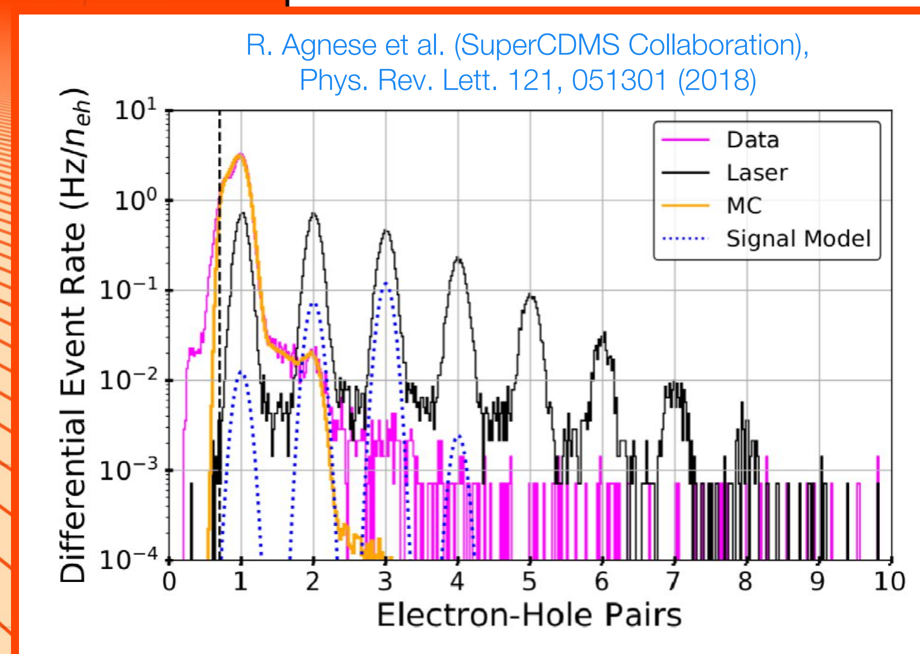

Possible models - WDB distribution

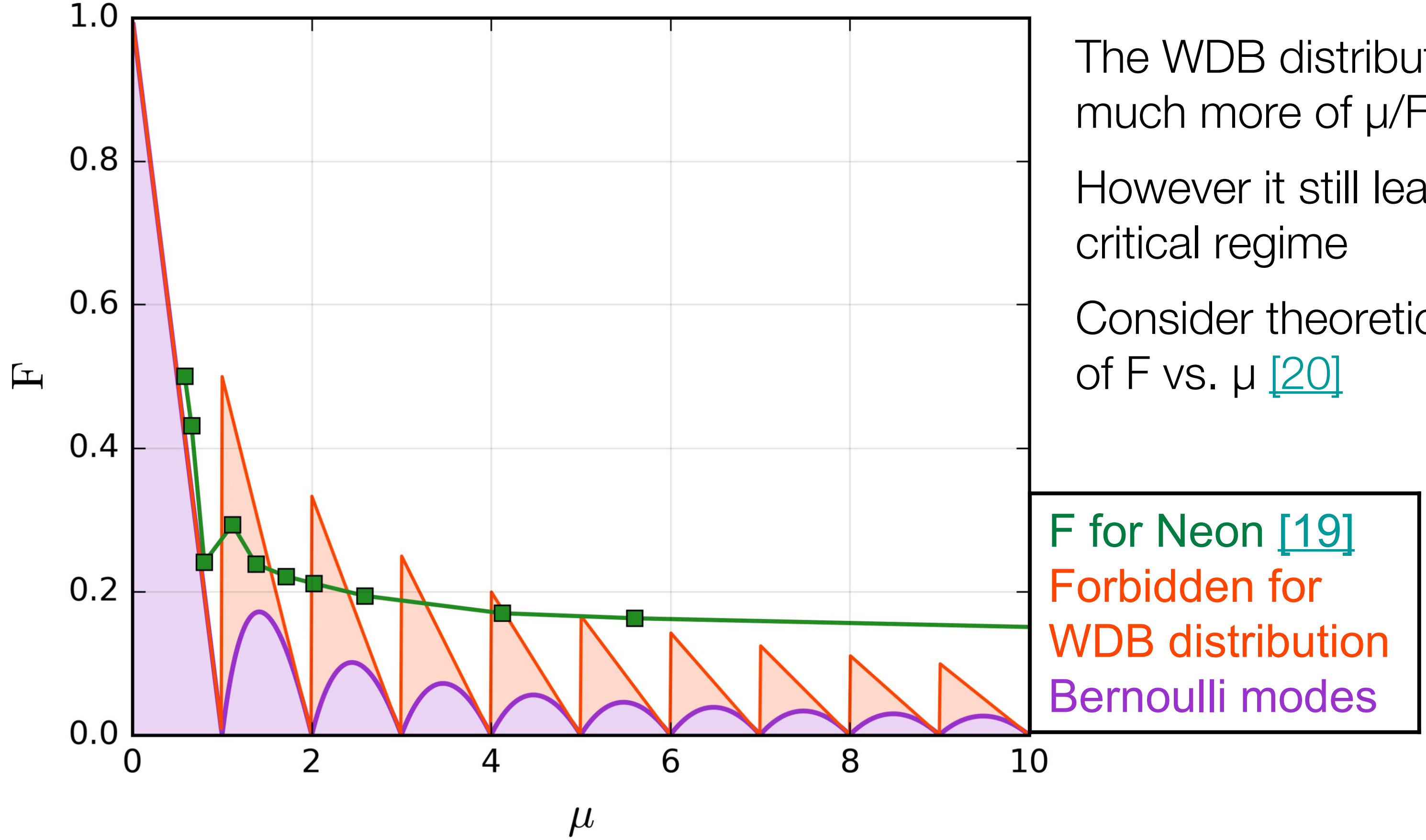

The WDB distribution [2] covers much more of μ/F space

However it still leaves gaps in a critical regime

Consider theoretical expectations of F vs. μ [20]

$$n_l = \left\lfloor \frac{\mu}{1-F} \right\rfloor \quad P_l\left(x|\mu, F\right) = P_{\mathrm{Binom}}\left(x|n_l, 1-F_l\right)$$

$$n_u = \left\lceil \frac{\mu}{1-F} \right\rceil \quad P_u\left(x|\mu, F\right) = P_{\mathrm{Binom}}\left(x|n_u, 1-F_u\right)$$

$$\mathcal{P}\left(x|\mu, F\right) = (1-\Delta F) P_l\left(x|\mu, F\right) + (\Delta F) P_u\left(x|\mu, F\right)$$

Possible models

Many other distributions to consider:

Negative binomial distribution
→ Only defined for F > 1 [17]

Generalized Poisson
→ Not defined for F < 0.25 [10]

Double Poisson
→ Requires truncation, not a true PMF [29]

Weighted Poisson with 3 or more parameters
→ Non-physical parameters, very complicated [14]

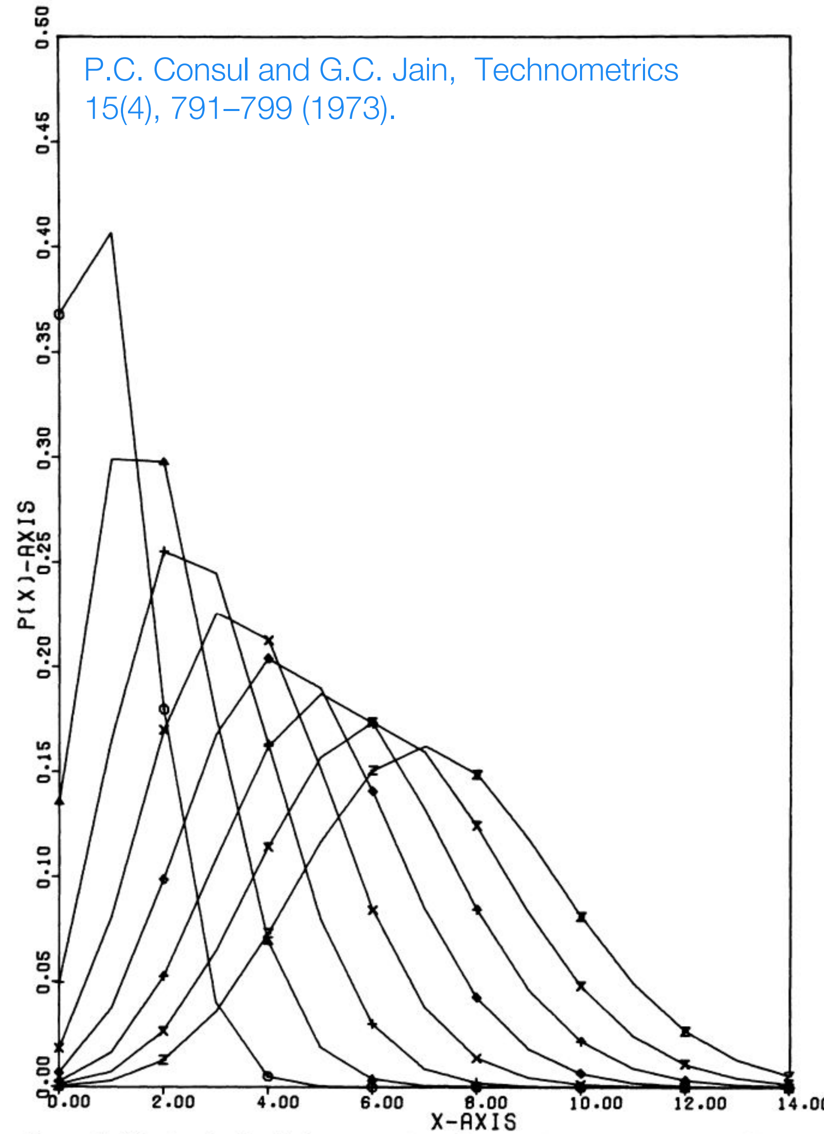

FIGURE 1—Showing the Graphs for $\lambda_2 = -0.1$ and $\lambda_1 = 1, 2, 3, 4, 5, 6, 7, 8$ according to the Symbols ○, △, +, ×, ◇, ⇑, X and $\overline{Z}$ respectively.

The COnway Maxwell - Poisson (COM-Poisson) distribution [11]:

$$P(x|\lambda,\nu) = \frac{\lambda^x}{(x!)^\nu Z(\lambda,\nu)}$$

$$Z(\lambda,\nu) = \sum_{j=0}^{\infty} \frac{\lambda^j}{(j!)^\nu} \qquad \lambda \in \{\mathbb{R} > 0\}, \quad \nu \in \{\mathbb{R} \geq 0\}$$

Many applications in other fields for modeling over and under-dispersion:

» Queuing systems [11]
» Linguistics: modelling word lengths [8]
» Marketing studies and online sales modelling [33]
» Vehicle crash statistics at types of intersections [25]
» Ecology: bird egg production/nest sizes [32]

... However it is new to physics!

The COnway Maxwell - Poisson (COM-Poisson) distribution [11]:

$$P(x|\lambda,\nu) = \frac{\lambda^x}{(x!)^\nu Z(\lambda,\nu)}$$

$$Z(\lambda,\nu) = \sum_{j=0}^{\infty} \frac{\lambda^j}{(j!)^\nu} \quad \lambda \in \{\mathbb{R} > 0\}, \quad \nu \in \{\mathbb{R} \geq 0\}$$

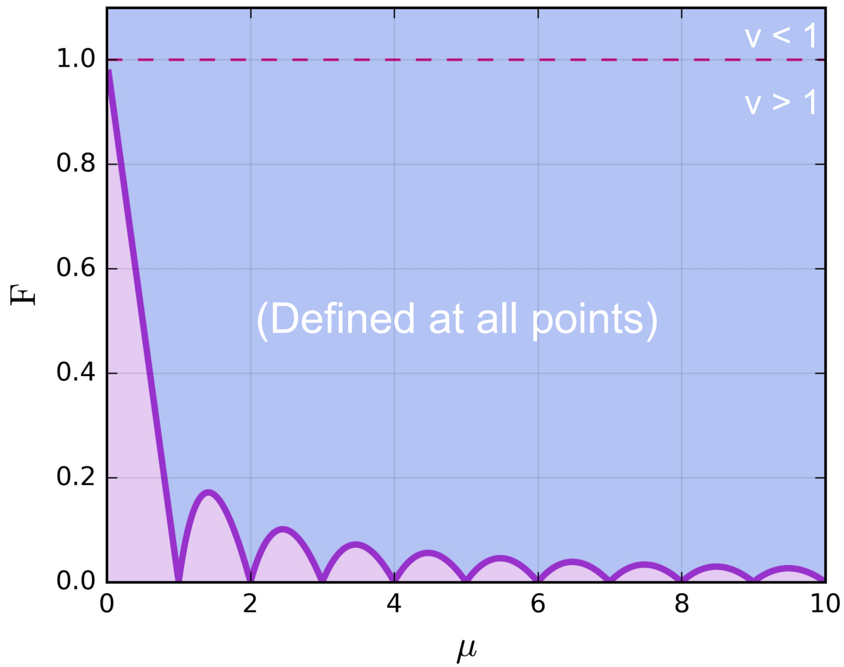

It is defined at every point in μ/F space (including over-dispersion)

Mean and variance given by [27]:

$$\mu(\lambda,\nu) = \sum_{j=0}^{\infty} \frac{j\lambda^j}{(j!)^\nu Z(\lambda,\nu)} \quad \sigma^2(\lambda,\nu) = \sum_{j=0}^{\infty} \frac{j^2\lambda^j}{(j!)^\nu Z(\lambda,\nu)} - \mu(\lambda,\nu)^2$$

Higher moments calculated with:

$$E\left(X^{n+1}\right) = \lambda \frac{\partial}{\partial \lambda} E\left(X^n\right) + E(X)\,E\left(X^n\right), \quad \text{for } n \geq 1$$

The problem...

$$\mu\left(\lambda,\nu\right)=\sum_{j=0}^{\infty}\frac{j\lambda^{j}}{\left(j!\right)^{\nu}Z\left(\lambda,\nu\right)} \qquad \sigma^{2}\left(\lambda,\nu\right)=\sum_{j=0}^{\infty}\frac{j^{2}\lambda^{j}}{\left(j!\right)^{\nu}Z\left(\lambda,\nu\right)}-\mu\left(\lambda,\nu\right)^{2}$$

$$P(x|\lambda,\nu) \qquad\qquad P(x|\mu,F)$$

???

$$???\quad \lambda\left(\mu,F\right)\quad \nu\left(\mu,F\right)\quad ???$$

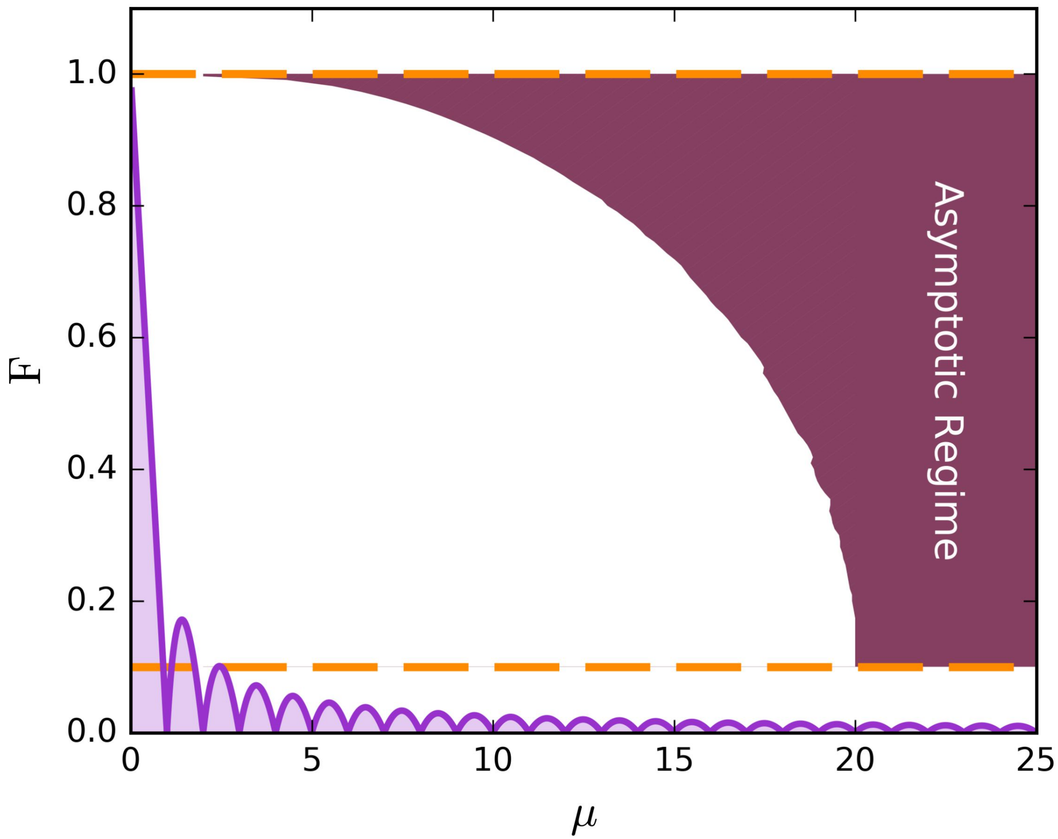

$$\lambda(\mu, F) \approx (\nu\mu F)^{\nu}$$

$$\nu(\mu, F) \approx \frac{2\mu + 1 + \sqrt{4\mu^2 + 4\mu + 1 - 8\mu F}}{4\mu F}$$

At high μ/F, there are asymptotic expressions that can be used to solve for the distribution parameters [27]

Accurate to ≤ 0.01% in μ and F

Using COM-Poisson

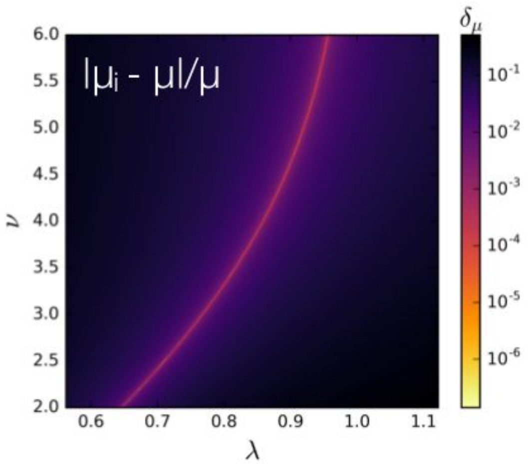

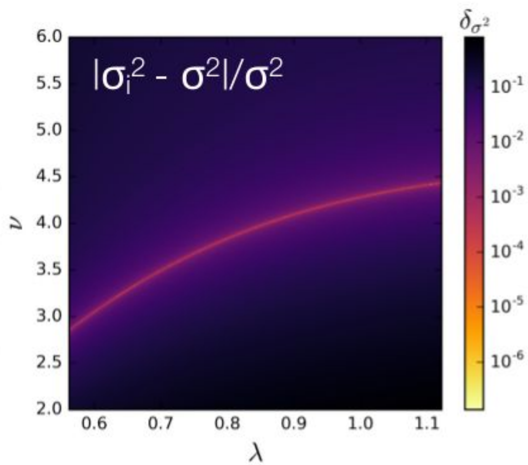

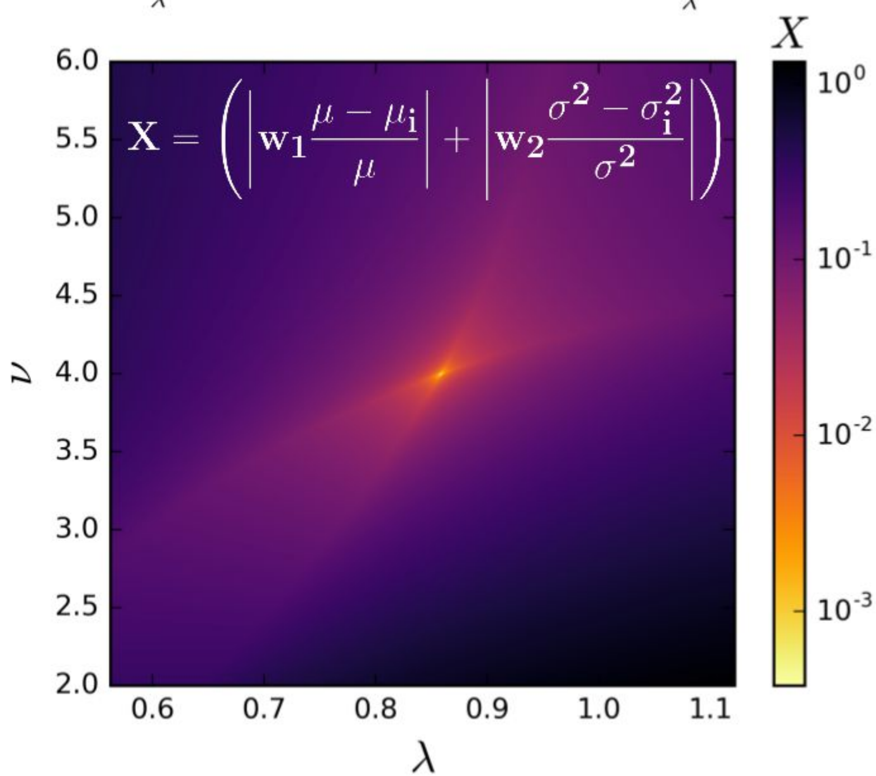

At high μ/F, there are asymptotic expressions that can be used to solve for the distribution parameters [27]

Accurate to ≤ 0.01% in μ and F

At low μ/F, a 2D optimization algorithm is used to find the correct values of λ and ν

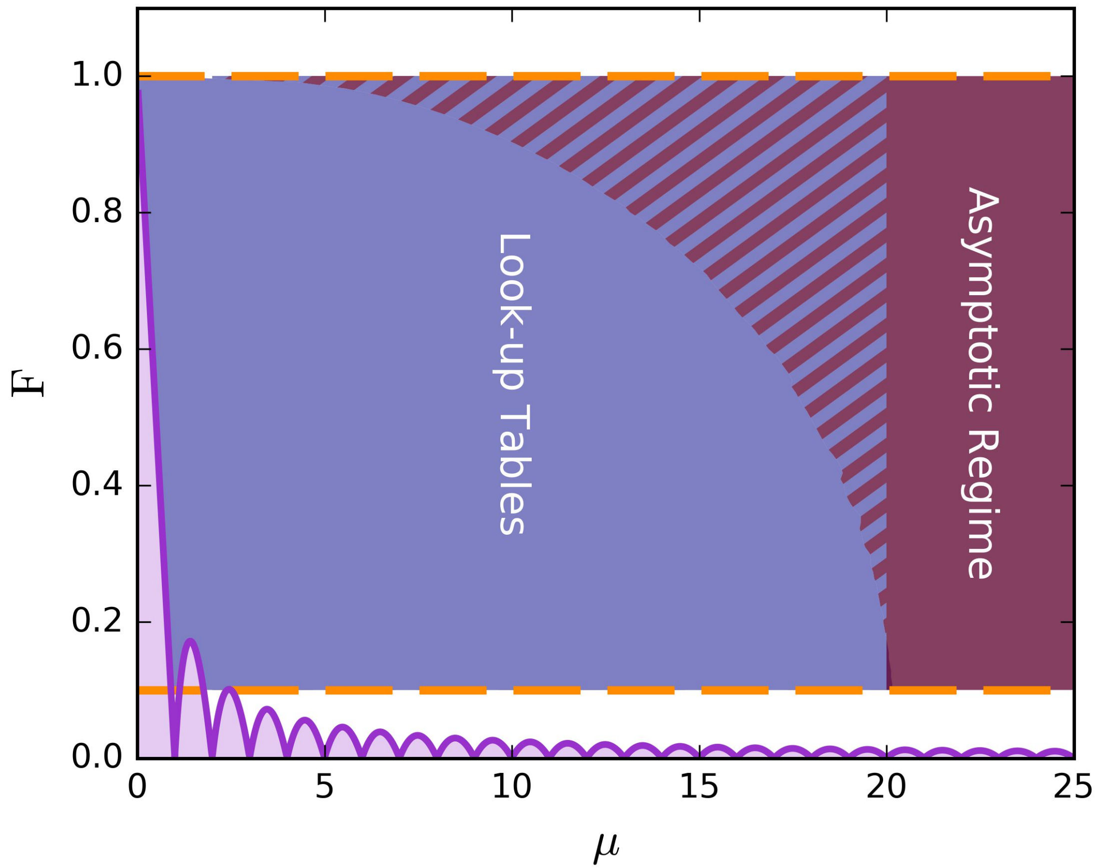

D. Durnford, Q. Arnaud, and G. Gerbier
Phys. Rev. D 98, 103013 (2018)

At high μ/F, there are asymptotic expressions that can be used to solve for the distribution parameters [27]

Accurate to ≤ 0.01% in μ and F

At low μ/F, a 2D optimization algorithm is used to find the correct values of λ and ν

Results are stored in look-up tables for quick interpolation, accurate to ≤ 0.1%

Tables and code to use them available at: https://news-g.org/com-poisson-code/

We can compare the theoretically predicted behaviour of F to what is possible for COM-Poisson, other models: COM-Poisson is defined where F(μ) is expected

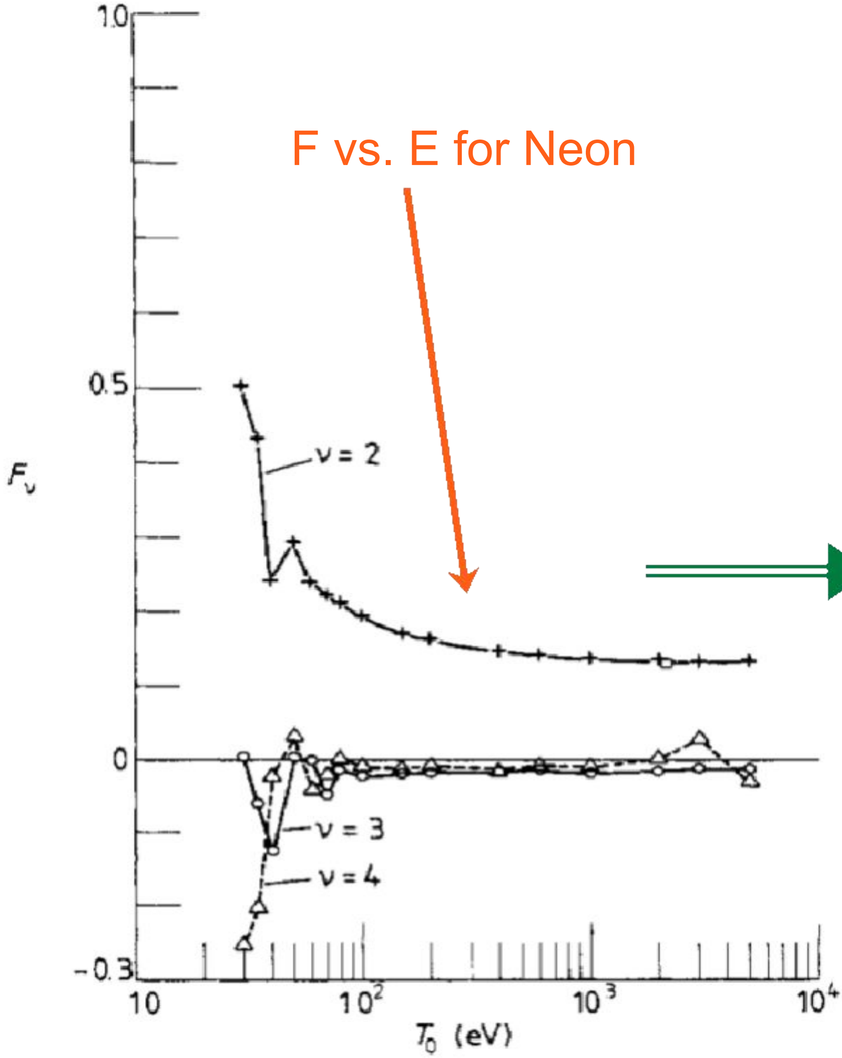

B. Grosswendt, J. Phys. B 17(7), 1391–1404 (1984).

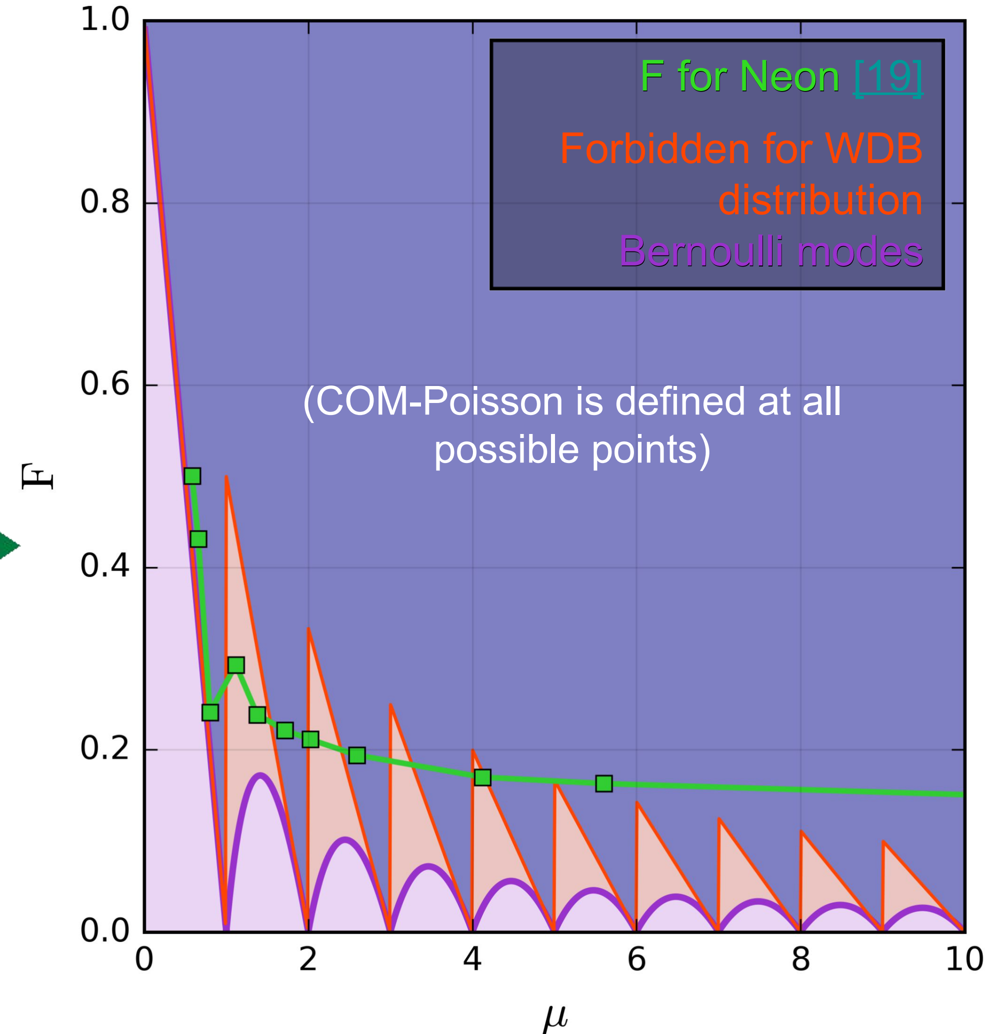

We can also examine other distribution shape parameters:
Compare higher moments along expected F(μ) curve

Central distribution moments vs. E for Neon

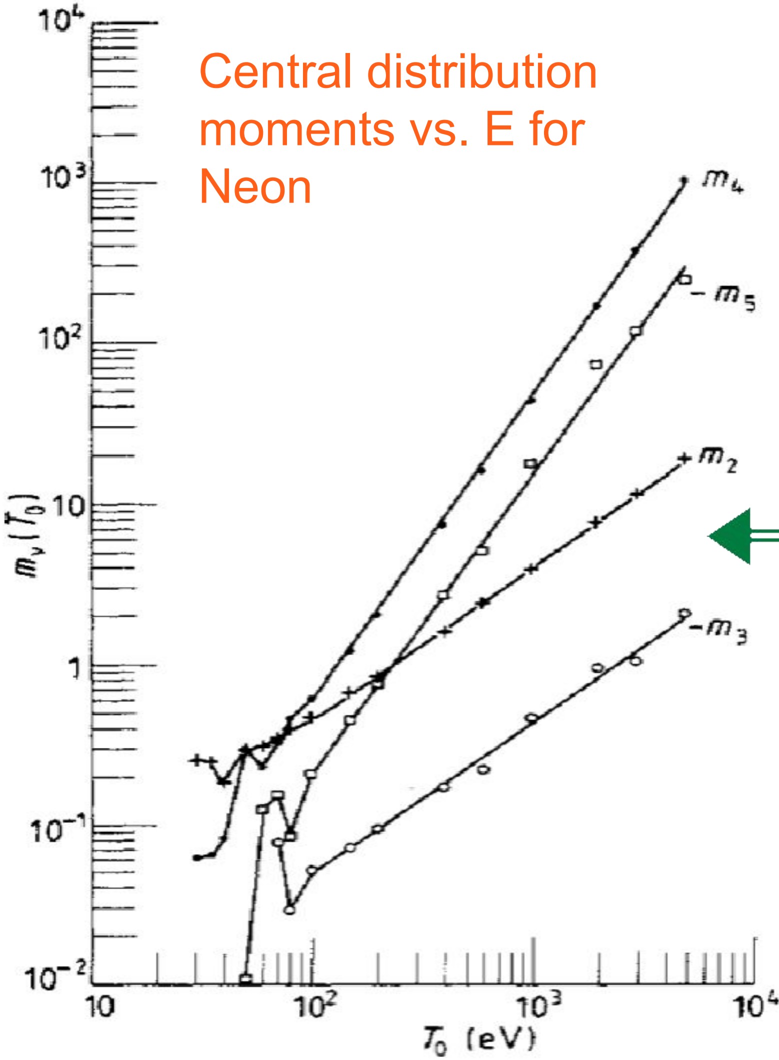

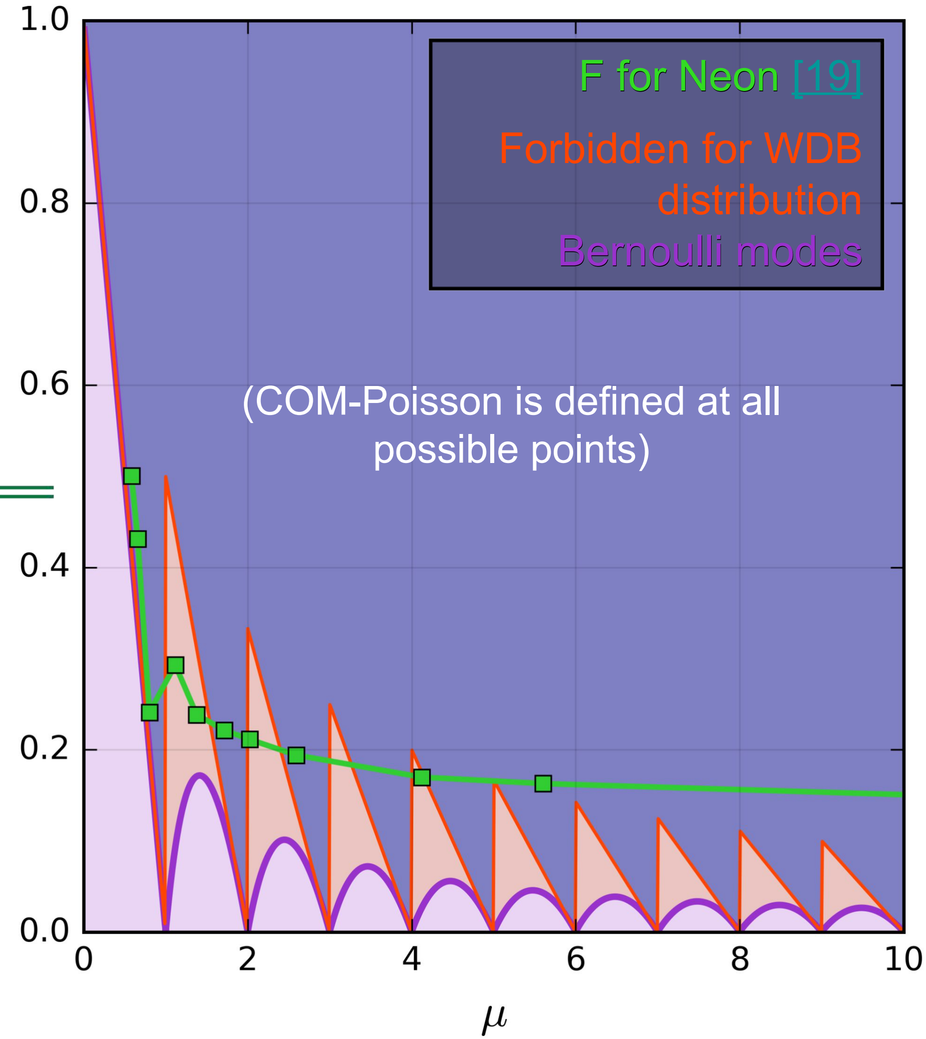

B. Grosswendt, J. Phys. B 17(7), 1391–1404 (1984).

We can compare the shape of COM-Poisson to theory:

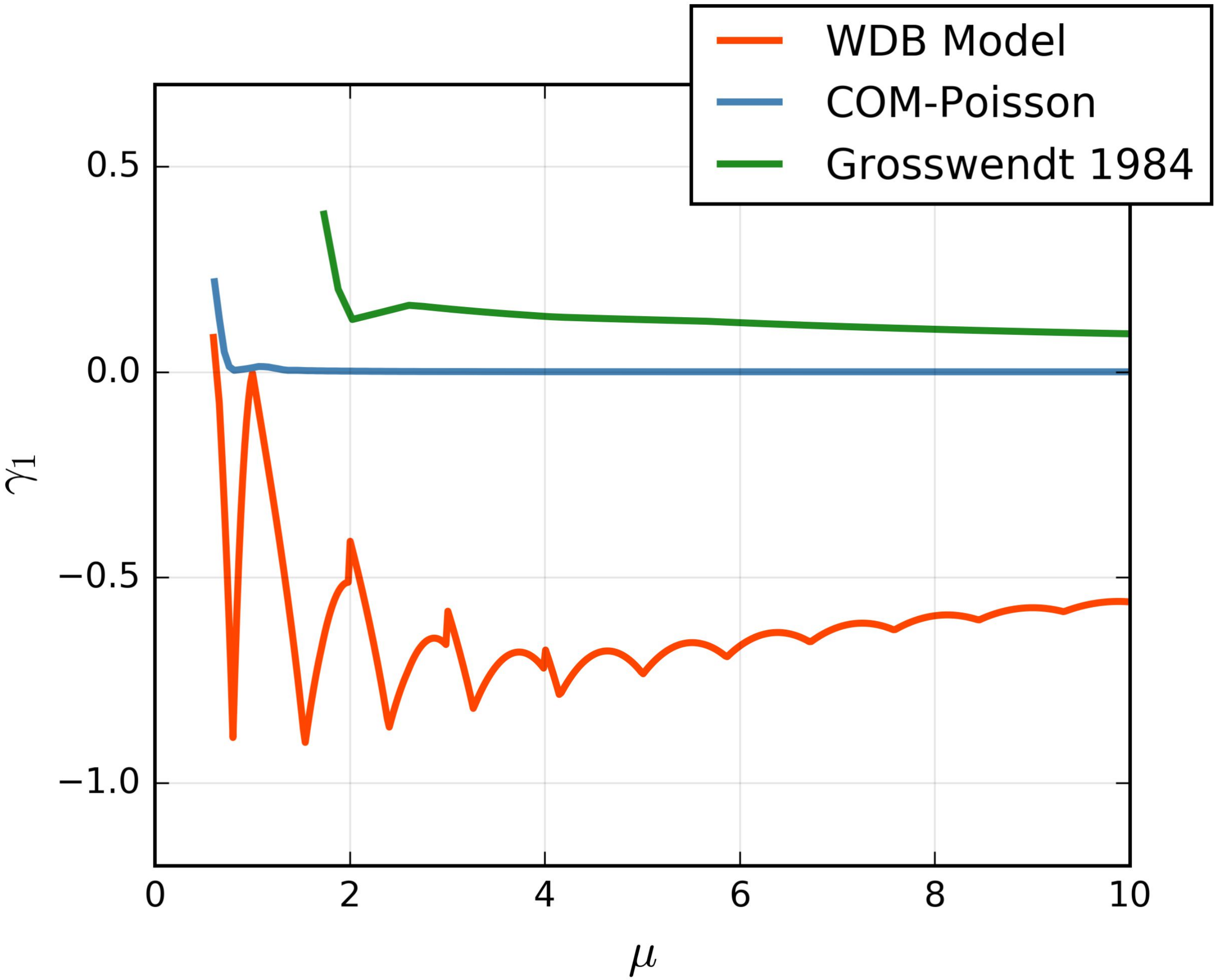

Skewness:

$$\gamma_1 = E\left[\left(\frac{X-\mu}{\sigma}\right)^3\right]$$

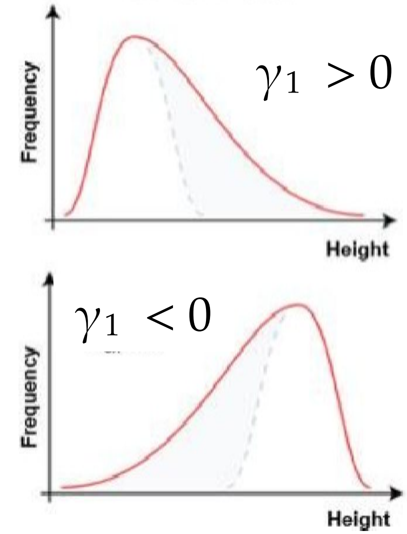

(Excess) Kurtosis:

$$\gamma_2 = E\left[\left(\frac{X-\mu}{\sigma}\right)^4\right] - 3$$

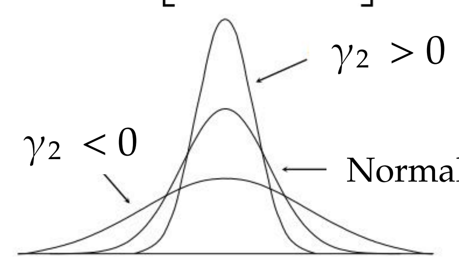

We can compare the shape of COM-Poisson to theory:

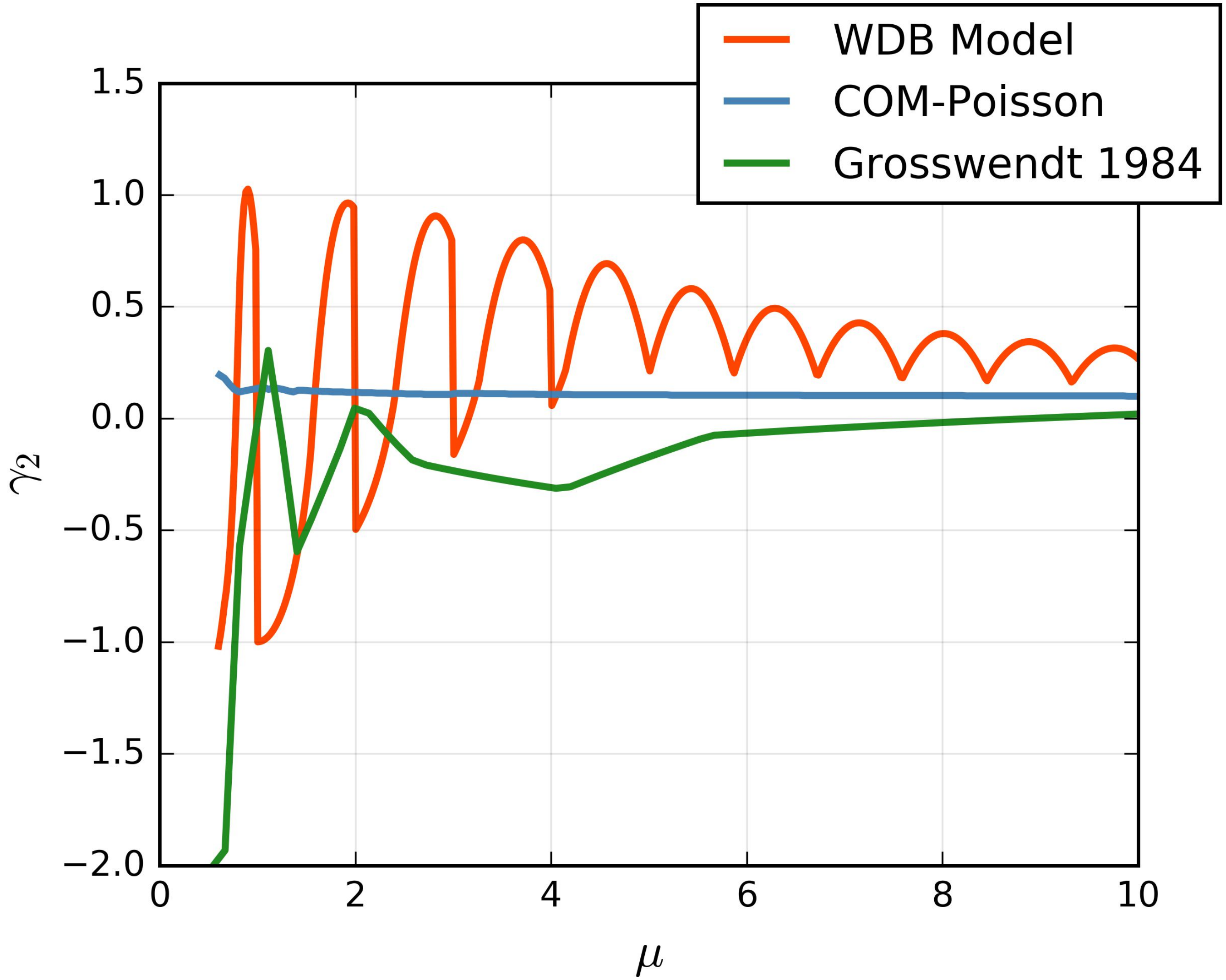

Skewness:

$$\gamma_1 = E\left[\left(\frac{X-\mu}{\sigma}\right)^3\right]$$

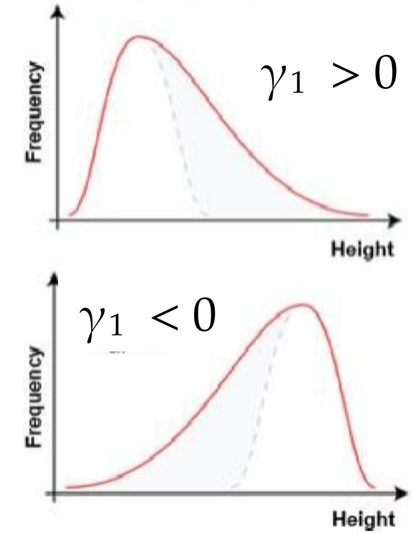

(Excess) Kurtosis:

$$\gamma_2 = E\left[\left(\frac{X-\mu}{\sigma}\right)^4\right] - 3$$

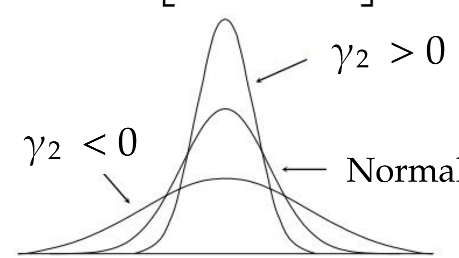

...Empirical support is still needed

The NEWS-G dark matter experiment

Spherical Proportional Counters (SPCs) to search for low-mass dark matter

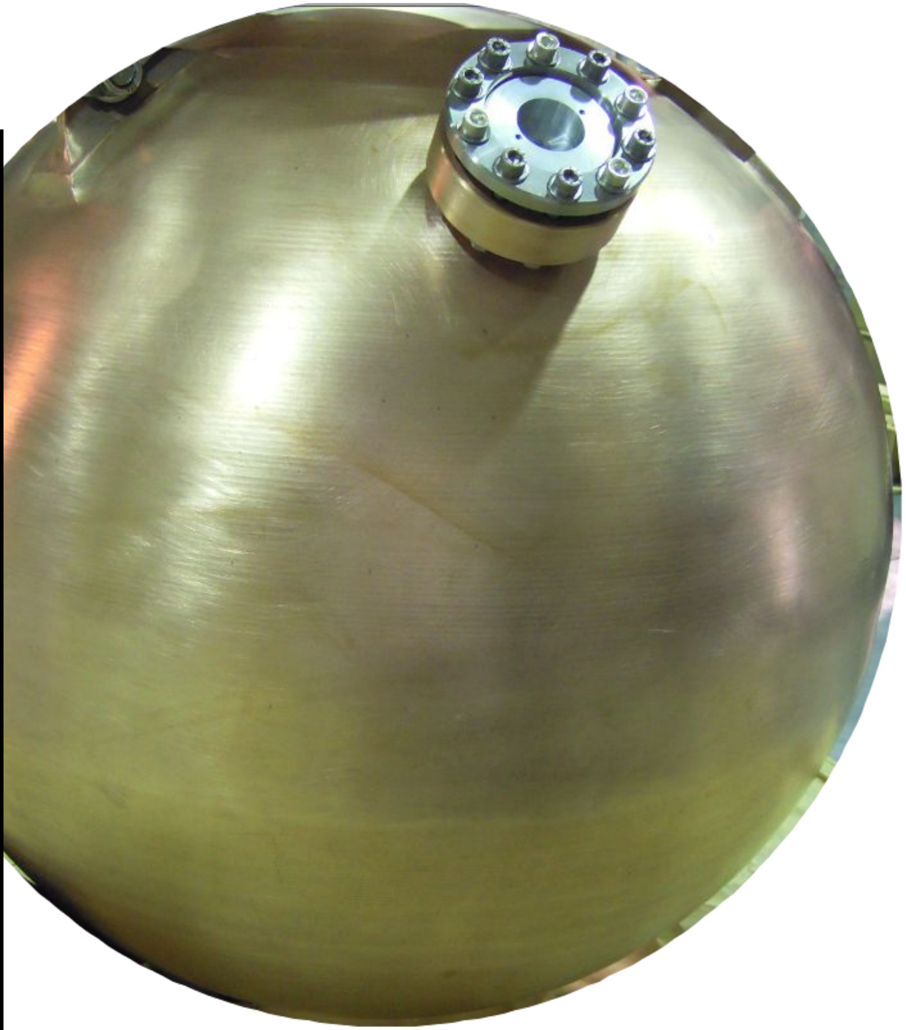

Low-A target atoms increase sensitivity to low-mass dark matter

Low intrinsic capacitance: ($C \approx 0.3$ pF)

High amplification gain from Townsend avalanche

Energy thresholds of ~10 eV!

NEWS-G is preparing to install a new detector at SNOLAB

Expected to be sensitive to WIMP masses ~100 MeV using H-rich gas and an energy threshold < 50 eV_{nr}

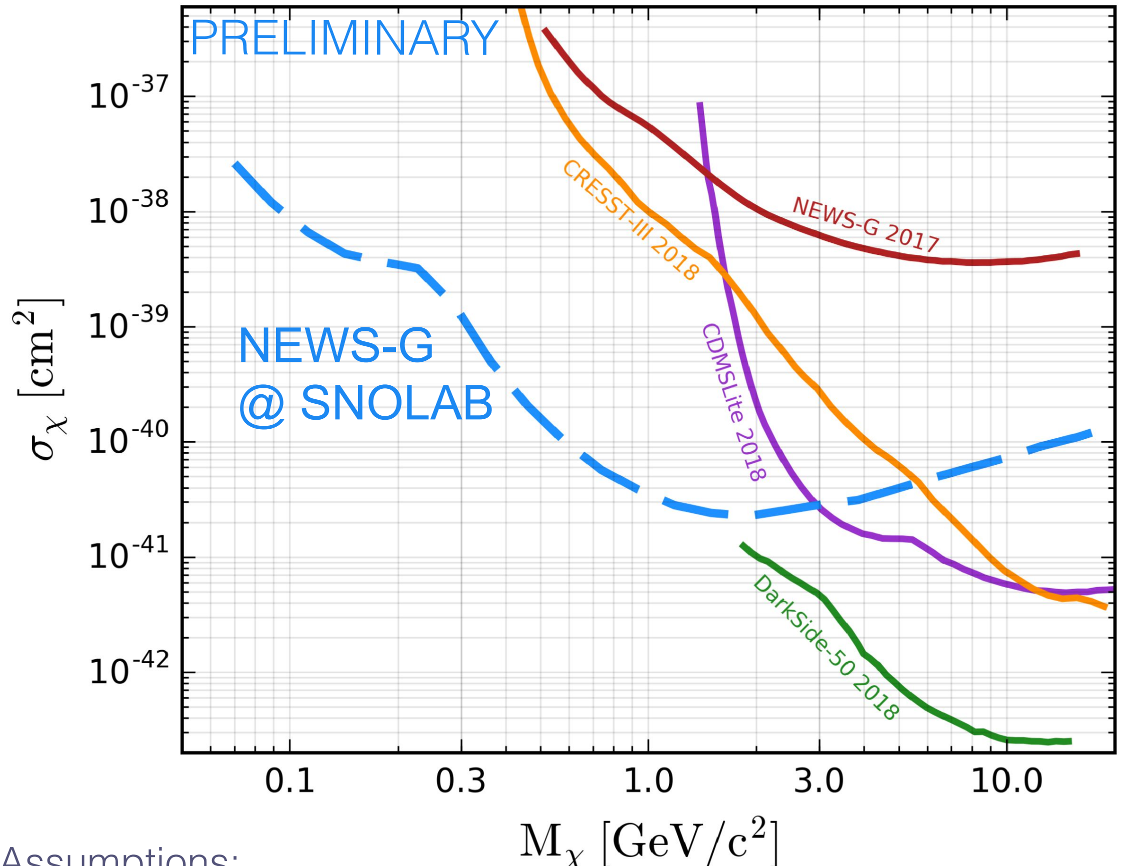

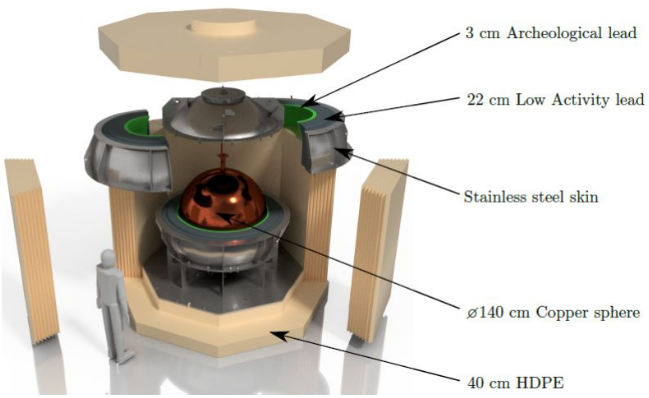

Assumptions:

Ne + 10% CH_4, Exposure: 20 kg days, F = 0.2, θ = 0.12,
SRIM quenching factor, Background: 1.78 dru, ROI: 14 eV_{ee} - 1 keV_{ee}
Optimum Interval Method

(1) Primary Ionization

$$\mu = \frac{E}{W(E)} \quad W_{\mathrm{nr}} = W_\gamma / Q(E)$$

(Neon: W_γ ~ 36 eV, Q ~ 0.2)

(2) Drift of charges

Typical drift time surface -> sensor: ~ 100 μs

(3) Avalanche of secondary e^-/ion pairs

Amplification of signal through Townsend avalanche (proportional to V)

(4) Signal formation

Current induced by the secondary ions drifting away from anode

(5) Signal readout

Induced current integrated by a charge sensitive pre-amplifier and digitized

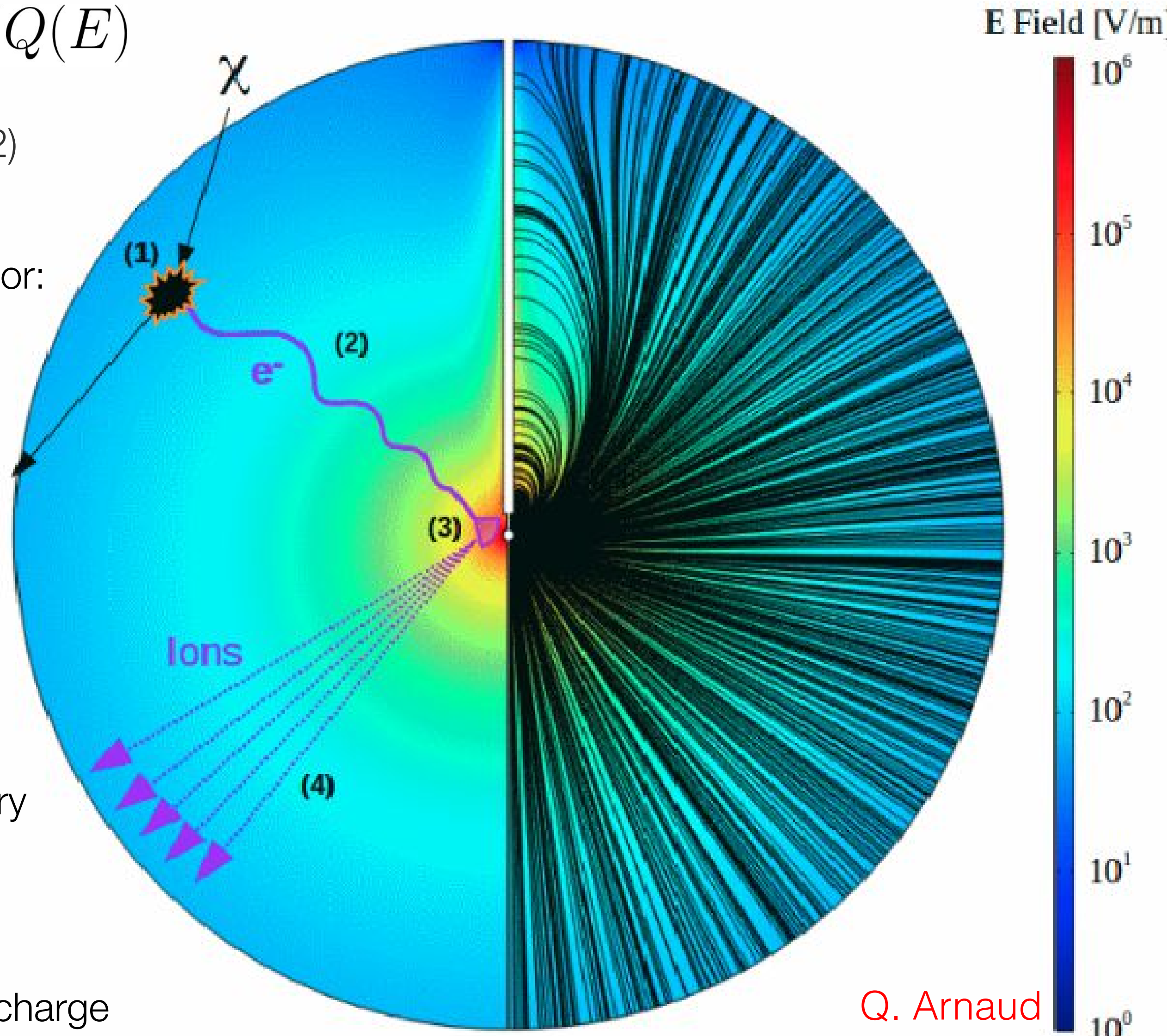

Q. Arnaud

(1) Primary Ionization

$$\mu = \frac{E}{W(E)} \quad W_{\mathrm{nr}} = W_\gamma / Q(E)$$

(Neon: W_γ ~ 36 eV, Q ~ 0.2)

(2) Drift of charges

Typical drift time surface -> sensor: ~ 100 μs

(3) Avalanche of secondary e⁻/ion pairs

Amplification of signal through Townsend avalanche (proportional to V)

(4) Signal formation

Current induced by the secondary ions drifting away from anode

(5) Signal readout

Induced current integrated by a charge sensitive pre-amplifier and digitized

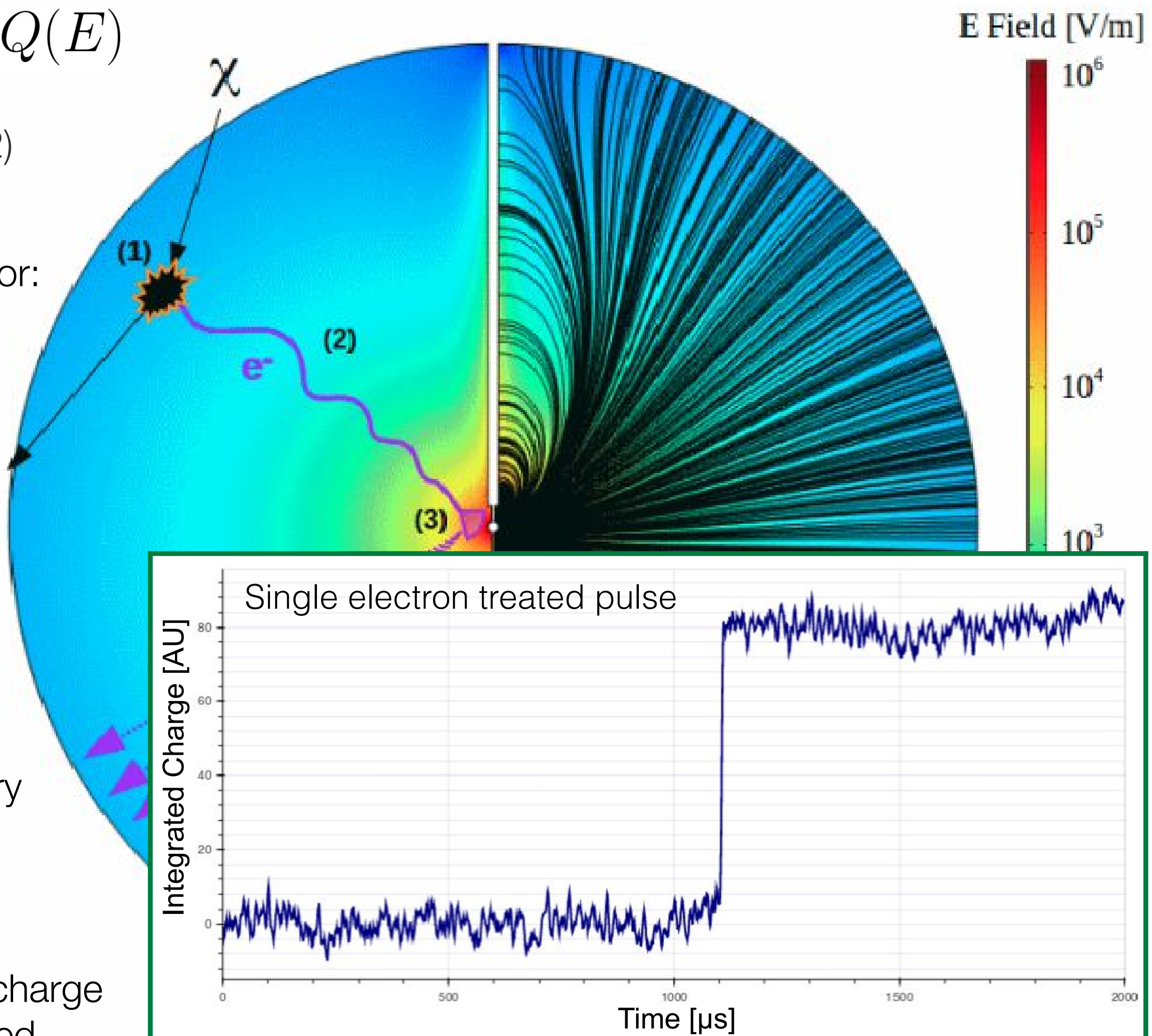

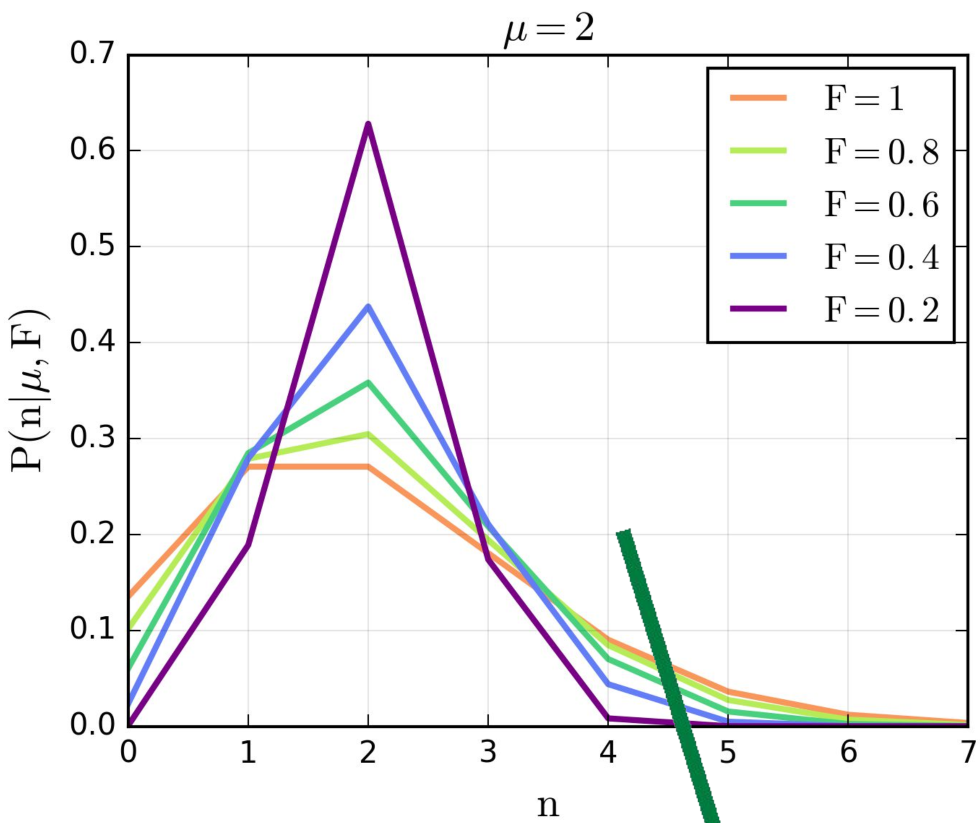

$$\mathcal{F}\left(E|E_0\right) = \sum_{n=1}^{n_{\max}} P_{\mathrm{COM}}\left(n|\lambda\left(\mu, F\right), \nu\left(\mu, F\right)\right) \times P_{\mathrm{Polya}}^{(n)}\left(E|\theta, \langle G\rangle\right)$$

$$\mu = \frac{E_0}{W\left(E_0\right)} \qquad n_{\max} = \left\lfloor \frac{E_0}{I} \right\rfloor$$

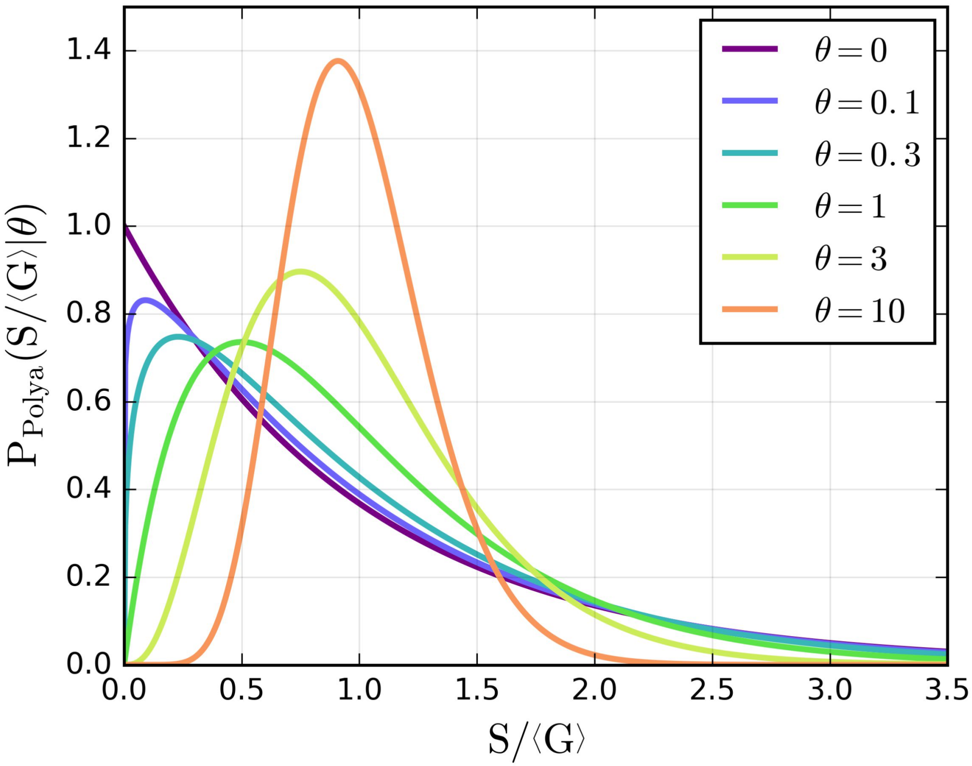

$$P_{\text{Polya}}\left(S|\left\langle G\right\rangle,\theta\right) = \frac{1}{\left\langle G\right\rangle}\left(\frac{\left(1+\theta\right)^{1+\theta}}{\Gamma\left(1+\theta\right)}\right) \times \left(\frac{S}{\left\langle G\right\rangle}\right)^{\theta}\exp\left(-\left(1+\theta\right)\frac{S}{\left\langle G\right\rangle}\right)$$

The distribution of the number of avalanche pairs S is roughly exponential

It is thought to be well-described by the Polya distribution [7,24,35], with shape parameter θ

$$\mathcal{F}\left(E|E_0\right) = \sum_{n=1}^{n_{\max}} P_{\text{COM}}\left(n|\lambda\left(\mu,F\right),\nu\left(\mu,F\right)\right)\times P_{\text{Polya}}^{(n)}\left(E|\theta,\left\langle G\right\rangle\right)$$

$$\mu = \frac{E_0}{W\left(E_0\right)} \qquad n_{\max} = \left\lfloor\frac{E_0}{I}\right\rfloor$$

$$P_{\text{Polya}}^{(n)}\left(E|\theta,\langle G\rangle\right)=\frac{1}{\langle G\rangle}\left(\frac{(1+\theta)^{1+\theta}}{\Gamma(1+\theta)}\right)^{n}$$
$$\times\left(\frac{E}{\langle G\rangle}\right)^{n(1+\theta)-1}\exp\left(-(1+\theta)\left(\frac{E}{\langle G\rangle}\right)\right)$$
$$\times\prod_{i=1}^{n-1}B\left((i+i\theta),(1+\theta)\right)$$

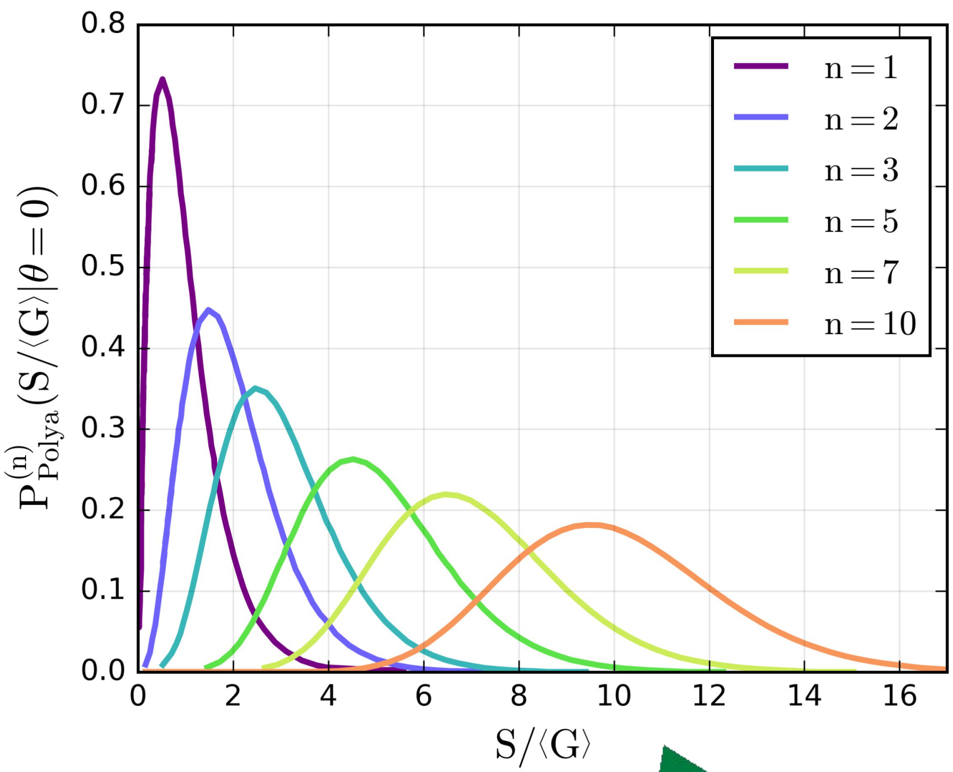

If the avalanche response of each primary electron is independent, then the avalanche response is the n^th^ convolution of Polya [5].

$$\mathcal{F}\left(E|E_0\right)=\sum_{n=1}^{n_{\max}}P_{\text{COM}}\left(n|\lambda(\mu,F),\nu(\mu,F)\right)\times P_{\text{Polya}}^{(n)}\left(E|\theta,\langle G\rangle\right)$$

$$\mu=\frac{E_0}{W(E_0)}\qquad n_{\max}=\left\lfloor\frac{E_0}{I}\right\rfloor$$

SPC detector response model

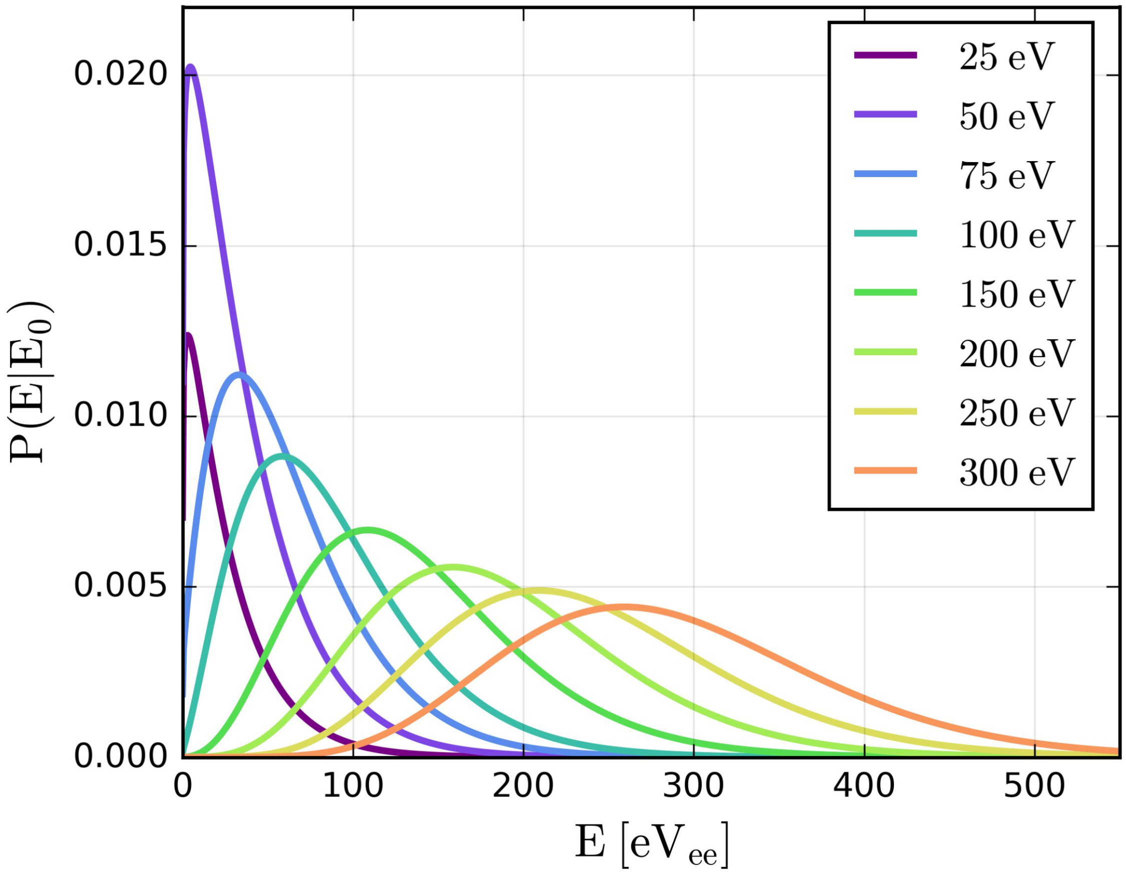

Analytical formula for overall detector response

This example:
F = 0.2, θ = 0.1

(Loss of signal at low energy because non-zero probability of having 0 primary electrons)

$$\mathcal{F}\left(E|E_0\right) = \sum_{n=1}^{n_{\max}} P_{\mathrm{COM}}\left(n|\lambda\left(\mu, F\right), \nu\left(\mu, F\right)\right) \times P_{\mathrm{Polya}}^{(n)}\left(E|\theta, \langle G\rangle\right)$$

$$\mu = \frac{E_0}{W\left(E_0\right)} \qquad n_{\max} = \left\lfloor \frac{E_0}{I} \right\rfloor$$

SPC detector response model

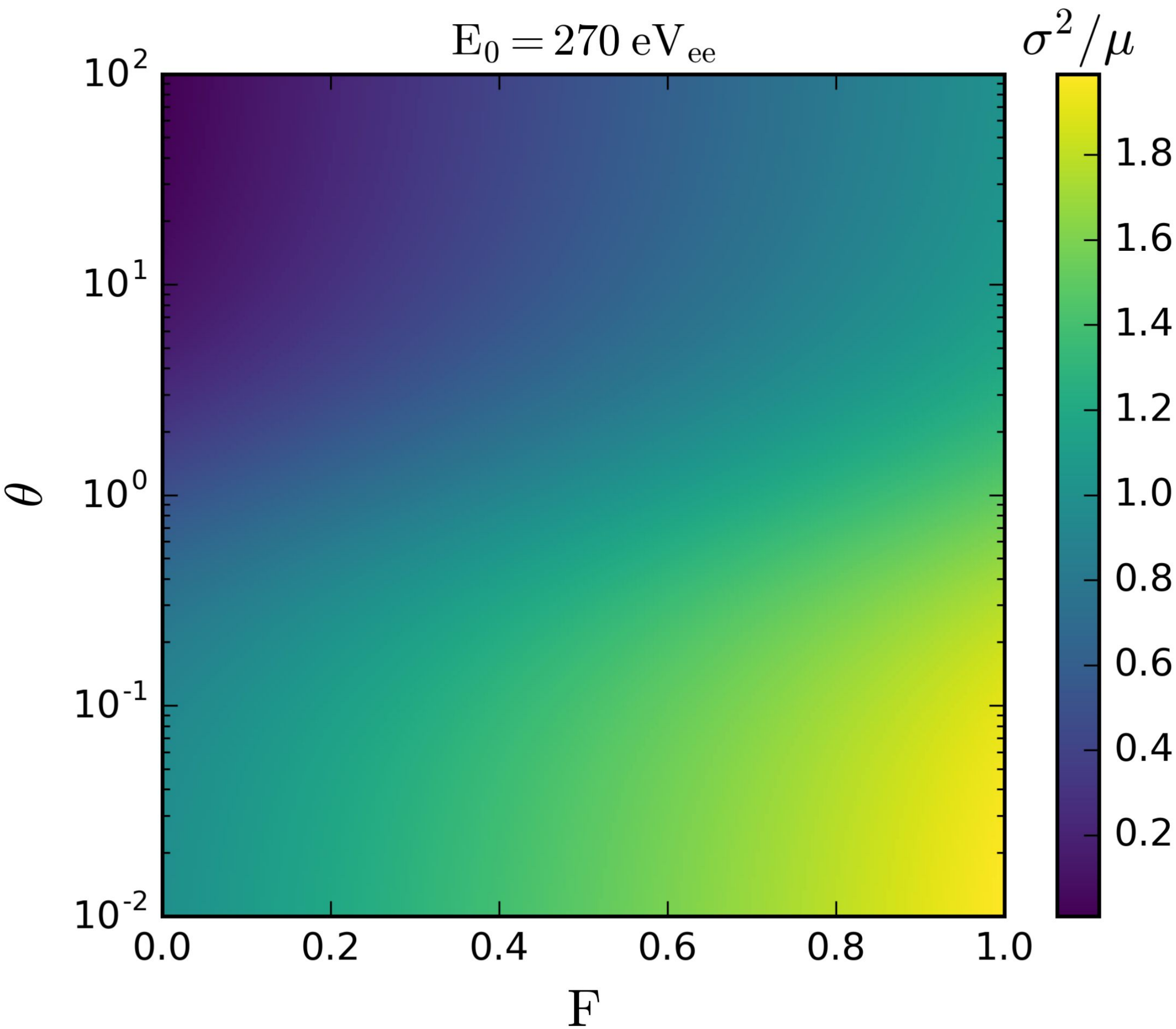

There's degeneracy between primary and secondary ionization for SPCs:

$$\frac{\sigma^2}{\mu} \approx F + \frac{1}{1+\theta}$$

Difficult (impossible?) to simultaneously fit avalanche response and COM-Poisson

We want a calibration source that only includes one process to disentangle them

Expected values of $F \approx 0.2$ and $\theta \approx 0.1$

UV laser setup

Q. Arnaud et al. (NEWS-G Collaboration), Phys. Rev. D 99, 102003 (2019)

Tunable transmission to control the mean number of electrons

Parallel photo-detector to tag laser events

Common DAQ for timing analysis between two channels

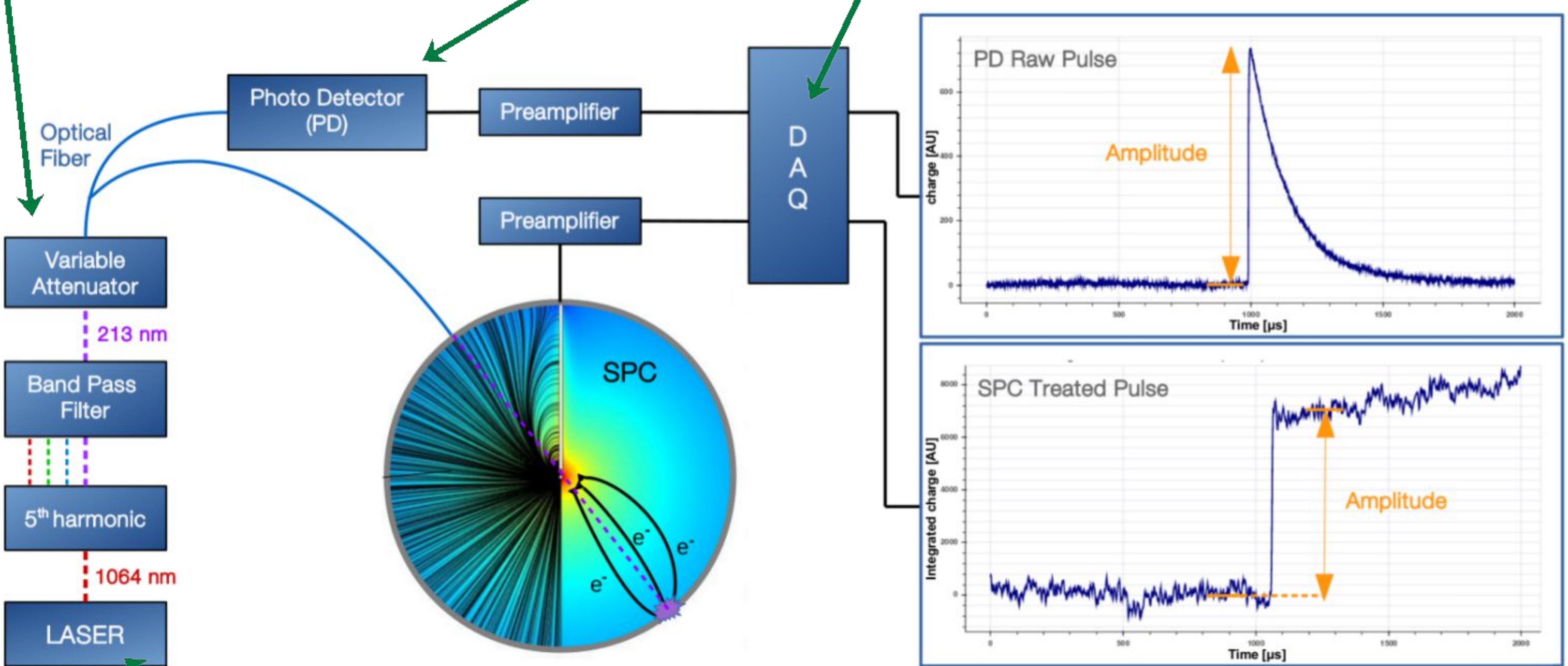

A powerful UV laser capable of extracting 100s of electrons

The excellent fit validates the avalanche response model [5]:

$$\mathcal{F}\left(E'\right) = P_{\text{Poisson}}\left(0|\mu\right) + \sum_{n=1}^{\infty} P_{\text{Polya}}^{(n)}\left(E'|\theta\left\langle G\right\rangle\right) \times P_{\text{Poisson}}\left(n|\mu\right)$$

(This is then convolved with a Gaussian to incorporate baseline noise)

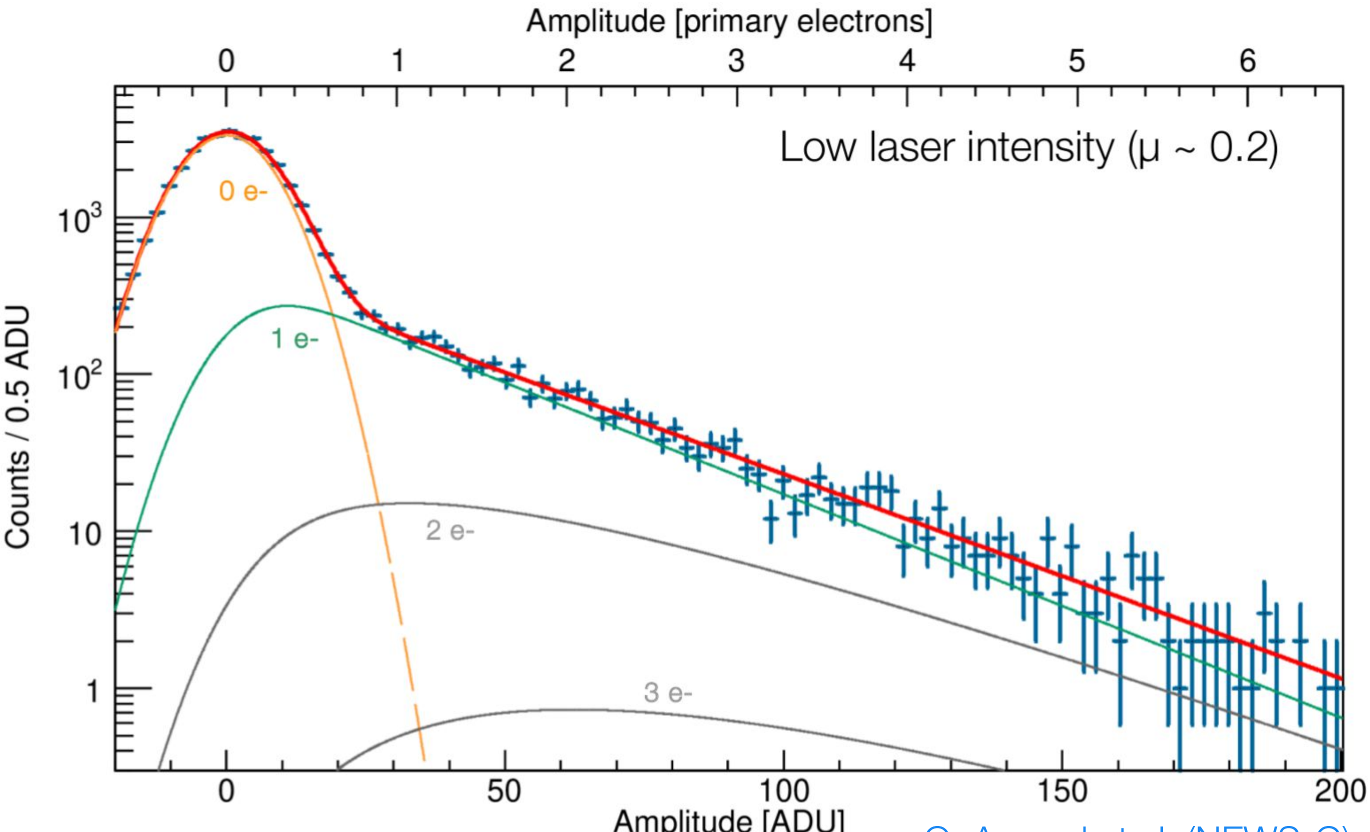

Q. Arnaud et al. (NEWS-G), Phys. Rev. D 99, 102003 (2019)

Data Parameters:

Ne + 2% CH4
P = 1.5 bar
HV = 1200 V

Fit results:

θ = 0.09 ±0.02
<G> = 30.26 ± 0.21 ADU
χ^2/ndf = 0.97

The excellent fit validates the avalanche response model [5]:

$$\mathcal{F}(E') = P_{\text{Poisson}}(0|\mu) + \sum_{n=1}^{\infty} P_{\text{Polya}}^{(n)}(E'|\theta\langle G\rangle) \times P_{\text{Poisson}}(n|\mu)$$

(This is then convolved with a Gaussian to incorporate baseline noise)

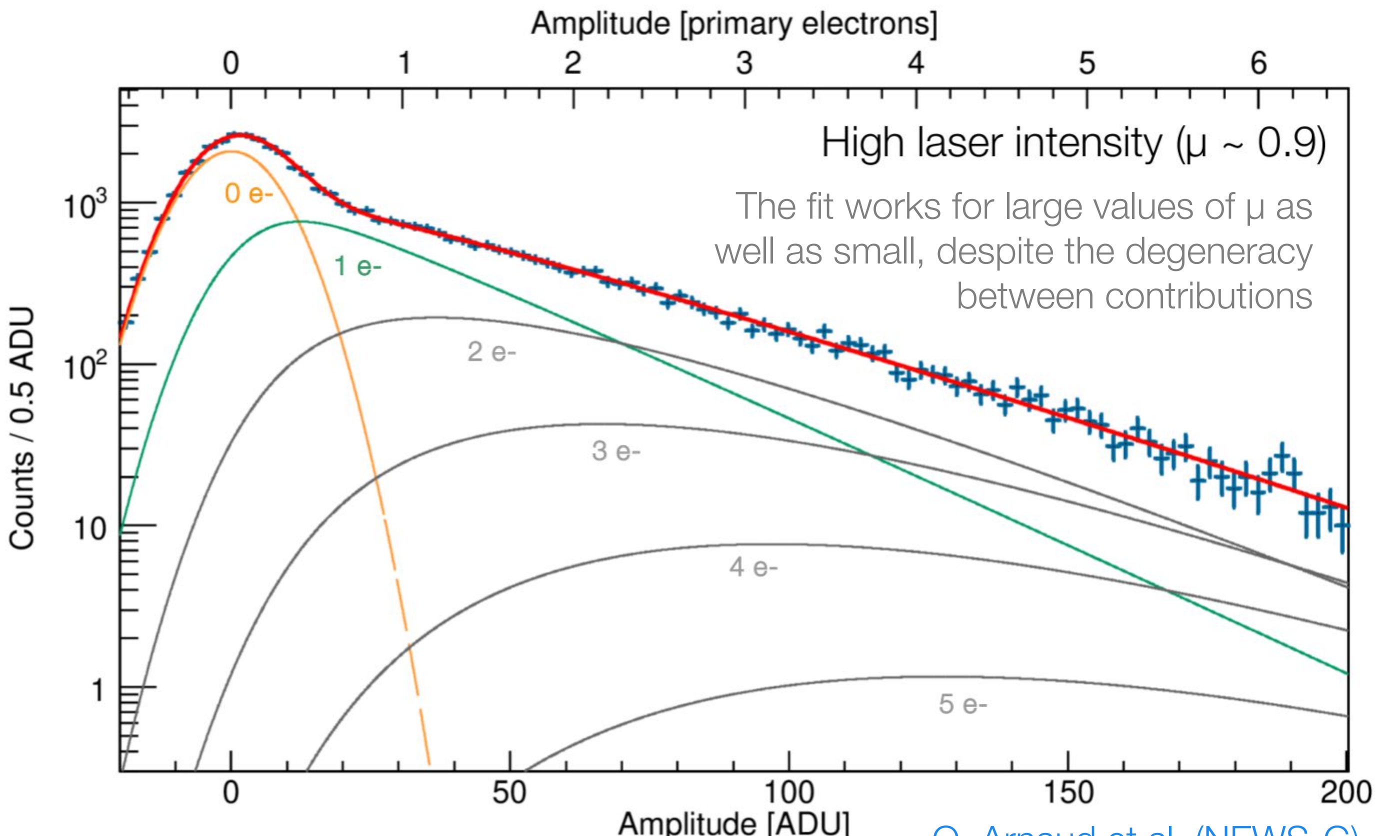

Data Parameters:

Ne + 2% CH4
P = 1.5 bar
HV = 1200 V

Fit results:

θ = 0.09 ±0.02
<G> = 30.26 ± 0.21 ADU
χ^2/ndf = 0.97

Q. Arnaud et al. (NEWS-G), Phys. Rev. D 99, 102003 (2019)

^{37}Ar: radioactive gas, decays via electron capture [23].
W-value measurement performed in 1.5 bar of Ne + 2% CH_4 [5]. Simultaneous operation of the UV laser also disentangles primary and secondary ionization.

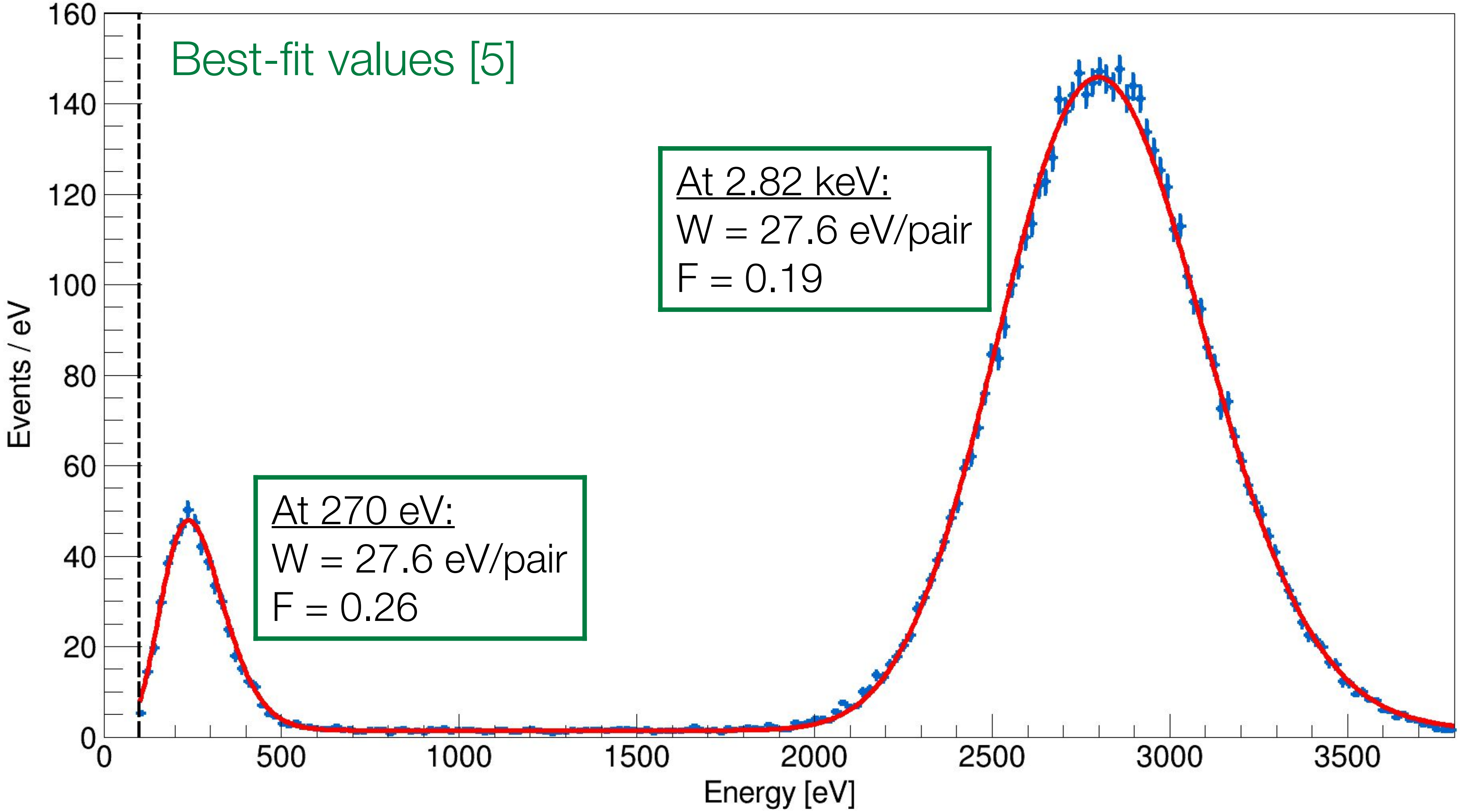

The W-value at 2.82 keV (calculated from <G>), θ, and branching ratios BR were fixed for this fit

In particular, the fit of the L-shell gives empirical support for COM-Poisson

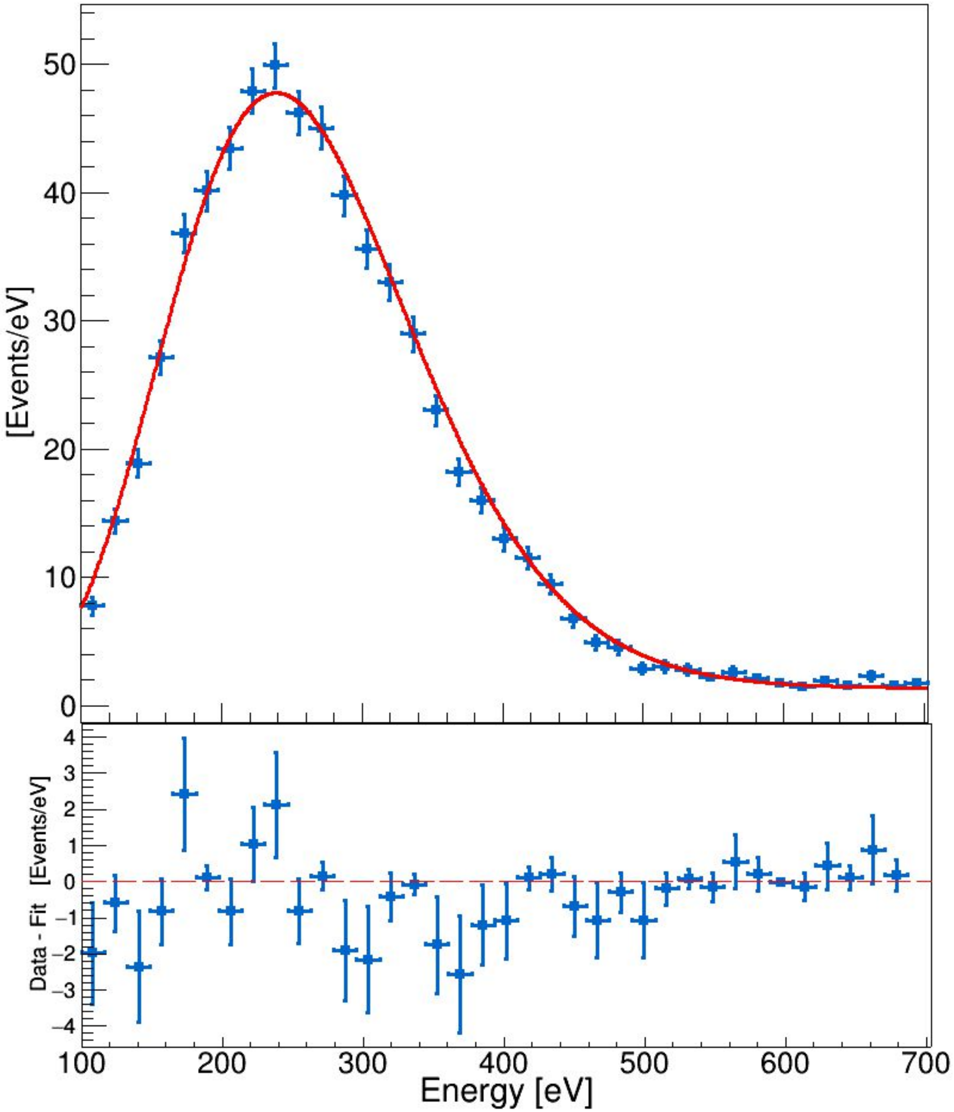

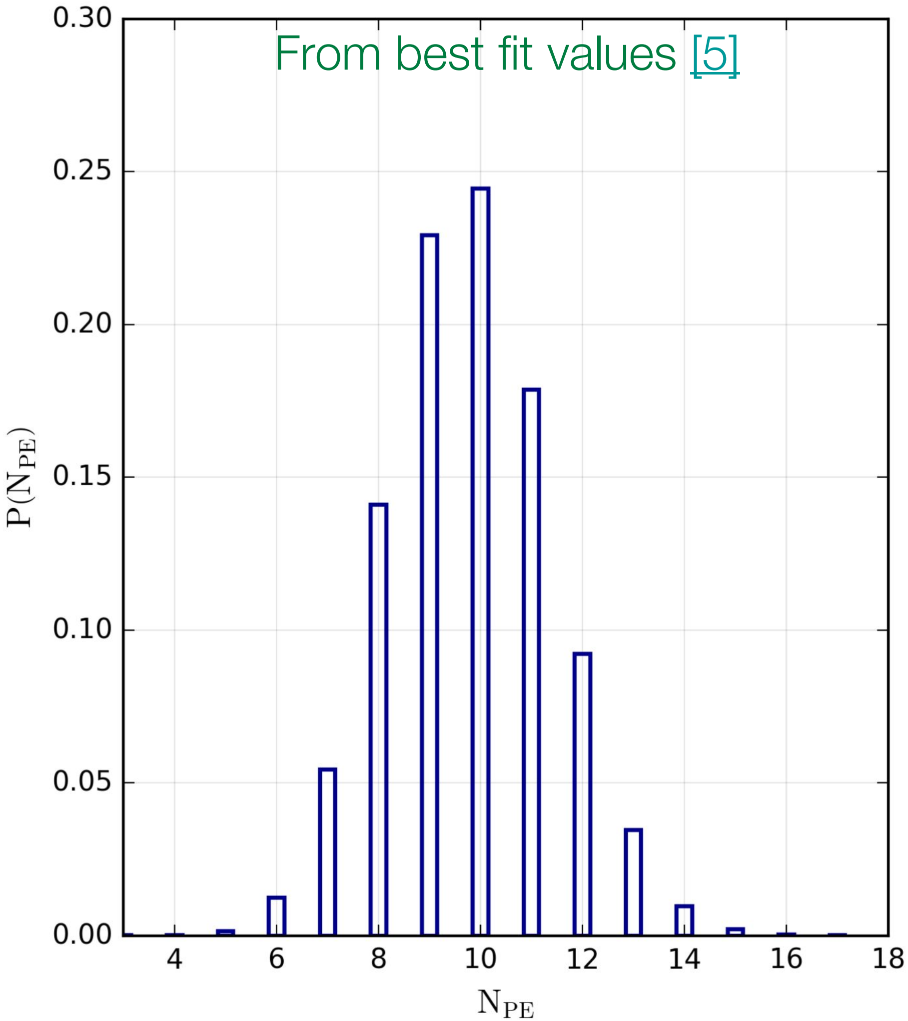

$\lambda = 1.03 \times 10^4$
$\nu = 3.99$

$\Longrightarrow$

$\mu = 9.79$
$F = 0.261$

What impact can the Fano factor have?

The impact of the Fano factor

Consider a hypothetical neon experiment with a finite energy threshold and Gaussian energy resolution of given width:

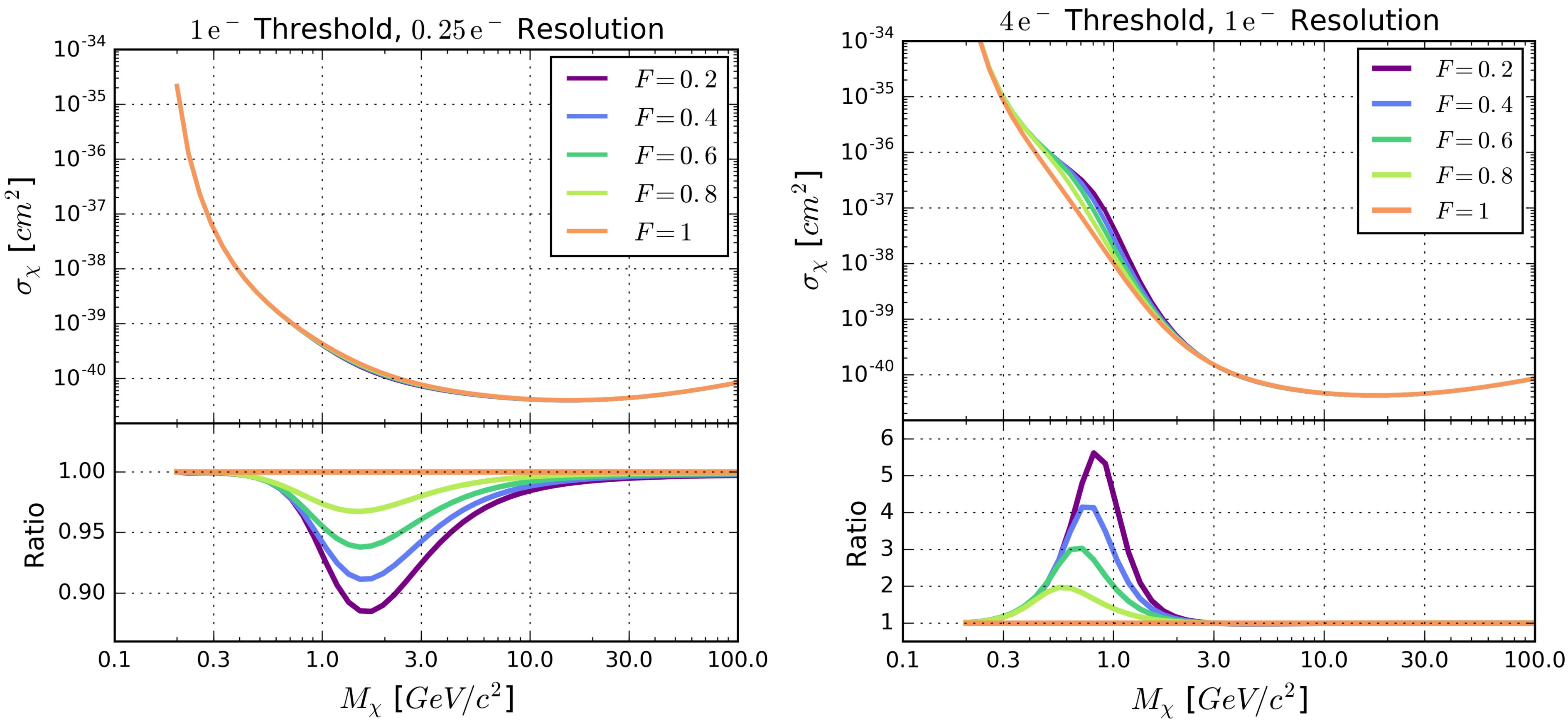

In these cases, the effect of the Fano factor is relatively small

At low DM mass, the expected signal is dominated by Bernoulli-mode events
At high DM mass, energy resolution has no effect on signal acceptance

The impact of the Fano factor on NEWS-G

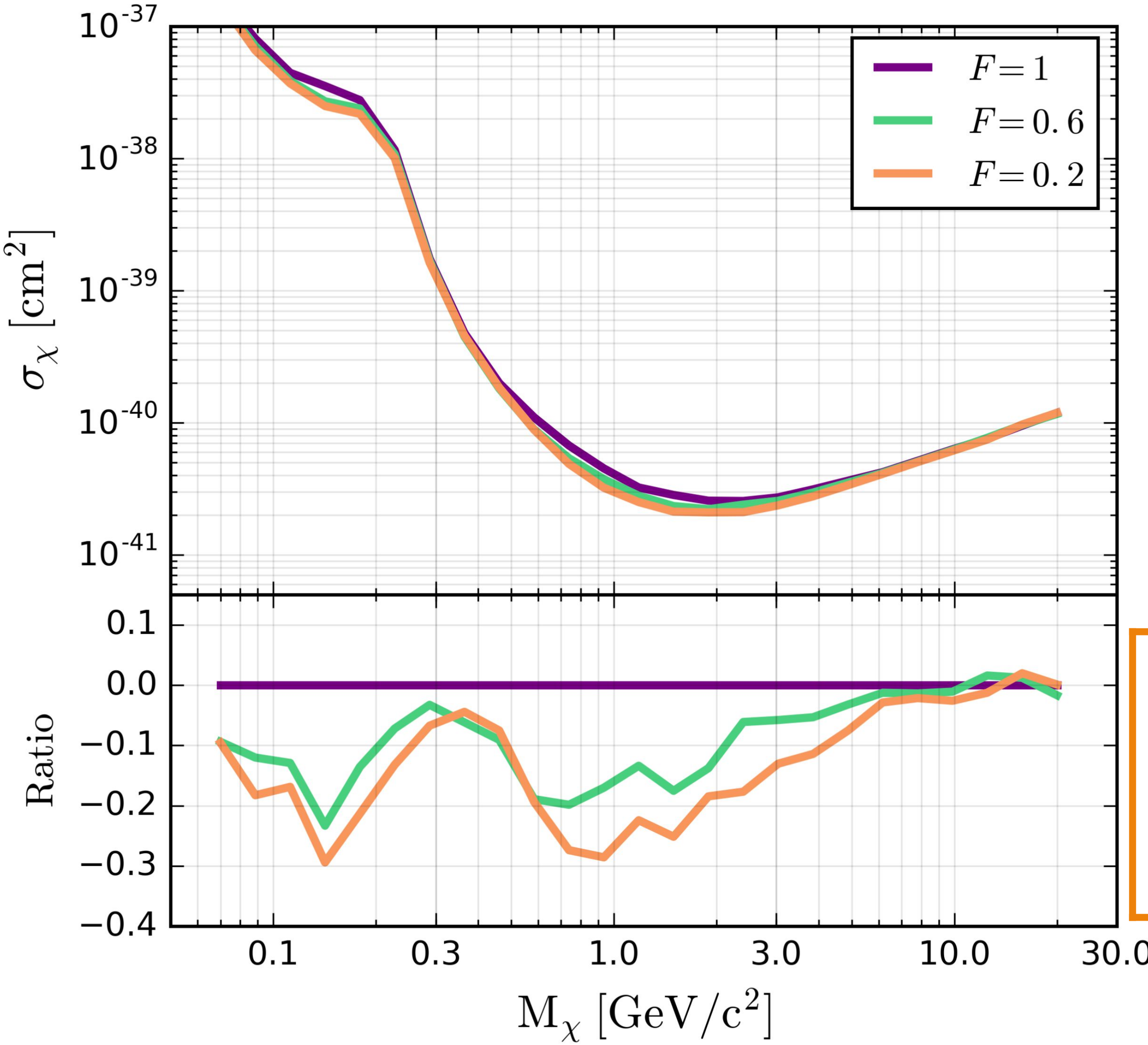

NEWS-G projected limits for SNOLAB with Ne + 10% CH_4 are produced with the Optimum Interval Method

The Fano factor has very little impact in this case as well (low energy threshold and broad resolution scenario)

OI Method: 1000 MCs
Gas: Ne + 10% CH_4
ROI: 0.5 e^- → 1 keV_{ee}
Response: θ = 0.12
Background: 1.67±0.5 dru
Exposure: 20 kg.days

The impact of the Fano factor

In cases where a detector has good energy resolution and a "high" energy threshold, F can have a large impact on sensitivity to low-mass DM

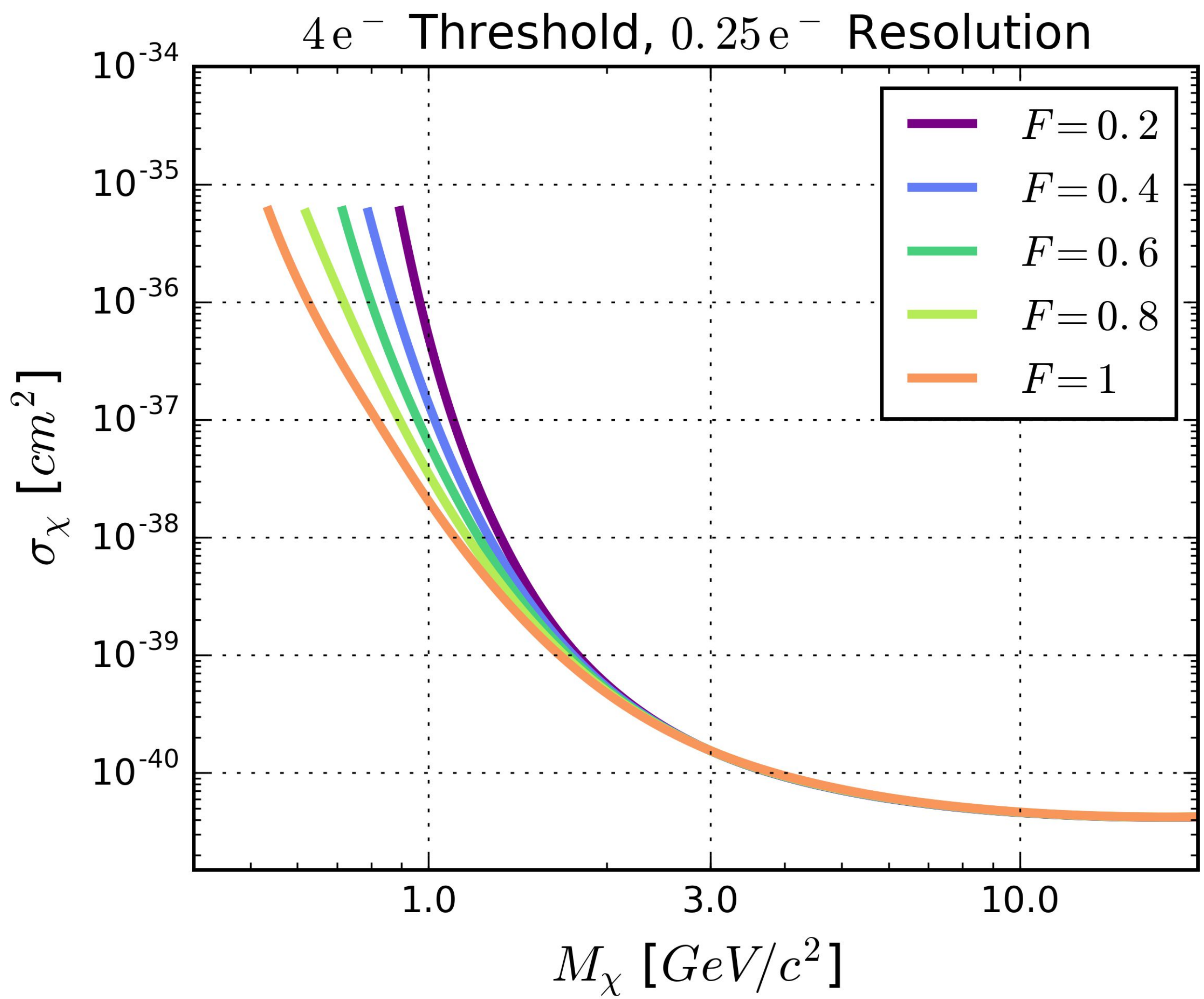

The impact of the Fano factor

This situation is realistic for some current direct detection experiments:

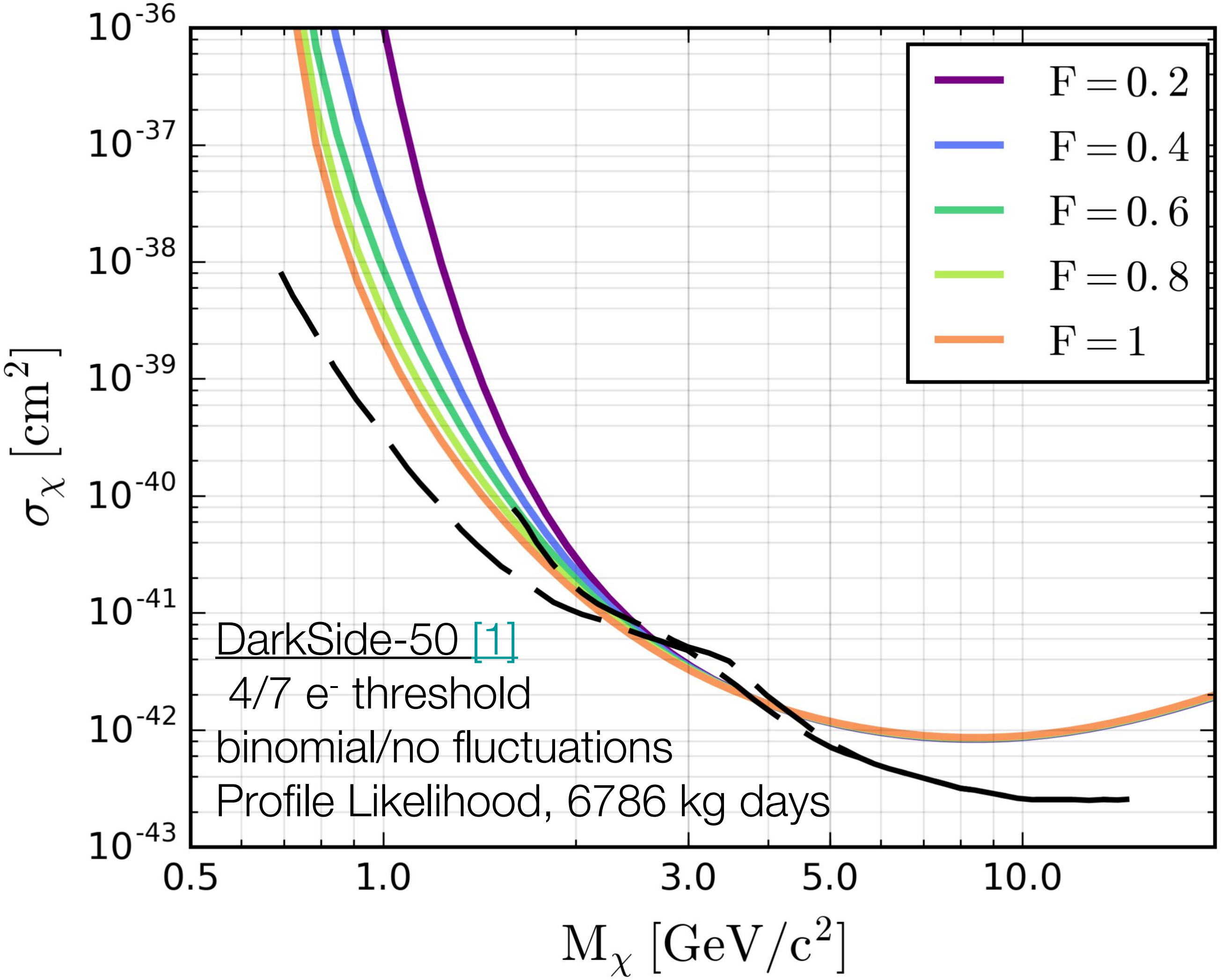

COM-Poisson with σ = 0.22 e⁻ Gaussian noise

4e⁻ threshold

Same ionization yield [9]

Poissonian limit, exposure equivalent to **1/√Exposure** background subtraction

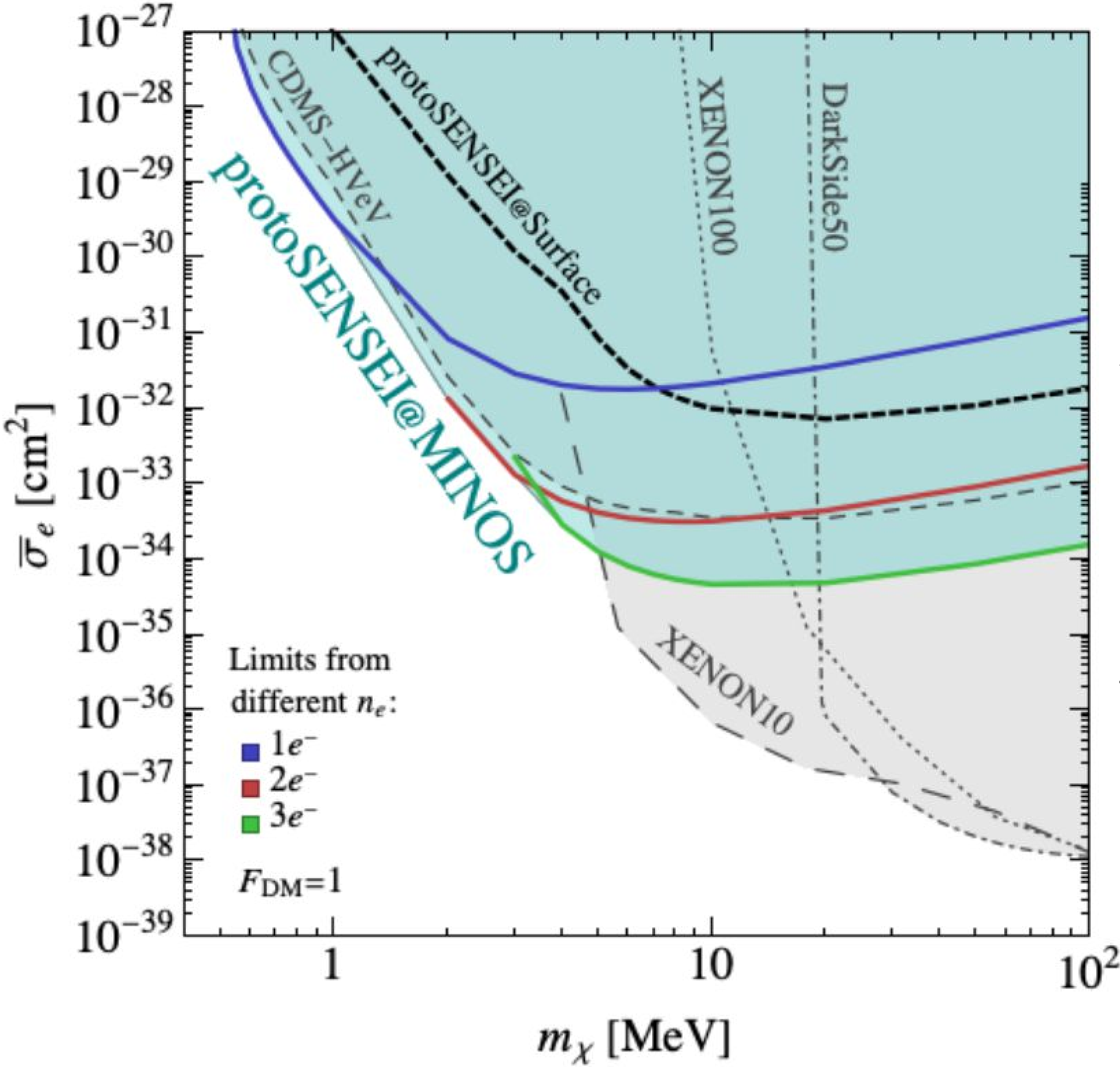

New parameter spaces are being probed in which F has a more direct impact:

I.e. dark matter scattering with electrons [2,4,34]

In analyses where regions of interest are defined in terms of # of ionizations (rather than deposited energy), then F could dramatically affect claimed limits

O. Abramoff et al. (SENSEI Collaboration), Phys. Rev. Lett. 121, 161801 (2019)

Summary

» Modeling ionization fluctuations at low energy is a relevant issue for low-mass dark matter direct detection experiments

» The COM-Poisson distribution is a possibly suitable model for this purpose

» Code to use COM-Poisson for modeling primary ionization is publicly available (https://news-g.org/com-poisson-code/)

» Ar-37 calibration data from NEWS-G provides some empirical support for this choice of model

» In some cases (such as for NEWS-G), the Fano factor does not have a significant impact on low-mass dark matter sensitivity

» In other cases, it could have a significant impact, and a model such as COM-Poisson could be used to incorporate F as a systematic

Thank you!

Queen's University Kingston - G Gerbier, P di Stefano, R Martin, G Giroux, S Crawford, M Vidal, G Savvidis, A Brossard, F Vazquez de Sola, Q Arnaud, K Dering, J McDonald, M Chapellier, A Ronceray, P Gros, A Rolland, C Neyron, JF Caron
- Copper vessel and gas set-up specifications, calibration, project management
- Gas characterization, laser calibration on smaller scale prototypes
- Simulations/Data analysis

IRFU (Institut de Recherches sur les Lois fondamentales de l'Univers)/**CEA Saclay** - **I Giomataris**, M Gros, T Papaevangelou, JP Bard, JP Mols
- Sensor/rod (low activity, optimization with 2 electrodes)
- Electronics (low noise preamps, digitization, stream mode)
- DAQ/soft

LSM (Laboratoire Souterrain de Modane), IN2P3, U of Chambéry - M Zampaolo, A DastgheibiFard
- Low activity archaeological lead
- Coordination for lead/PE shielding and copper sphere

Aristotle University of Thessaloníki - I Savvidis, A Leisos, S Tzamarias
- Simulations, neutron calibration
- Studies on sensor

LPSC (Laboratoire de Physique Subatomique et Cosmologie) **Grenoble** - D Santos, JF Muraz, O Guillaudin
- Quenching factor measurements at low energy with ion beams

Pacific Northwest National Laboratory - E Hoppe, R Bunker
- Low activity measurements, copper electro-forming

RMCC (Royal Military College of Canada) **Kingston** - D Kelly, E Corcoran
- ^{37}Ar source production, sample analysis

SNOLAB Sudbury - P Gore, S Langrock
- Calibration system/slow control

University of Birmingham - K Nikolopoulos, P Knights, I Katsioulas, R Ward
- Simulations, analysis, R&D

University of Alberta - MC Piro, D Durnford
- Gas purification, data analysis

Associated labs: TRIUMF - F Retiere

The NEWS-G Collaboration
(November 2018)

References

[1] P. Agnes et al., Phys. Rev. Lett. 121, 081307 (2018).

[2] R. Agnese et al., Phys. Rev. Lett. 121, 51301 (2018).

[3] G.D. Alkhazov, A.P. Komar, and A.A Vorob'ev, Nucl. Instrumen. Methods 48(1), 1–12 (1967).

[4] E. Armengaud, et al., Phys. Rev. D 99, 82003 (2019).

[5] Q. Arnaud et al., Phys. Rev. D 99, 102003 (2019).

[6] Q. Arnaud et al., Astropart. Phys. 97, 54–62 (2018).

[7] R. Bellazzini et al., NIM A 581(1), 246–253 (2007).

[8] K.-H. Best, Journal of Quantitative Linguistics 8(1), 1–11 (2001).

[9] F. Bezrukov, F. Kahlhoefer, and M. Lindner, Astropart. Phys. 35(3), 119–127 (2011).

[10] P.C. Consul and G.C. Jain, Technometrics 15(4), 791–799 (1973).

[11] R.W. Conway and W.L. Maxwell, Journal of Industrial Engineering 12, 132–136 (1962).

[12] M. Crisler et al., Phys. Rev. Lett. 121(6), 61803 (2018).

[13] J.R.T. de Mello Netoet al., Proc. Sci. ICRC2015, 1221 (2016).

[14] D. Durnford, M.Sc. Thesis (2018) https://qspace.library.queensu.ca/handle/1974/24878

[15] D. Durnford, Q. Arnaud, and G. Gerbier, Phys. Rev. D 98, 103013 (2018).

[16] U. Fano, Phys. Rev. 72(1), 26–29 (1947).

[17] W. Gardner, E.P. Mulvey, and E.C. Shaw, Psycol. Bull., 118(3), 392–404 (1995).

[18] B. Grosswendt and E. Waibel, Radiation Protection Dosimetry 13(1–4), 95–102 (1985).

References

[19] B. Grosswendt, J. Phys. B 17(7), 1391–1404 (1984).

[20] B. Grosswendt, Monte Carlo Transport of Electrons and Photons pp. 345–360 (1987).

[21] A. Hashiba et al., NIM A 227(2), 305–310 (1984).

[22] M. Kase et al., Nucl. Instrum. Methods Phys. Res. 227(2), 311–317 (1984).

[23] D.G. Kelly et al., Journal of Radioanalytical and Nuclear Chemistry 318(1) (2018).

[24] M. Kobayashi et al., NIM A 845, 236–240 (2017).

[25] D. Lord and Y.-J. Park, Accident Analysis & Prevention 40(4), 1441–1457 (2008).

[26] B.G. Lowe, NIM A 399(2), 354–364 (1997).

[27] T.T.P. Minka et al. (2003), http://lib.stat.cmu.edu/cmu-stats/tr/tr776/tr776.pdf

[28] A. Owens, G.W. Fraser, and K.J. McCarthy, NIM A 491(3), 437–443 (2002).

[29] E.L. Plan, CPT: Pharmacometrics and Systems Pharmacology, 3(8), 129 (2014).

[30] A.J.P.L. Policarpo et al., NIM 118(1), 221–226 (1974).

[31] J. Seguinot, J. Tischhauser, and T. Ypsilantis NIM A 354(2–3), 280–287 (1995).

[32] K.F. Sellers, S. Borle, and G.Shmueli, Appl. Stoch. Models Bus. Ind. 28(2), 104 (2011).

[33] G. Shmueli et al., J. R. Stat. Soc. C 54(1), 127 (2004).

[34] J. Tiffenberg et al., Phys. Rev. Lett. 119(13), 131802 (2017).

[35] T. Zerguerras et al., NIM A 608(3), 397–402 (2009).

Extra Slides

COM-Poisson

Mean and variance

$$\mu = \frac{\partial log Z(\lambda,\nu)}{\partial log\lambda}$$
$$= \lambda\frac{\partial log Z(\lambda,\nu)}{\partial\lambda}$$
$$= \frac{\lambda}{Z(\lambda,\nu)}\frac{\partial Z(\lambda,\nu)}{\partial\lambda}$$
$$= \frac{\lambda}{Z(\lambda,\nu)}\frac{\partial}{\partial\lambda}\sum_{j=0}^{\infty}\frac{\lambda^j}{(j!)^\nu}$$
$$= \frac{\lambda}{Z(\lambda,\nu)}\sum_{j=0}^{\infty}\frac{j\lambda^{j-1}}{(j!)^\nu}$$
$$= \sum_{j=0}^{\infty}\frac{j\lambda^j}{(j!)^\nu Z(\lambda,\nu)}$$

$$\sigma^2 = \frac{\partial\mu(\lambda,\nu)}{\partial log\lambda} = \lambda\frac{\partial\mu(\lambda,\nu)}{\partial\lambda} = \lambda\frac{\partial}{\partial\lambda}\sum_{j=0}^{\infty}\frac{j\lambda^j}{(j!)^\nu Z(\lambda,\nu)}$$
$$= \lambda\left(Z^{-1}\sum_{j=0}^{\infty}\frac{j^2\lambda^{j-1}}{(j!)^\nu} - Z^{-2}\frac{\partial Z}{\partial\lambda}\sum_{j=0}^{\infty}\frac{j\lambda^j}{(j!)^\nu}\right)$$
$$= \sum_{j=0}^{\infty}\frac{j^2\lambda^j}{(j!)^\nu Z(\lambda,\nu)} - \lambda Z^{-2}\sum_{j=0}^{\infty}\frac{j\lambda^{j-1}}{(j!)^\nu}\sum_{j=0}^{\infty}\frac{j\lambda^j}{(j!)^\nu}$$
$$= \sum_{j=0}^{\infty}\frac{j^2\lambda^j}{(j!)^\nu Z(\lambda,\nu)} - \left(\sum_{j=0}^{\infty}\frac{j\lambda^j}{(j!)^\nu Z(\lambda,\nu)}\right)^2$$
$$= \sum_{j=0}^{\infty}\frac{j^2\lambda^j}{(j!)^\nu Z(\lambda,\nu)} - \mu(\lambda,\nu)^2$$

9

For COM-Poisson, there are asymptotic approximations already known:

$$\gamma_1 \approx \frac{1}{\sqrt{\nu}}\lambda^{-1/2\nu} + \mathcal{O}\left(\lambda^{-3/2\nu}\right) \quad \gamma_2 \approx \frac{1}{\nu}\lambda^{-1/\nu} + \mathcal{O}\left(\lambda^{-2\nu}\right)$$

As well as a recursive formula to calculate the higher distribution moments very easily:

$$E\left(X^{n+1}\right) = \lambda\frac{\partial}{\partial\lambda}E\left(X^n\right) + E\left(X\right)E\left(X^n\right), \quad \text{for } n \geq 1$$

To prove that this is true for COM-Poisson, take a grid of points in λ and ν,

Then map those points to the mean and variance plane

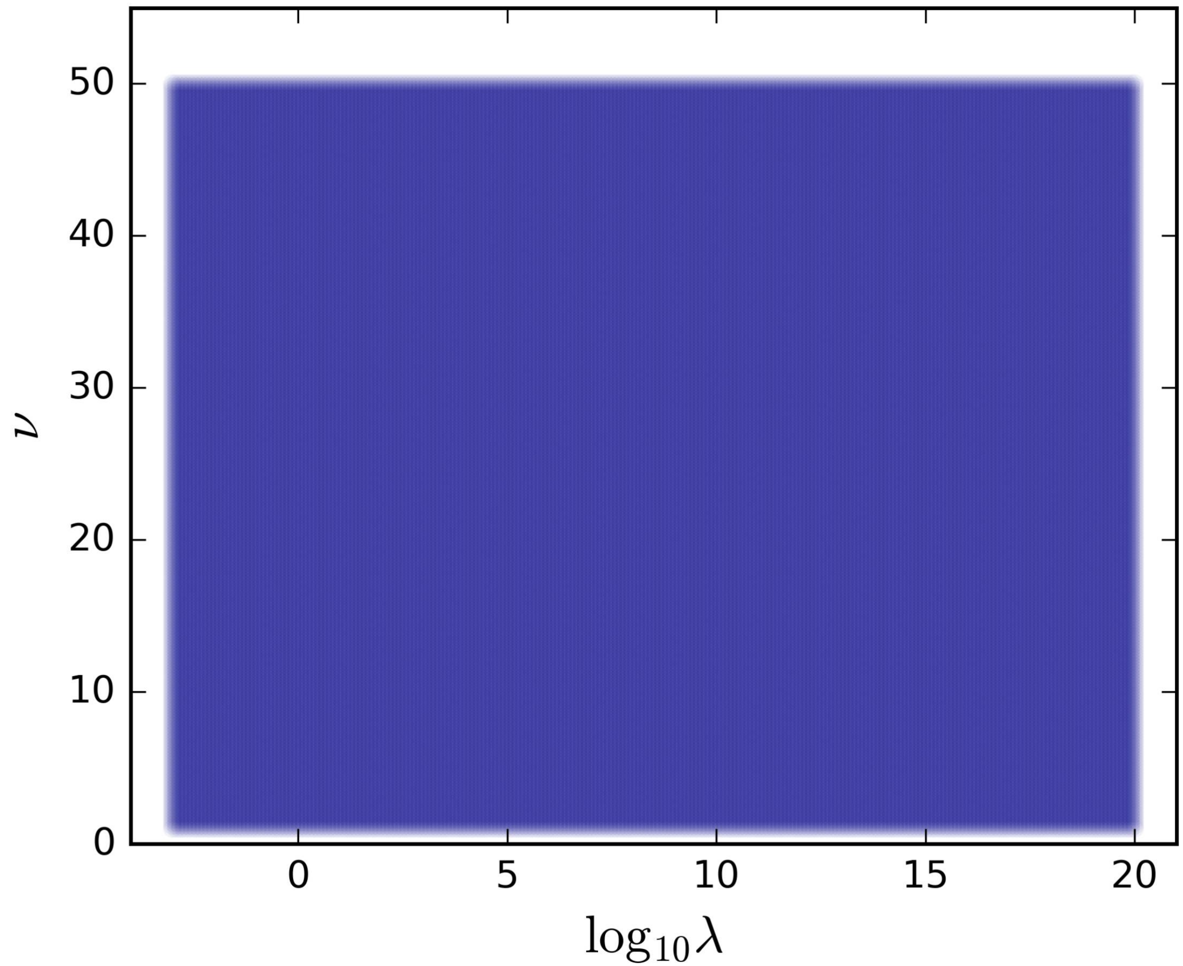

To prove that this is true for COM-Poisson, take a grid of points in λ and ν,

Then map those points to the mean and variance plane

The Bernoulli modes appear!

You cannot go into this forbidden parameter space!

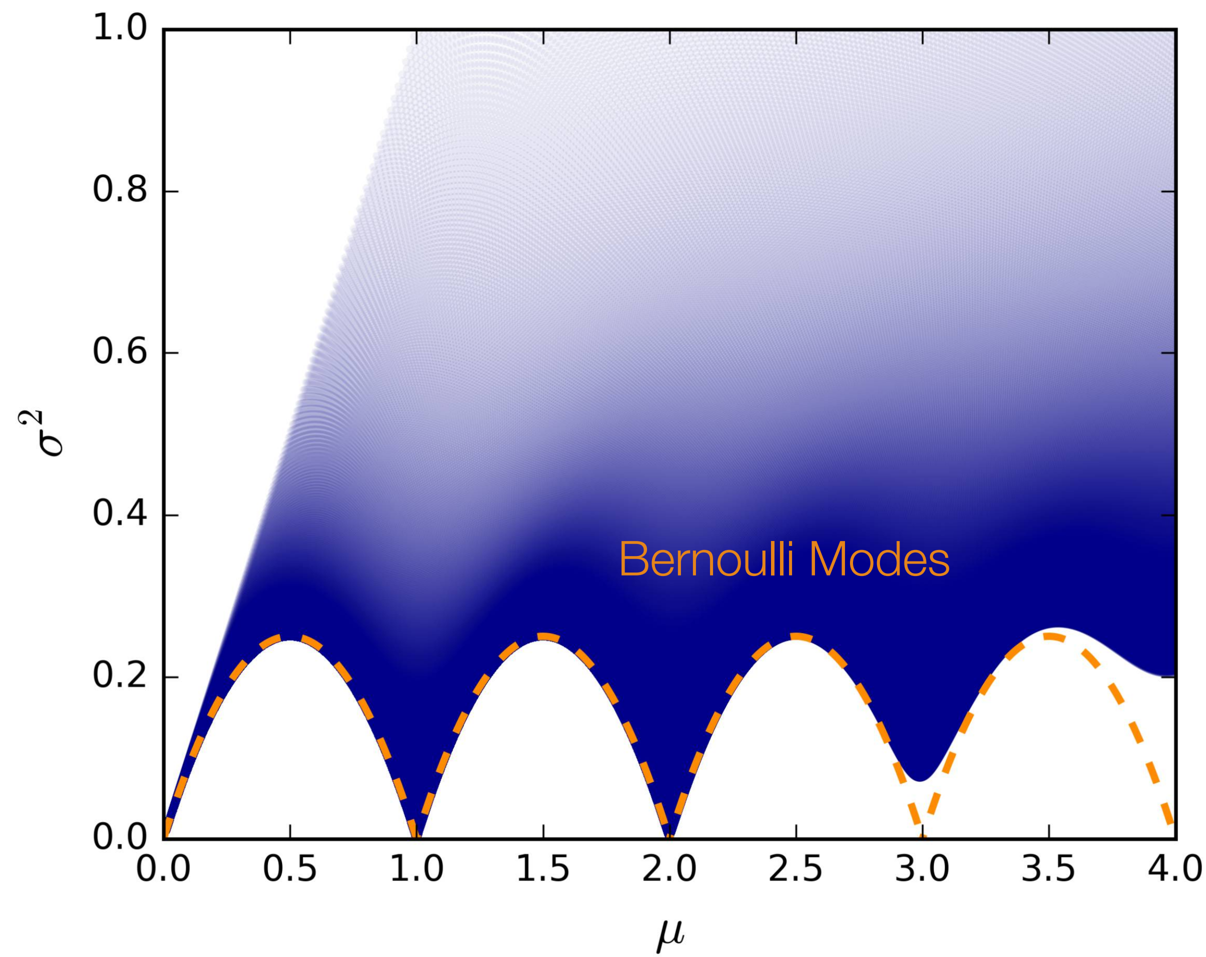

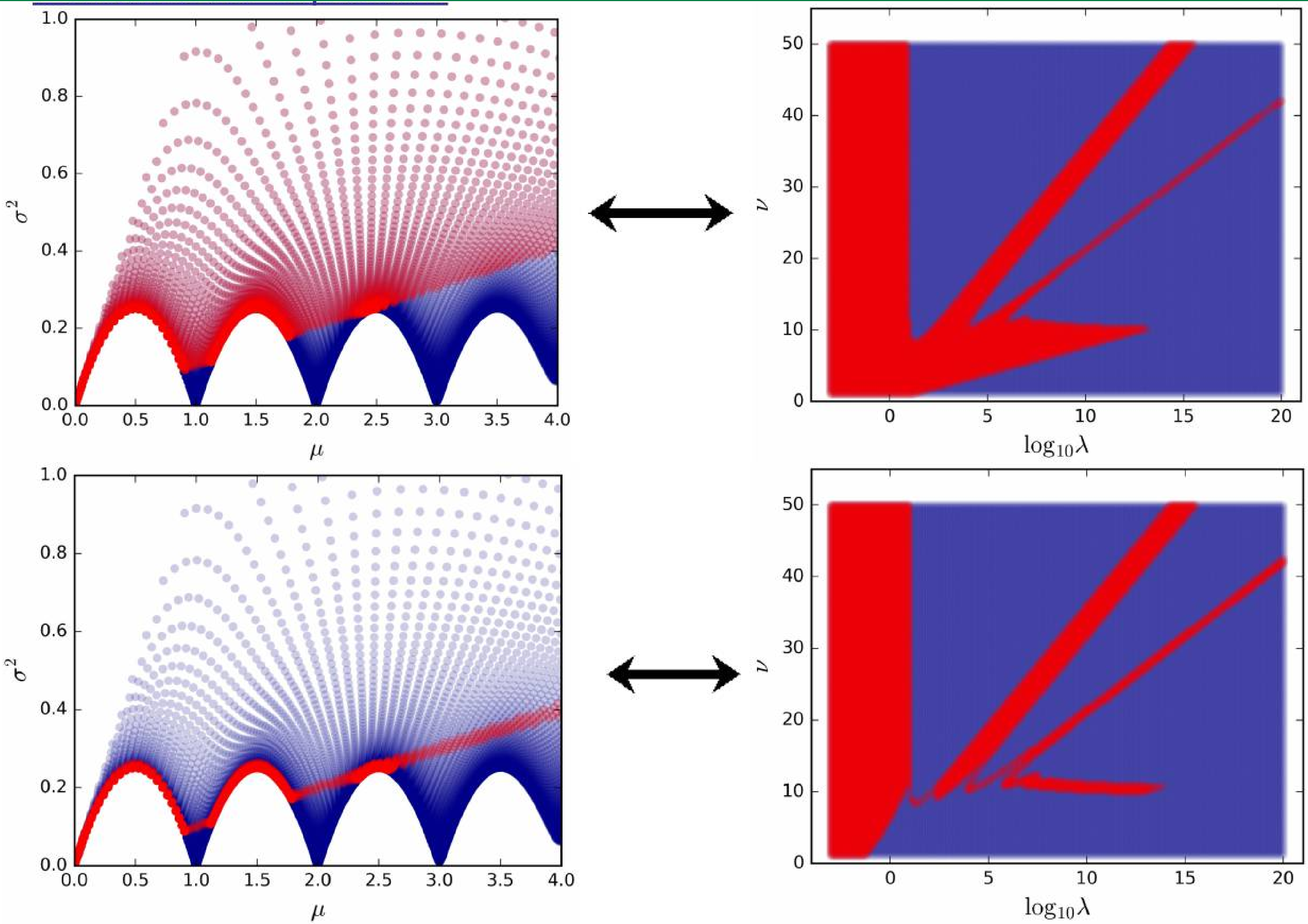
σ^2
μ
ν
$\log_{10}\lambda$
σ^2
μ
ν
$\log_{10}\lambda$

Asymptotic regime

At larger values of mean, there is an asymptotic formula that gives us a closed form expression for the mean and variance! No need to use the minimization algorithm here!

$$Z_2 = \frac{e^{\nu\lambda^{1/\nu}}}{\lambda^{\frac{\nu-1}{2\nu}}(2\pi)^{\frac{\nu-1}{2}}\sqrt{\nu}}\left(1+\mathcal{O}\left(\lambda^{-1/\nu}\right)\right)$$

$$\mu \approx \lambda^{1/\nu} - \frac{\nu-1}{2\nu} \qquad \sigma^2 \approx \frac{1}{\nu}\lambda^{1/\nu}$$

$$\lambda(\mu, F) \approx (\nu\mu F)^{\nu}$$

$$\nu(\mu, F) \approx \frac{2\mu + 1 + \sqrt{4\mu^2 + 4\mu + 1 - 8\mu F}}{4\mu F}$$

Asymptotic regime

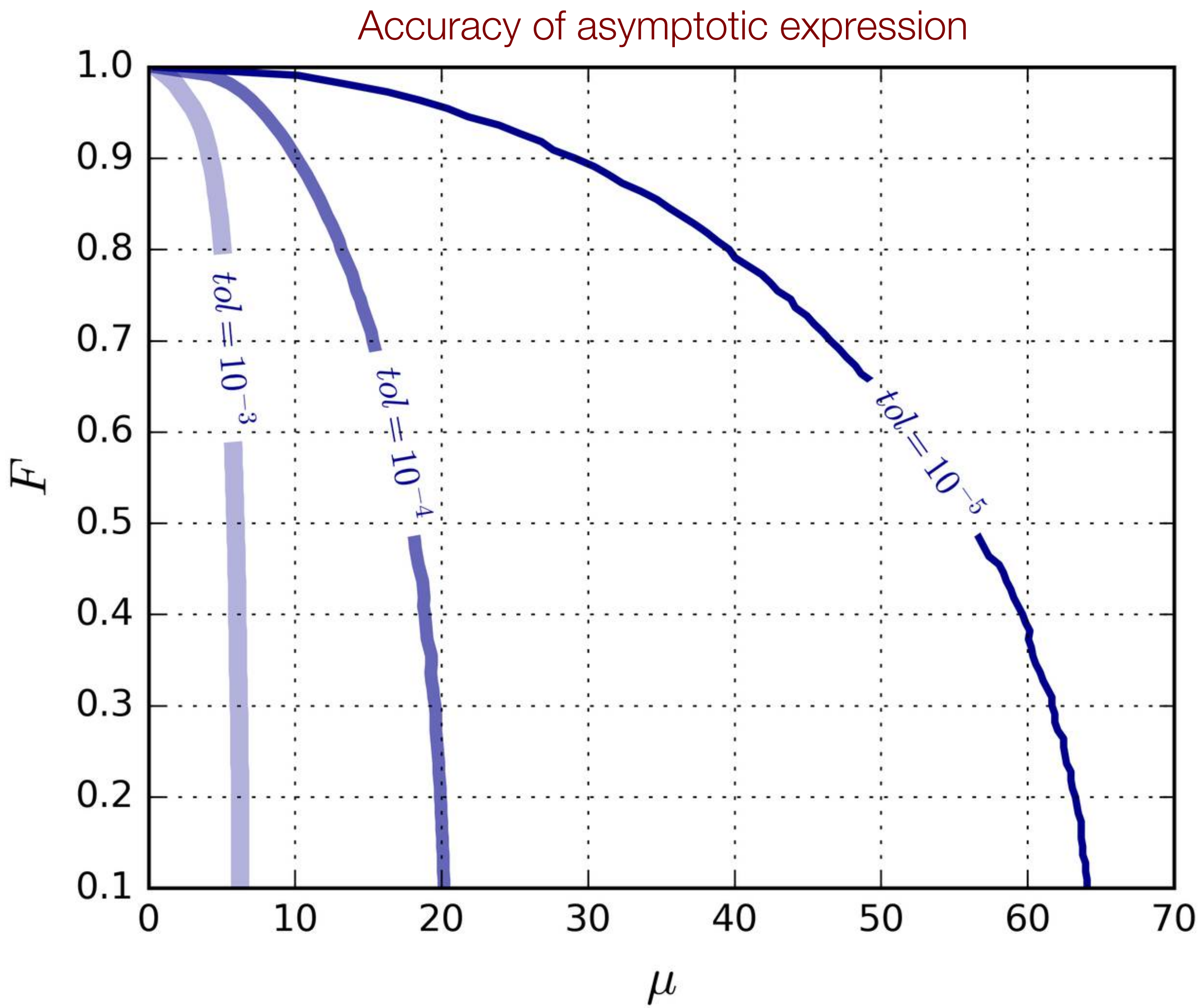

Nominally this approximation is valid when:

$$\lambda > 10^{\nu}$$

For us, it is valid to accuracy of 10^{-4} for all F above a μ of 20

Design of Table

The goal is to guarantee accuracy to within a given distance of the Bernoulli modes

We linearly interpolate points, so we have to guarantee that linear interpolation is good to given distance from Bernoulli modes

Therefore we have to have some points within given distance of Bernoulli modes

Table point density such that each time a F-line crosses a Bernoulli mode, it is bounded by points within D = 0.1% of Bernoulli mode

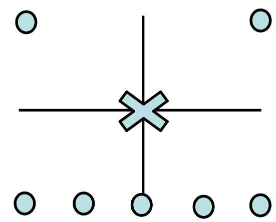

If any within Bernoulli mode and not, then "point within D of Bernoulli mode"

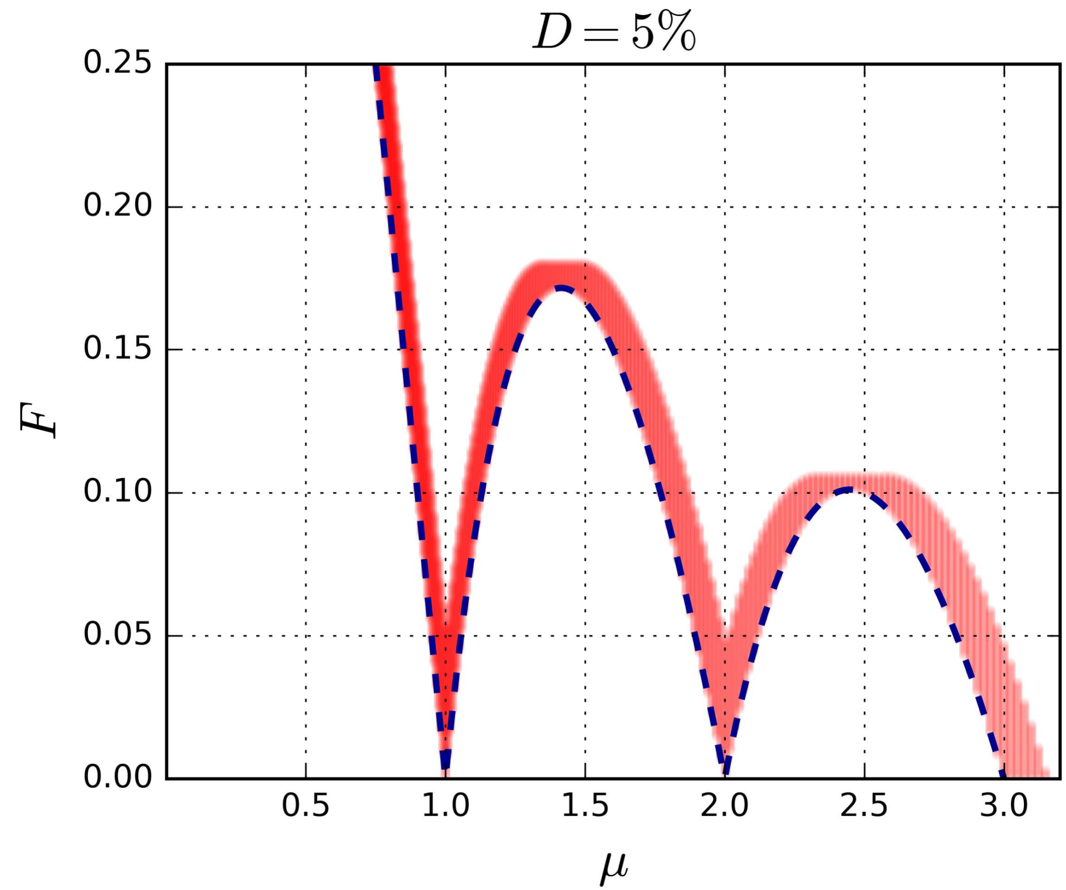

Look-up tables

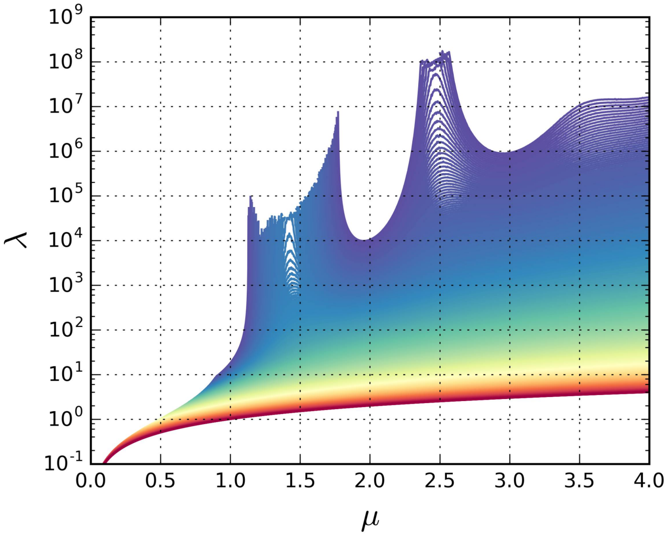

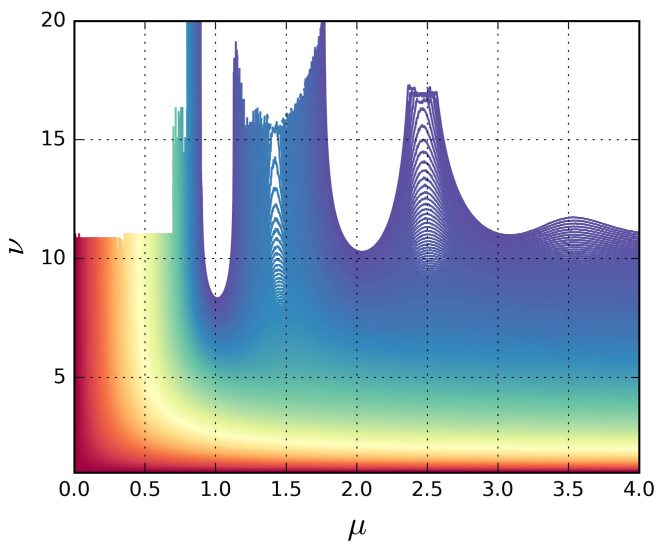

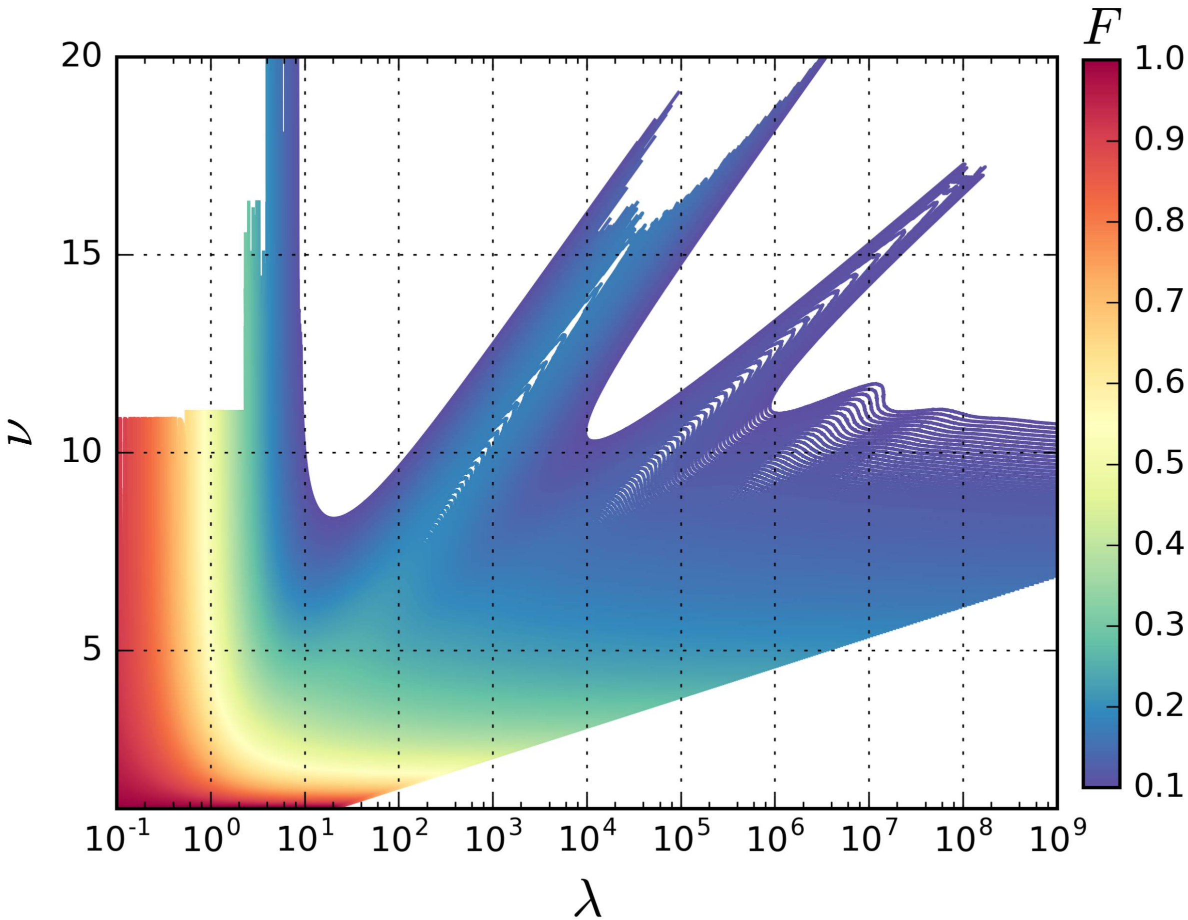

Accuracy of Look-up tables

Test done by choosing N random points in μ/F space, calculating resulting error using COM-Poisson code.

The look-up tables were iteratively corrected to ensure < 0.1% precision

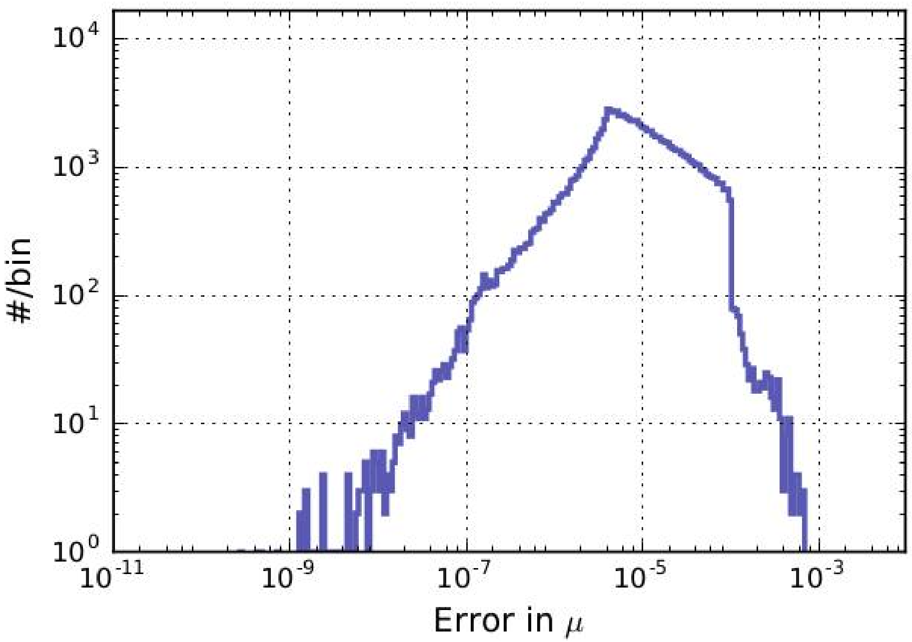

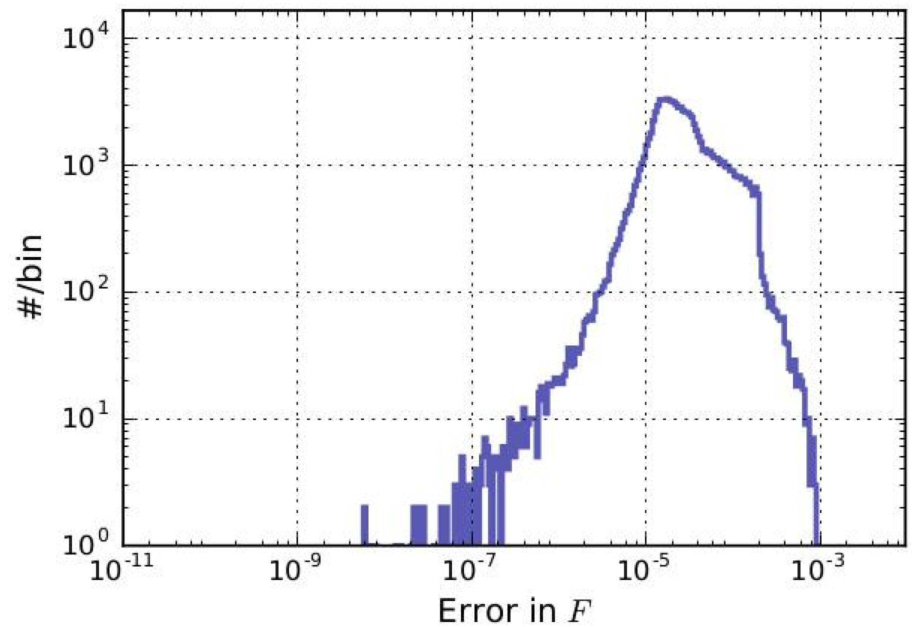

Fitting theoretical ionization distributions

No goodness of fit performed, but apparent agreement with simulated ionization distributions.

In the future, it could be tested against modern simulation packages (i.e. Garfield++)

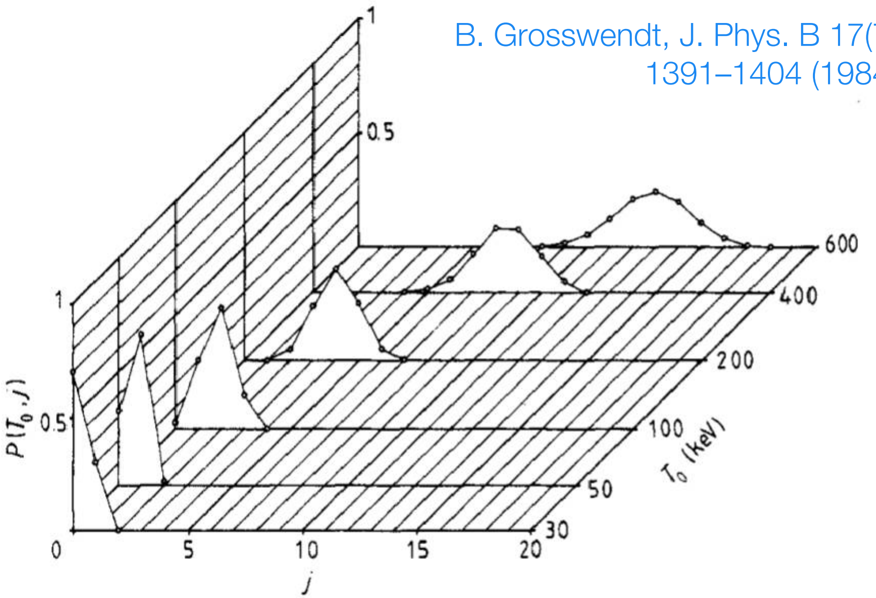

B. Grosswendt, J. Phys. B 17(7), 1391–1404 (1984).

Figure 4. Three-dimensional plot of the probability $P(T_0, j)$ that exact-j ionisations are produced upon the complete slowing down of electrons of initial energy T_0 in He.

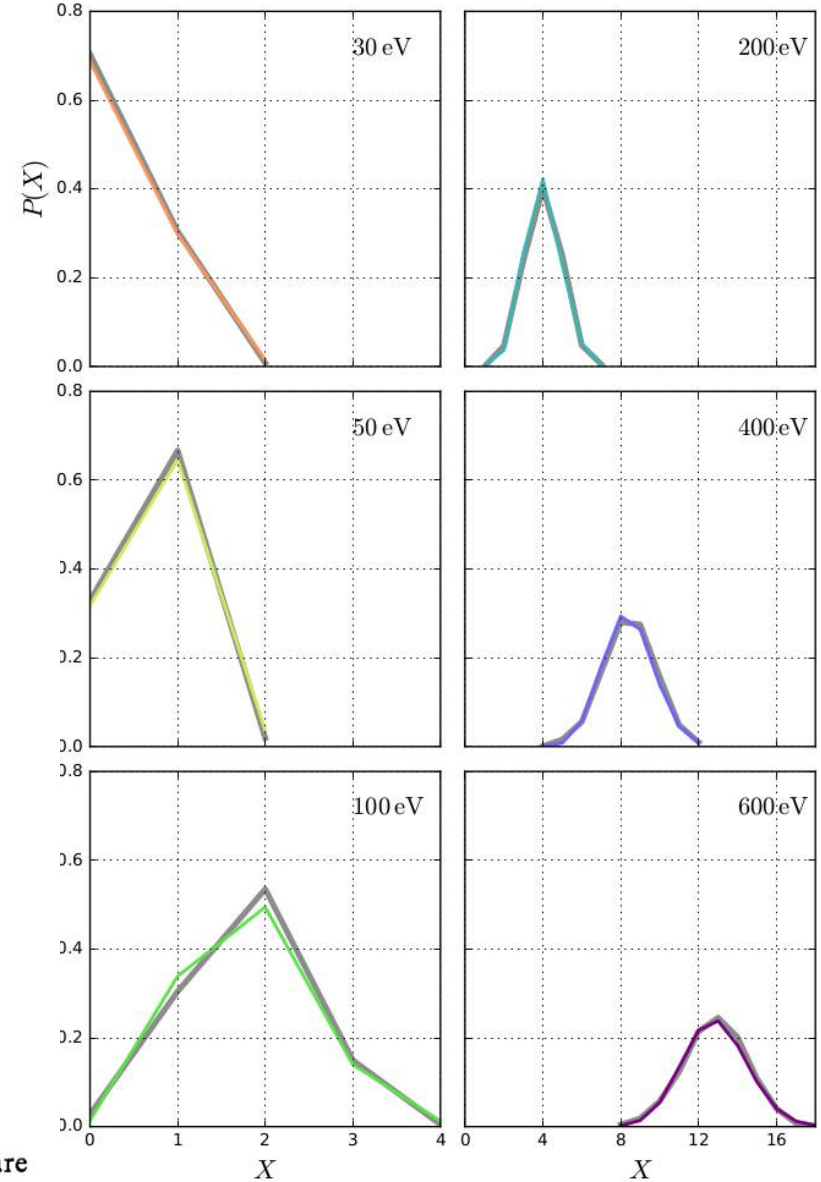

The size of the impact of F as a systematic can be understood intuitively by considering the signal acceptance near an energy threshold:

» At the single ionization/Bernoulli regime, allowed values of F converge, so the impact is small (i.e. low WIMP mass, low threshold)
» F will have a greater impact on signal acceptance if it dominates overall resolution
» At high WIMP mass, signal acceptance is ~ 1

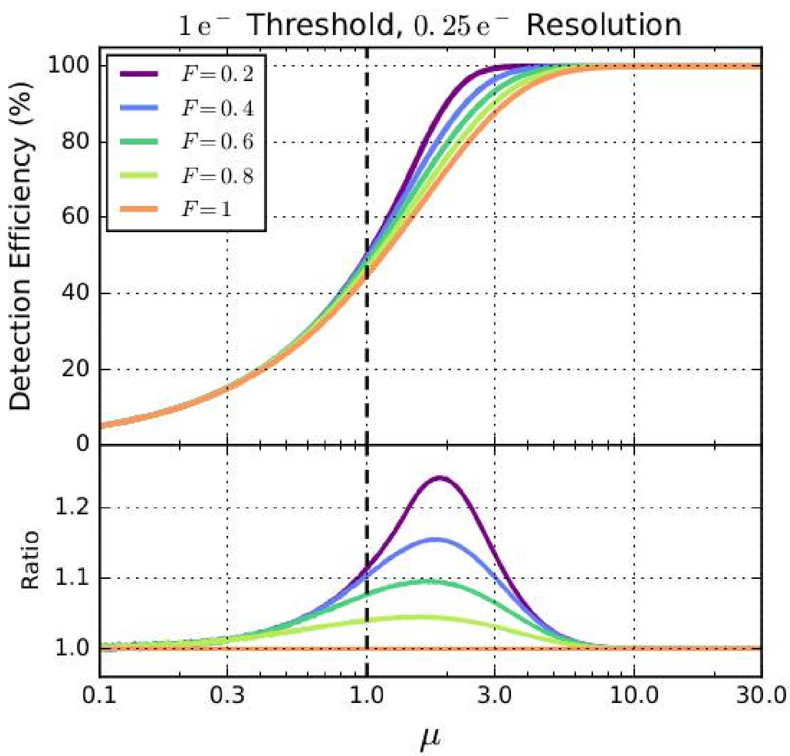

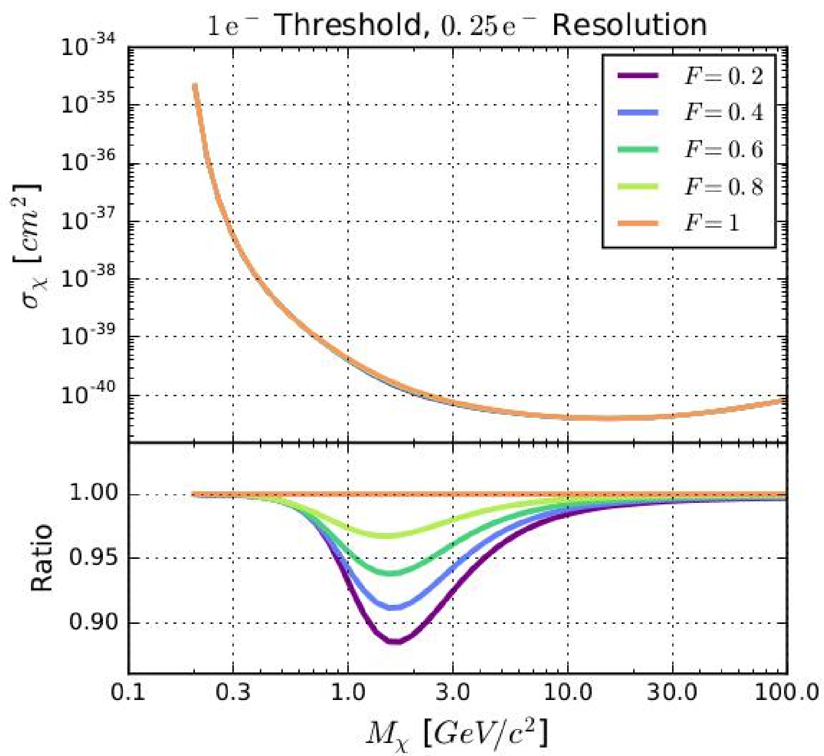

The size of the impact of F as a systematic can be understood intuitively by considering the signal acceptance near an energy threshold:

» At the single ionization/Bernoulli regime, allowed values of F converge, so the impact is small (i.e. low WIMP mass, low threshold)
» F will have a greater impact on signal acceptance if it dominates overall resolution
» At high WIMP mass, signal acceptance is ~ 1

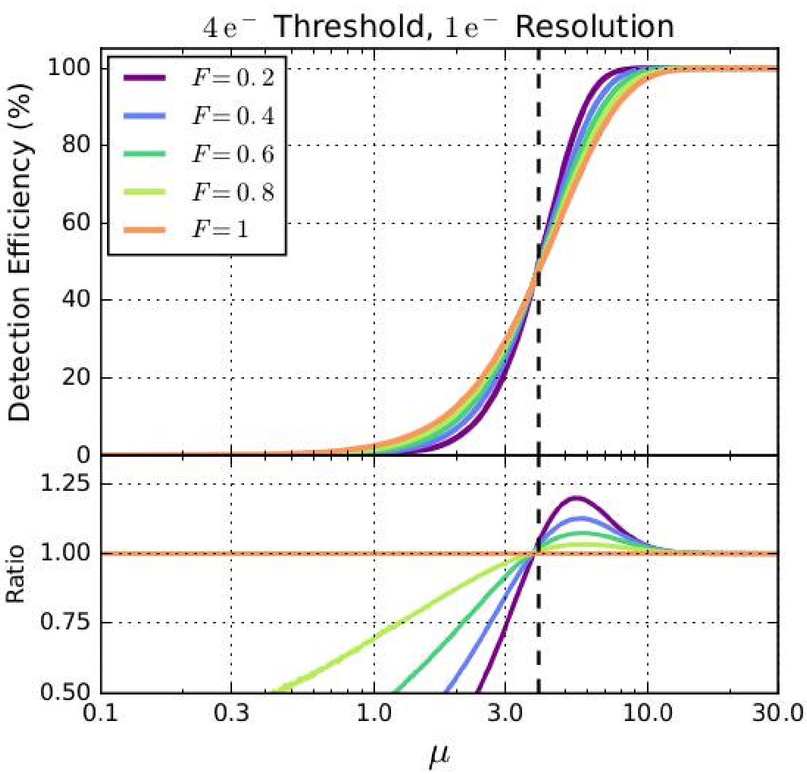

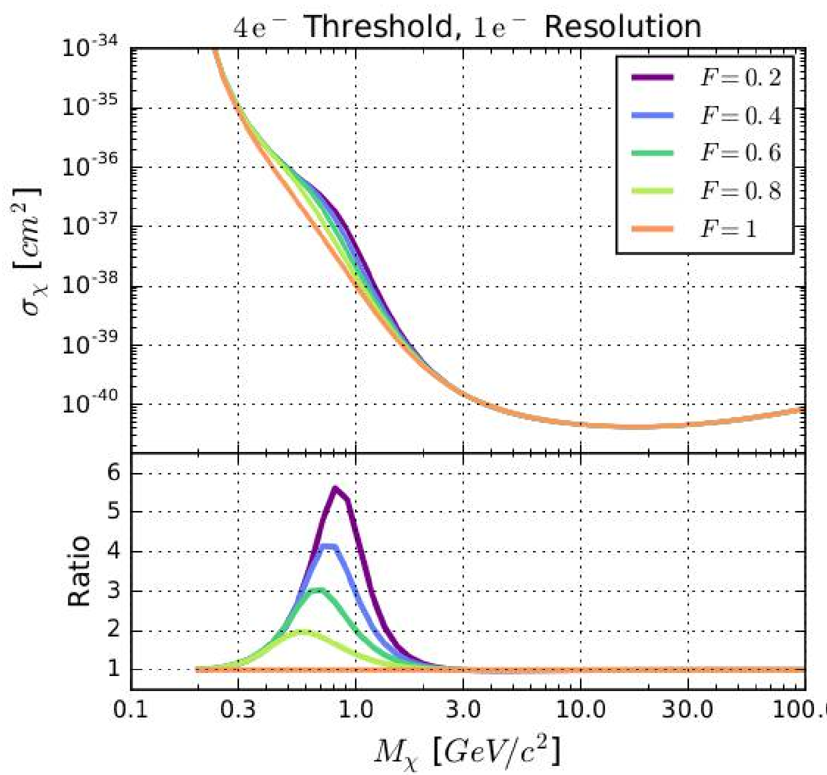

The size of the impact of F as a systematic can be understood intuitively by considering the signal acceptance near an energy threshold:

» At the single ionization/Bernoulli regime, allowed values of F converge, so the impact is small (i.e. low WIMP mass, low threshold)
» F will have a greater impact on signal acceptance if it dominates overall resolution
» At high WIMP mass, signal acceptance is ~ 1

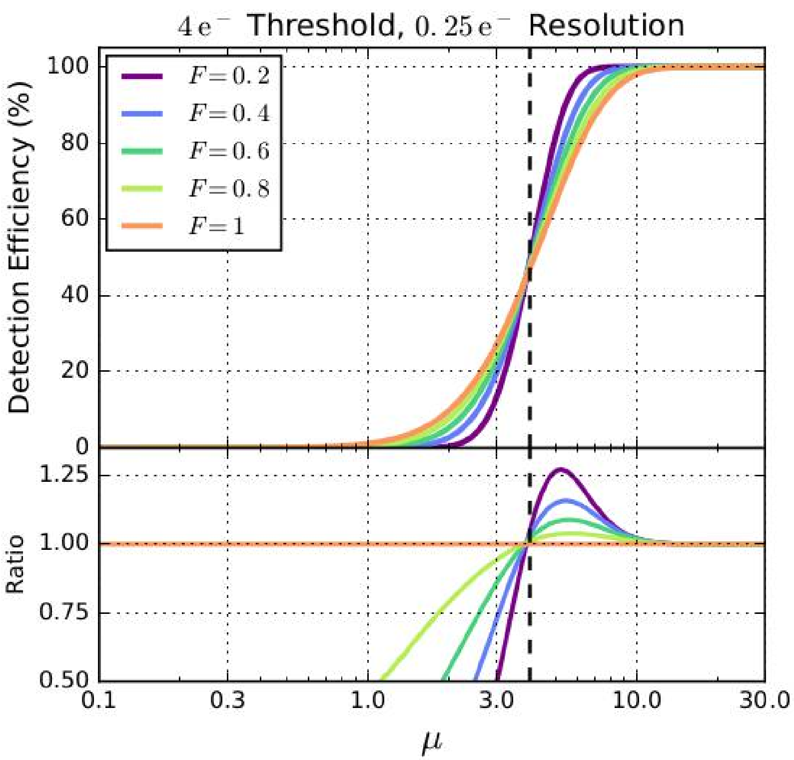

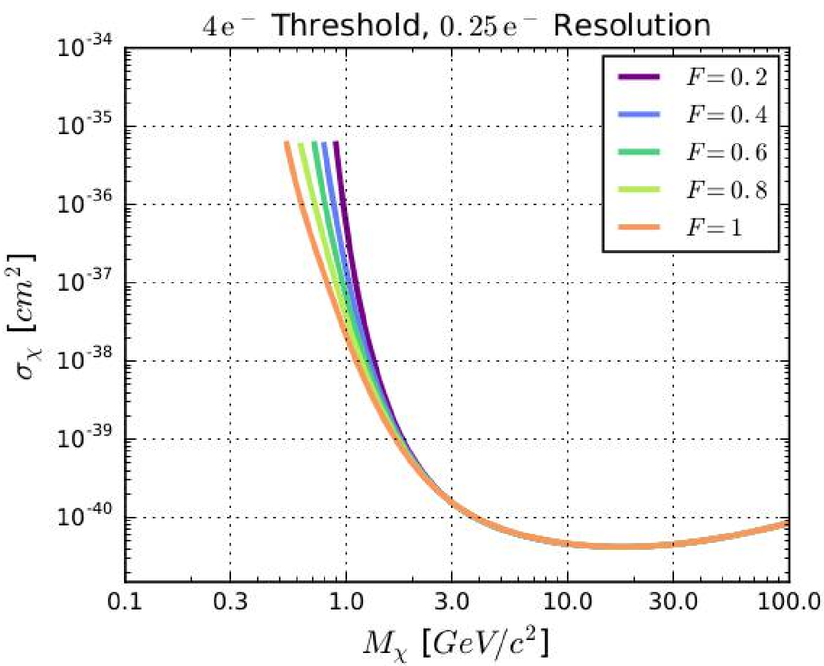

Ionization statistics models

A weighted sum of 2 binomial distributions:

For the binomial distribution:

$$\mu = np(1-p) \qquad F = 1-p$$

Define parameters fir two nearest binomial distributions:

$$n_l = \left\lfloor \frac{\mu}{1-F} \right\rfloor \qquad n_u = \left\lceil \frac{\mu}{1-F} \right\rceil$$

$$F_l = 1 - \frac{\mu}{n_l} \qquad F_u = 1 - \frac{\mu}{n_u}$$

Add weighted according to distance between desired F and possible binomials:

$$P_l\left(x|\mu, F\right) = P_{\text{Binom}}\left(x|n_l, 1-F_l\right)$$
$$P_u\left(x|\mu, F\right) = P_{\text{Binom}}\left(x|n_u, 1-F_u\right)$$

$$\Delta F = \frac{F - F_l}{F_u - F_l}$$

$$\mathcal{P}\left(x|\mu, F\right) = (1-\Delta F)P_l\left(x|\mu, F\right) + (\Delta F)P_u\left(x|\mu, F\right)$$

WDB Model

WDB equations:

$$\mathcal{P}\left(x|\mu,F\right)=(1-\Delta F)P_l\left(x|\mu,F\right)+(\Delta F)P_u\left(x|\mu,F\right) \qquad \Delta F=\frac{F-F_l}{F_u-F_l}$$

$$\begin{aligned}
\mu_{\mathrm{WDB}} &= E\left(X\right)\\
&=\sum_{i=0}^{\infty}P_{\mathrm{WDB}}\left(X_i\right)X_i\\
&=\sum_{i=0}^{\infty}\left[\left(1-\Delta F\right)P_l\left(X_i\right)+\Delta F P_u\left(X_i\right)\right]X_i\\
&=\left(1-\Delta F\right)\sum_{i=0}^{\infty}P_l\left(X_i\right)X_i+\Delta F\sum_{i=0}^{\infty}P_u\left(X_i\right)X_i\\
&=\left(1-\Delta F\right)\mu_l+\Delta F\mu_u\\
&=\left(1-\Delta F\right)n_lp_l+\Delta F n_up_u\\
&=\left(1-\Delta F\right)n_l\frac{\mu}{n_l}+\Delta F n_u\frac{\mu}{n_u}\\
&=\left(1-\Delta F\right)\mu+\Delta F\mu\\
&=\boxed{\mu}
\end{aligned}$$

$$\begin{aligned}
\sigma^2_{\mathrm{WDB}} &= E\left(X^2\right)-\mu^2\\
&=\sum_{i=0}^{\infty}P_{\mathrm{WDB}}\left(X_i\right)X_i^2-\mu^2\\
&=\sum_{i=0}^{\infty}\left[\left(1-\Delta F\right)P_l\left(X_i\right)+\Delta F P_u\left(X_i\right)\right]X_i^2-\mu^2\\
&=\left(1-\Delta F\right)\sum_{i=0}^{\infty}P_l\left(X_i\right)X_i^2+\Delta F\sum_{i=0}^{\infty}P_u\left(X_i\right)X_i^2-\mu^2\\
&=\left(1-\Delta F\right)\left(\sigma_l^2+\mu^2\right)+\Delta F\left(\sigma_u^2+\mu^2\right)-\mu^2\\
&=\left(1-\Delta F\right)\left(n_lp_l\left(1-p_l\right)+\mu^2\right)+\Delta F\left(n_up_u\left(1-p_u\right)+\mu^2\right)-\mu^2\\
&=\left(1-\Delta F\right)\left(\mu F_l+\mu^2\right)+\Delta F\left(\mu F_u+\mu^2\right)-\mu^2\\
\implies F_{\mathrm{WDB}} &=\left(1-\Delta F\right)\left(F_l+\mu\right)+\Delta F\left(F_u+\mu\right)-\mu\\
&=\left(1-\frac{F-F_l}{F_u-F_l}\right)\left(F_l+\mu\right)+\left(\frac{F-F_l}{F_u-F_l}\right)\left(F_u+\mu\right)-\mu\\
&=\frac{F_u-F}{F_u-F_l}\left(F_l+\mu\right)+\frac{FF_u-\mu F_l+\mu F-F_lF_u}{F_u-F_l}-\mu\\
&=\frac{\left(F_u-F_l\right)\left(F+\mu\right)}{F_u-F_l}-\mu\\
&=\boxed{F}
\end{aligned}$$

You get the correct μ and F by construction, wherever WDB (ΔF) is defined

Comparing skewness and kurtosis - WDB

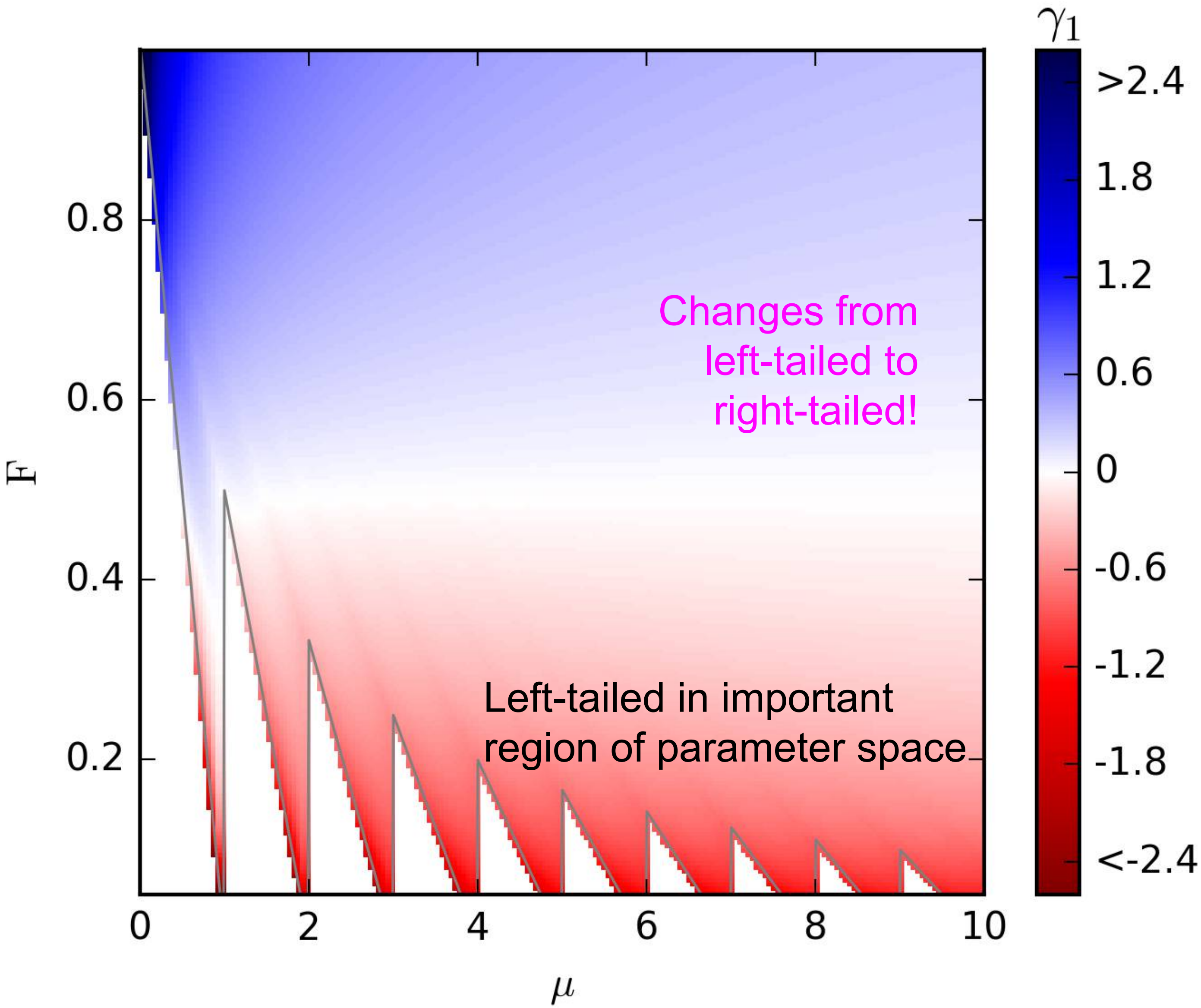

Comparing skewness and kurtosis - COM Poisson

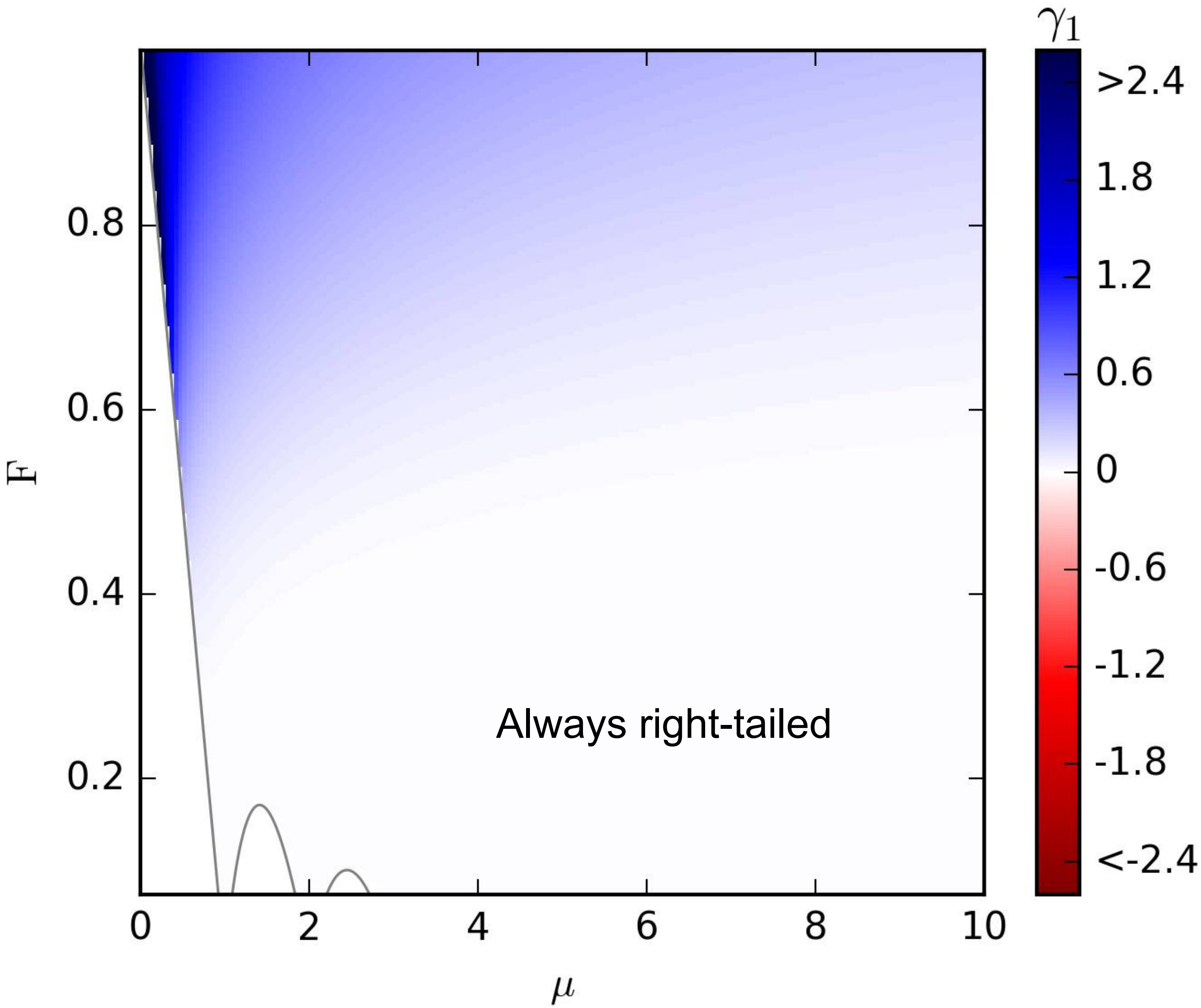

Comparing skewness and kurtosis - WDB

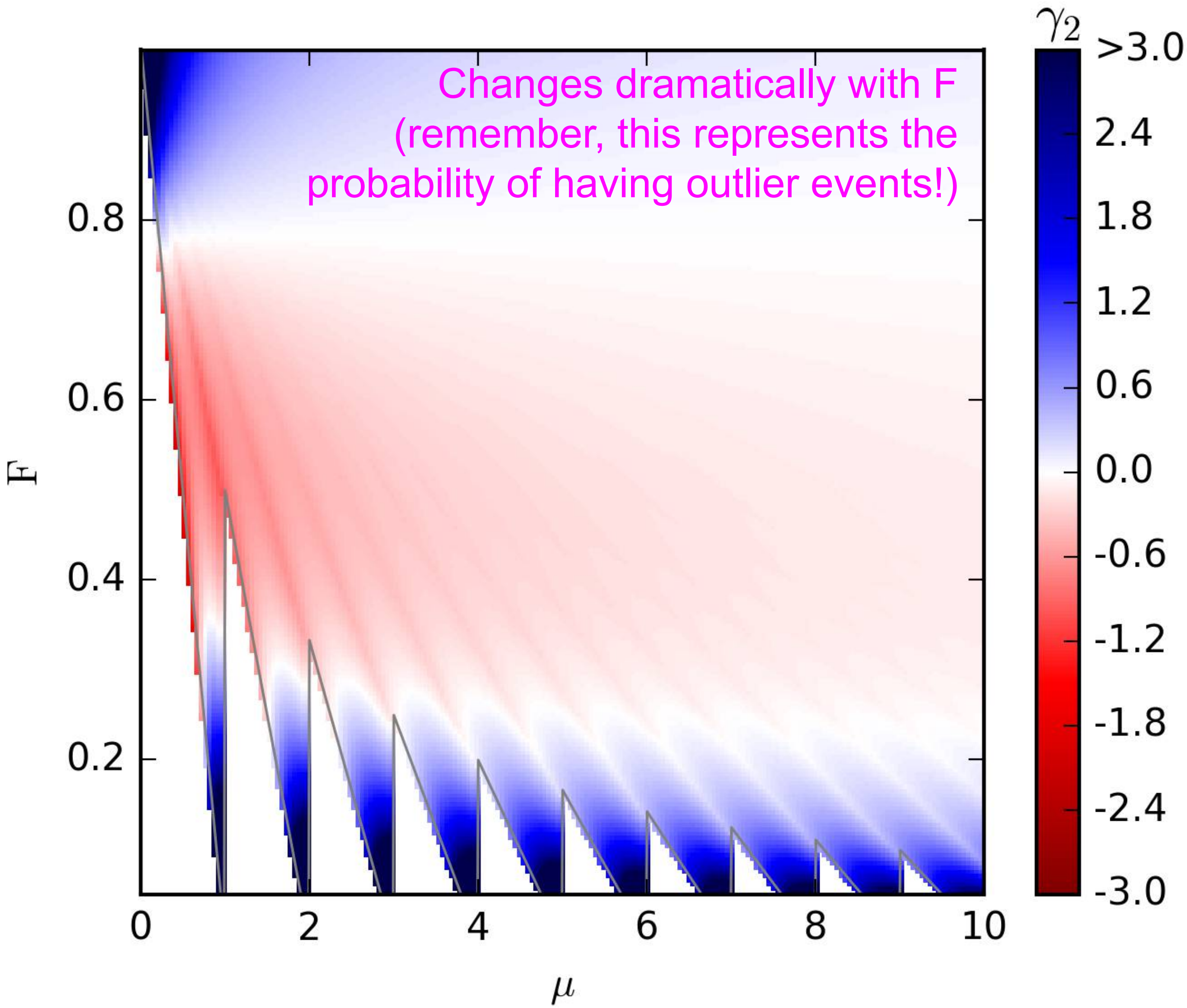

Comparing skewness and kurtosis - COM Poisson

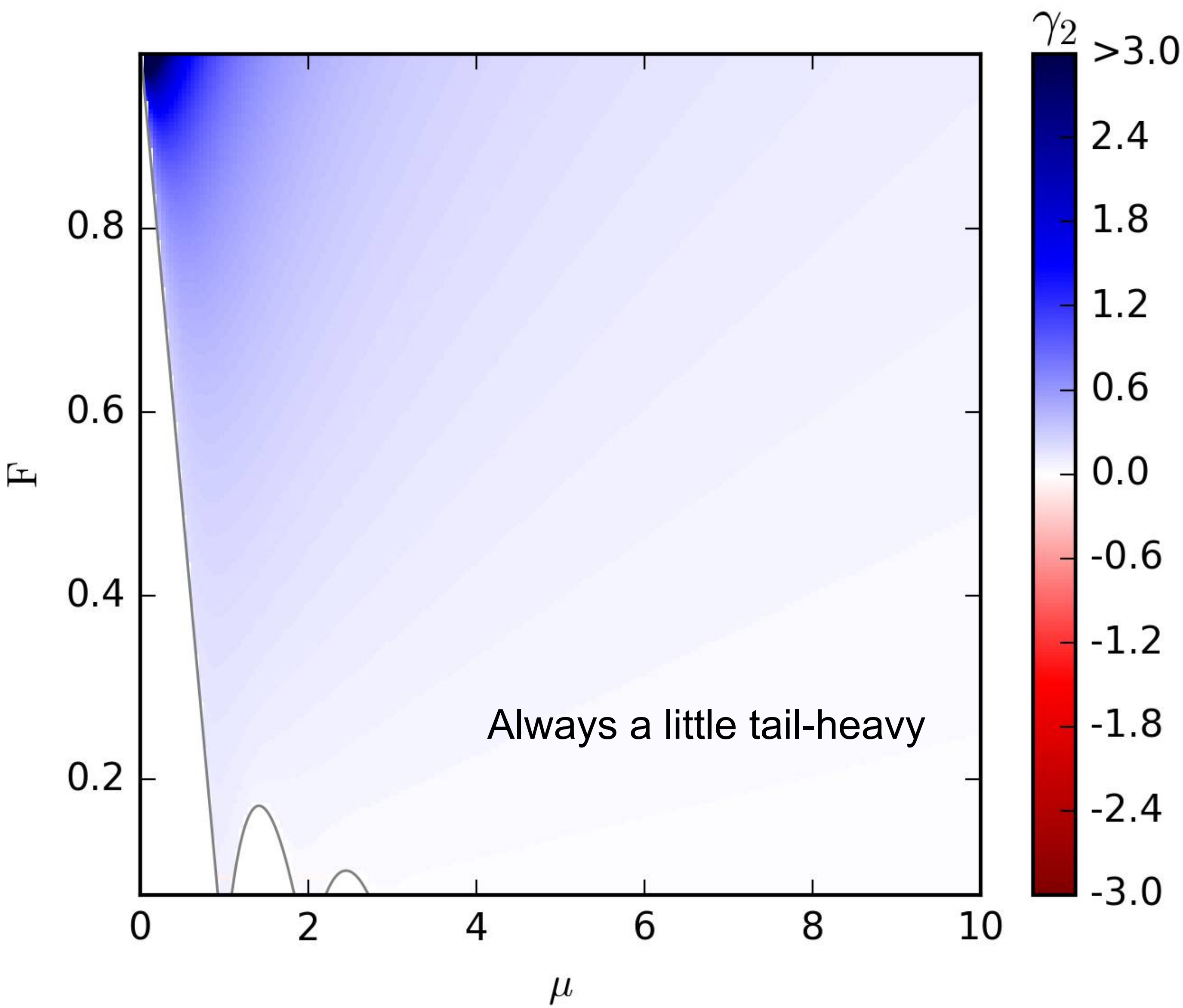

UV Laser Calibration

Laser power fluctuations

The laser power varies $O(10\%)$ from pulse to pulse

We deal with this problem by dividing data into subsets with fixed photo-detector amplitude ±5%

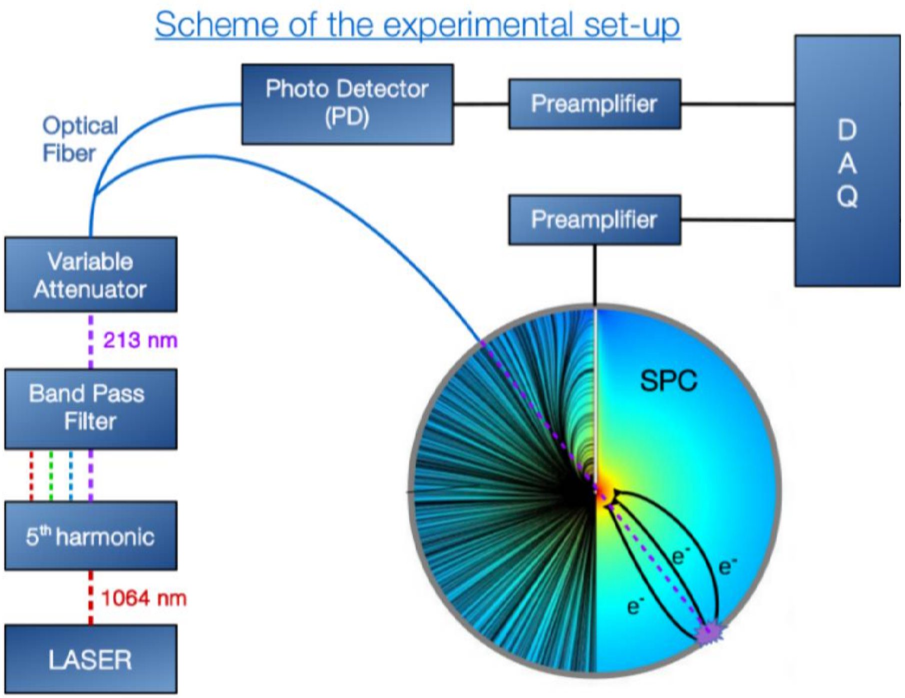

~10% dispersion in laser pulse size

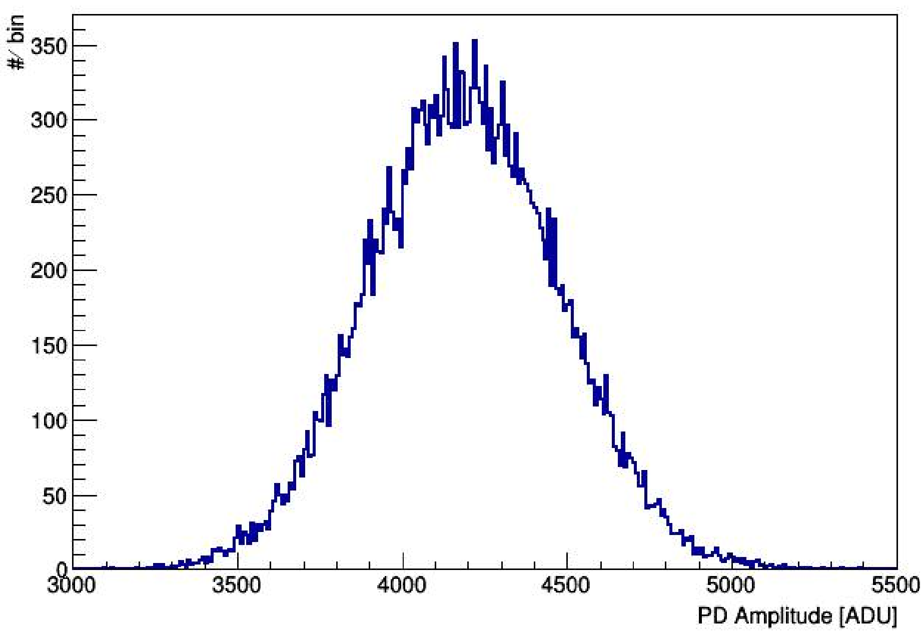

Laser power fluctuations

The laser power varies O(10%) from pulse to pulse

We deal with this problem by dividing data into subsets with fixed photo-detector amplitude ±5%

We disentangle the photo-detector resolution from laser power fluctuations by testing against a second photo-detector

[Scheme of the experimental set-up](#)

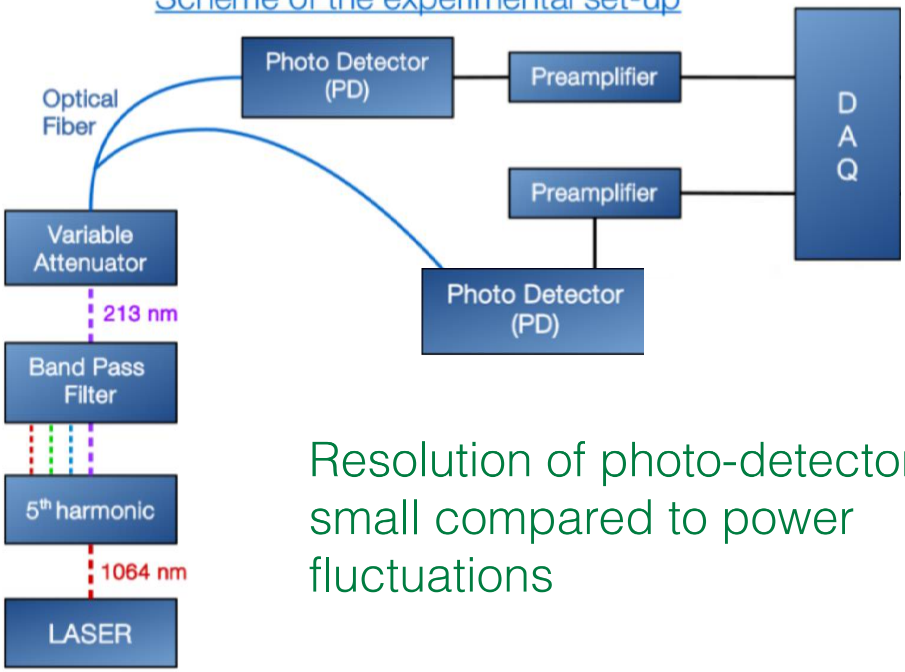

Resolution of photo-detector is small compared to power fluctuations

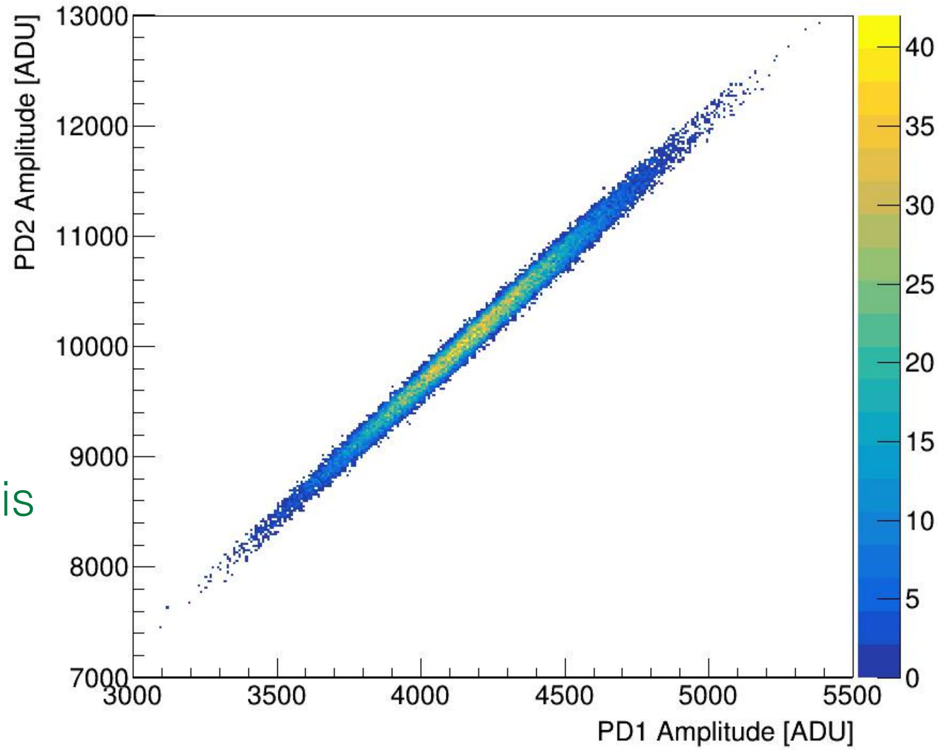

Data with varying laser intensity

This allows for combined fitting of data subsets, as well as data with different laser intensities:

Individual Fits | **Joint Fits**

The expected # of PE varies linearly with laser intensity

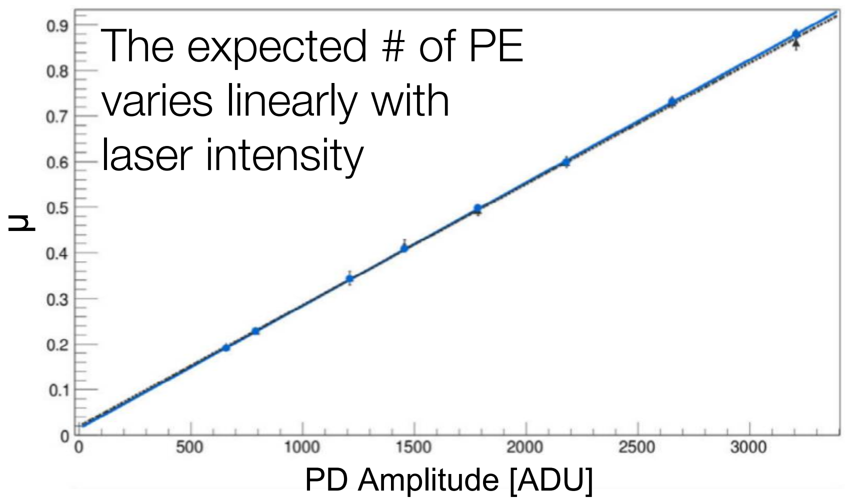

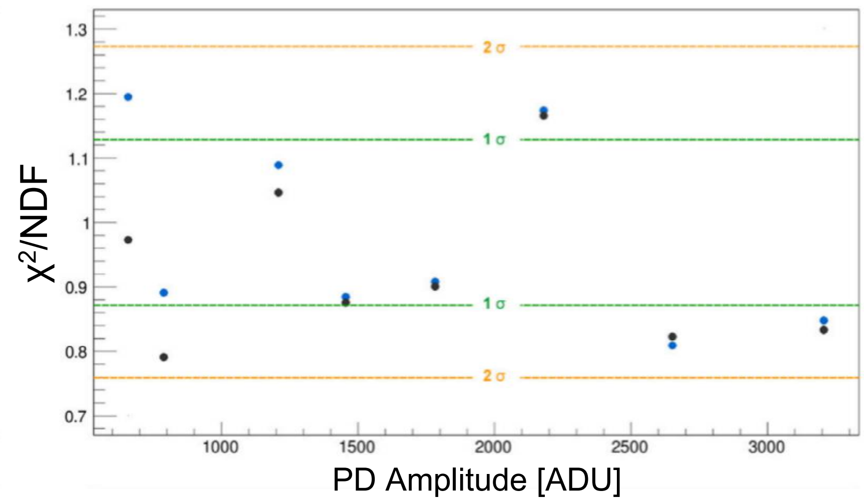

Single and joint fits are in agreement

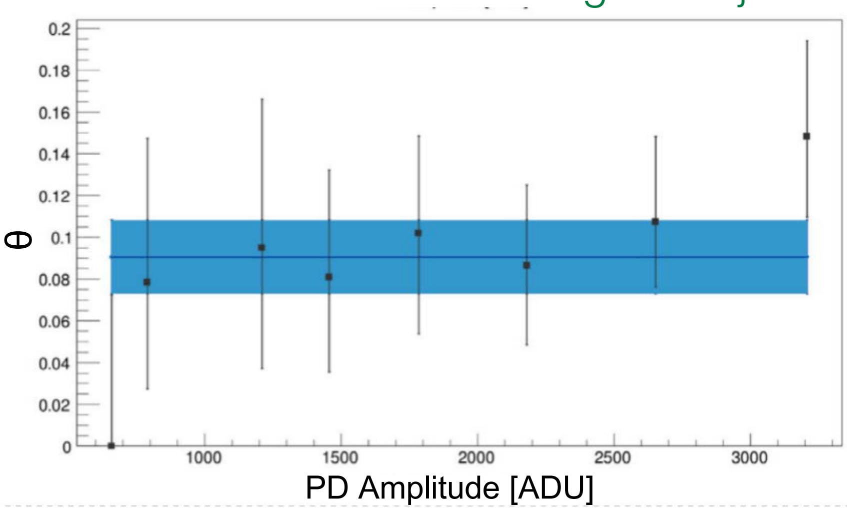

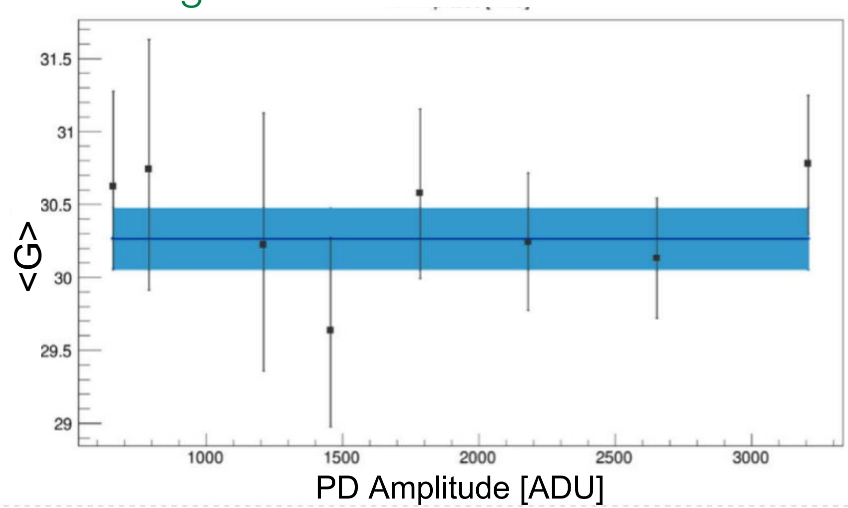

Q. Arnaud et al. (NEWS-G), Phys. Rev. D 99, 102003 (2019)

Trigger efficiency

The laser can be used to directly measure the efficiency of our triggering algorithm

Method 1:
SPC-triggered spectrum divided by photo-detector triggered spectrum (this does not account for null laser events)

Method 2:
Fit total spectrum (0 PE + > 0 PE events), then fit > 0 PE spectrum multiplied by error function with <G>, θ, and σ fixed.

Demonstration of ~10 eV energy threshold: 16 eV in this example

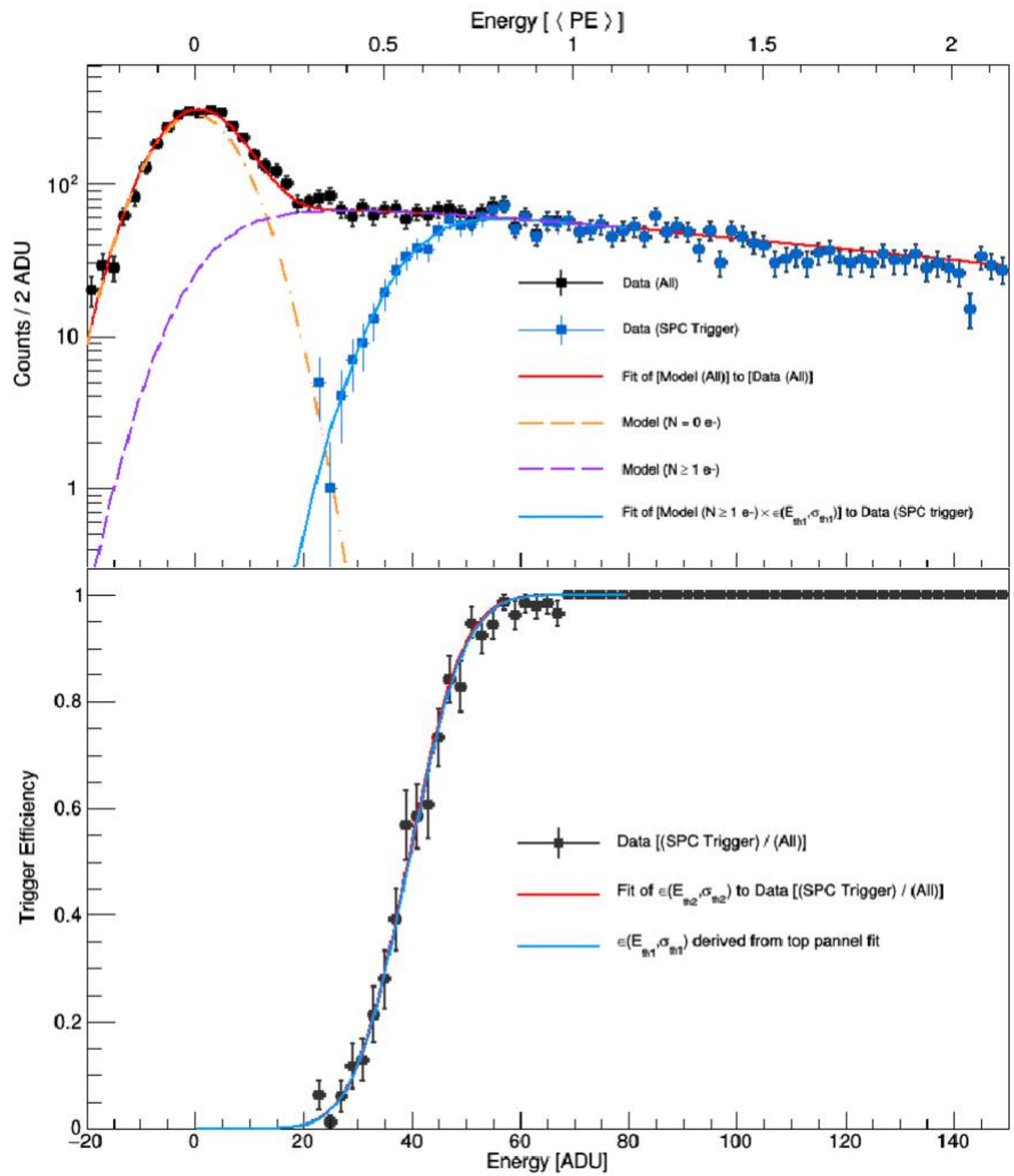

Q. Arnaud et al. (NEWS-G), Phys. Rev. D 99, 102003 (2019)

Detector monitoring

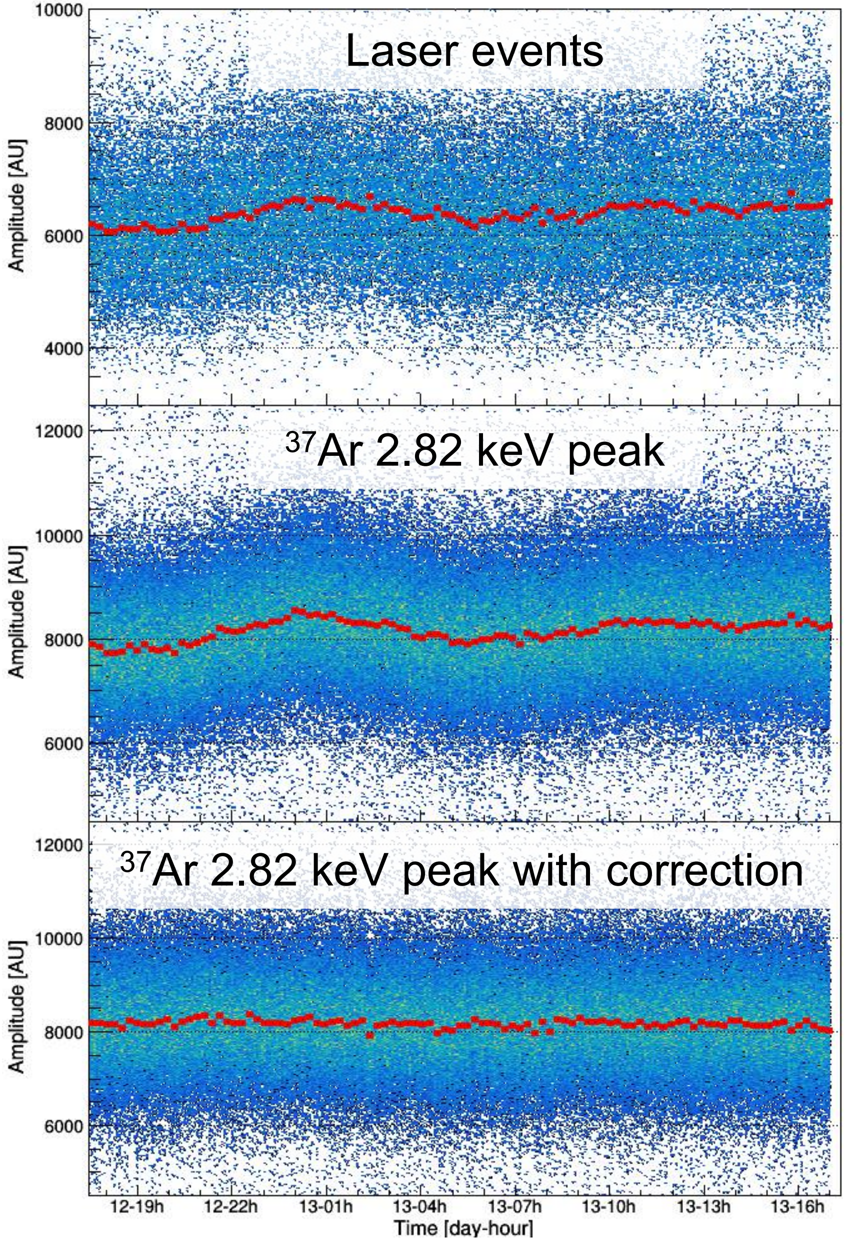

The laser can be used to monitor the detector response during physics runs

Long-term fluctuations in gain can be caused by temperature changes, O_2 contamination, sensor damage...

Laser monitoring data could even be used to correct for long-term fluctuations

Q. Arnaud et al. (NEWS-G), Phys. Rev. D 99, 102003 (2019)

NEWS-G

First results from NEWS-G

Competitive low-mass WIMP limit with a neon target at the Laboratoire Souterrain de Modane

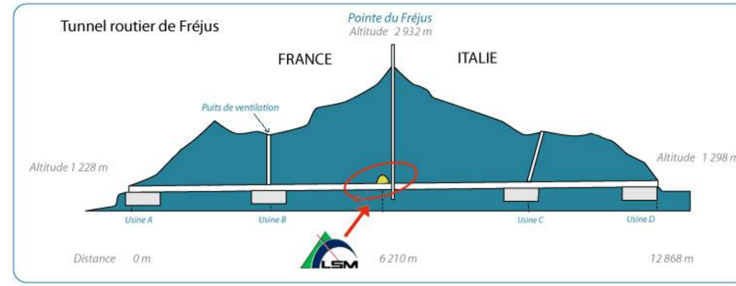

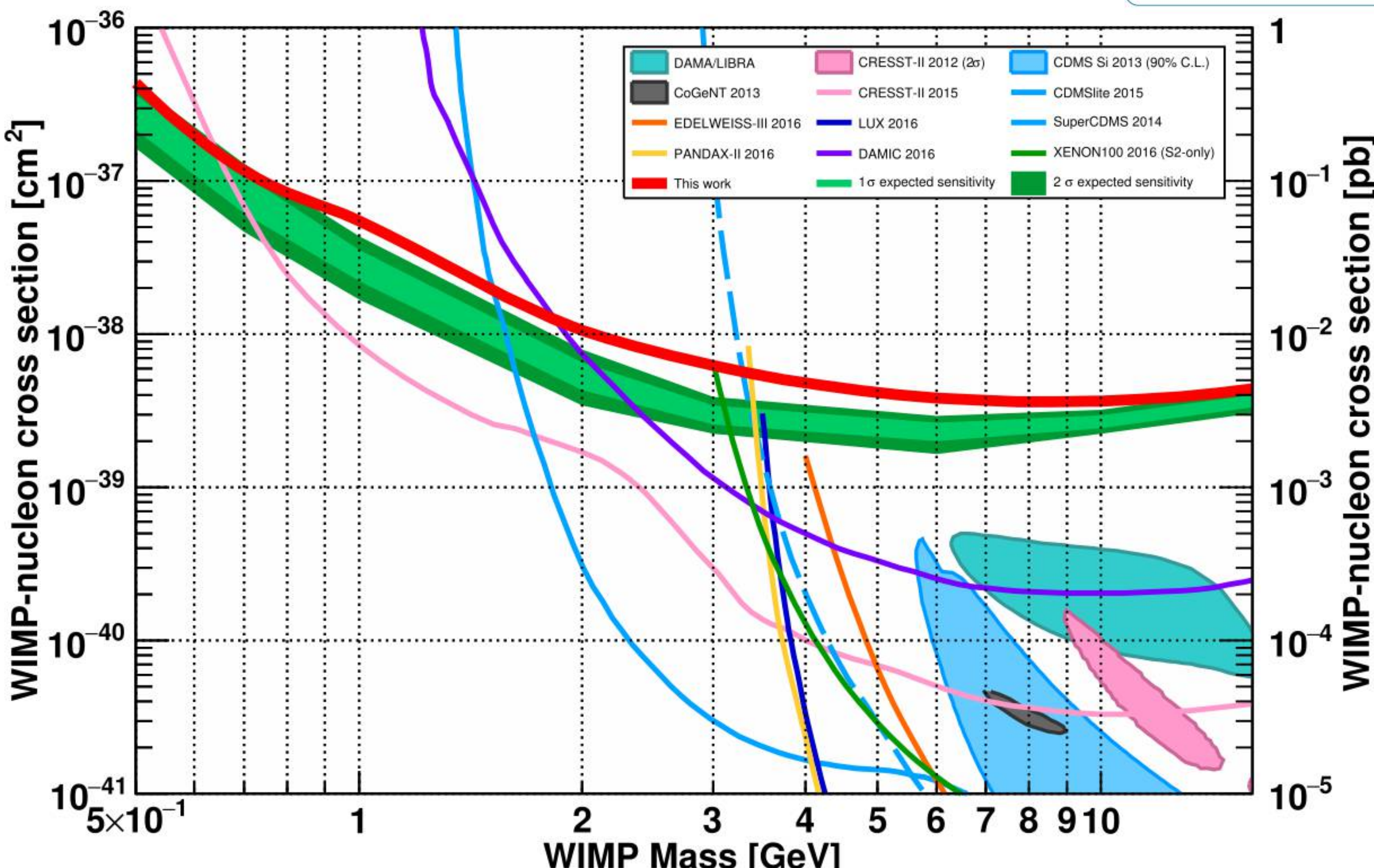

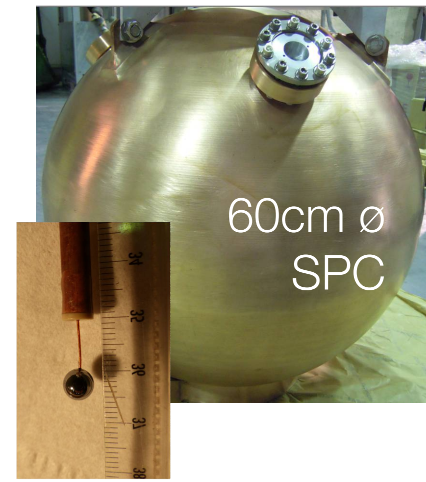

3.1 bars of Ne
+ 0.7% CH_4

42 days of data

Q. Arnaud et al. (NEWS-G), Astropart. Phys. 97, 54 (2018).

Pulse treatment

Deconvolve for amplifier response and ion-induced current

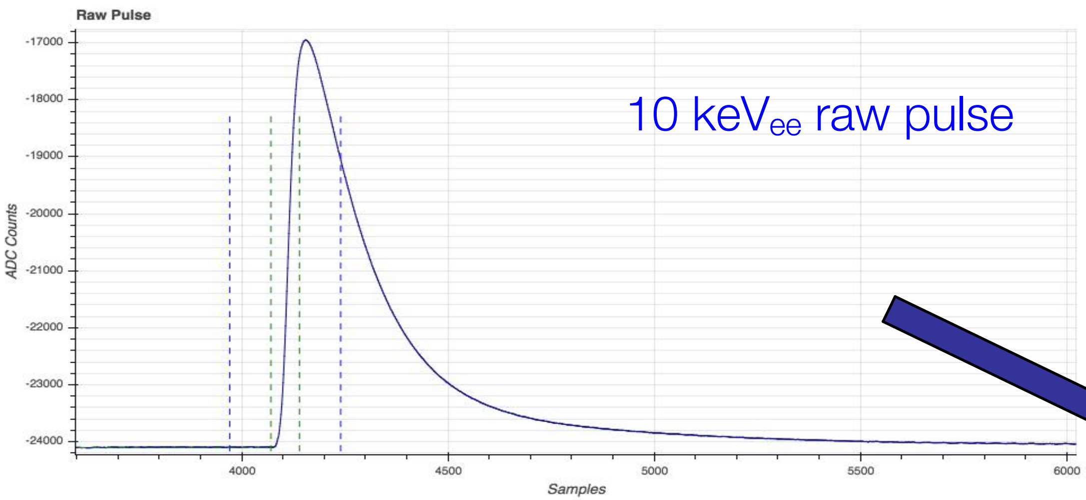

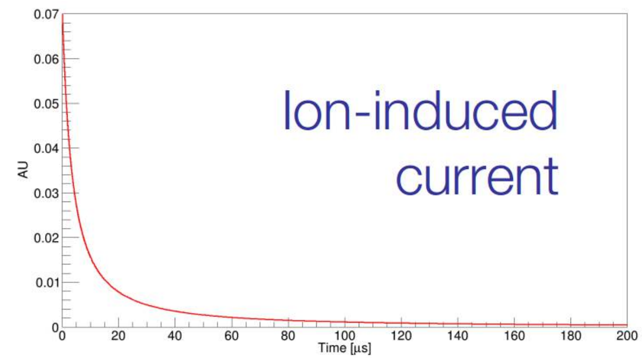

X

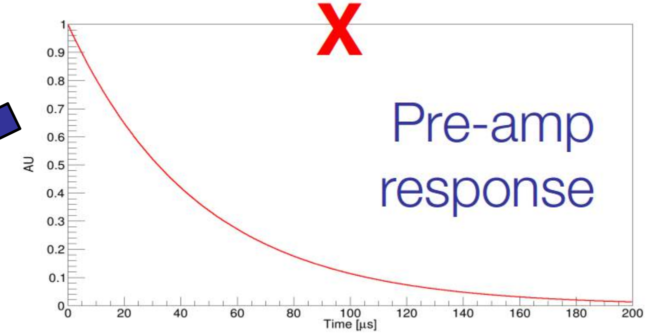

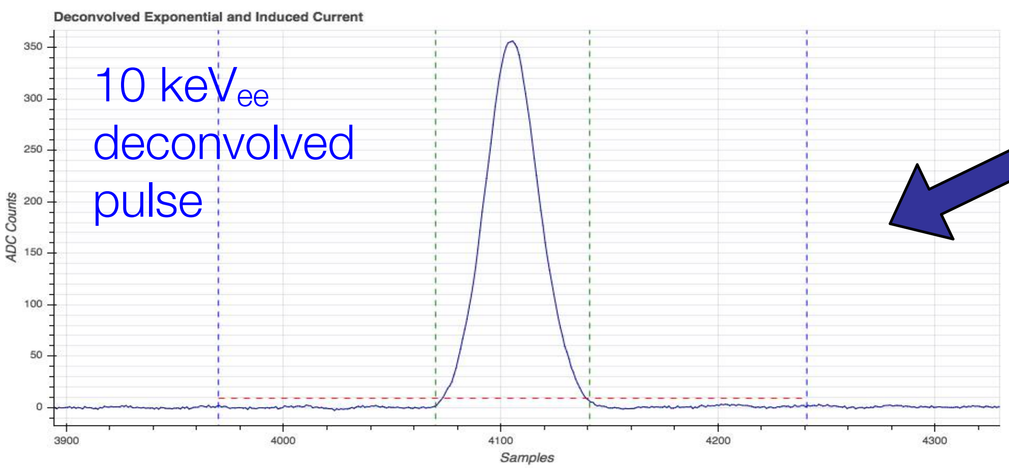

Quenching factor measurements

$$W_{\mathrm{nr}} = W_{\gamma}/Q(E)$$

Ongoing measurement campaigns at:

TUNL
TRIANGLE UNIVERSITIES NUCLEAR LABORATORY

Deuterium from a TANDEM accelerator used to produce neutrons: D(D,n)^{3}He

Neon measurement campaign:

Good data at 0.7 keV$_{nr}$

Working on 0.3 keV$_{nr}$!

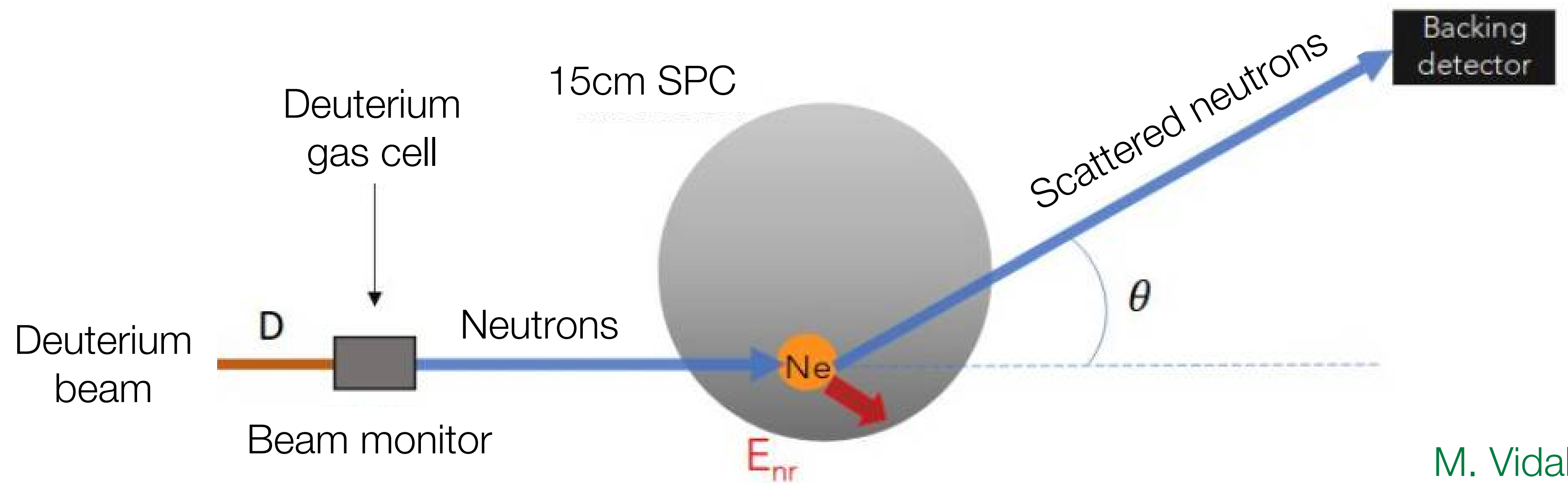

M. Vidal

Collaborators at the RMCC produce samples with a fission reactor:

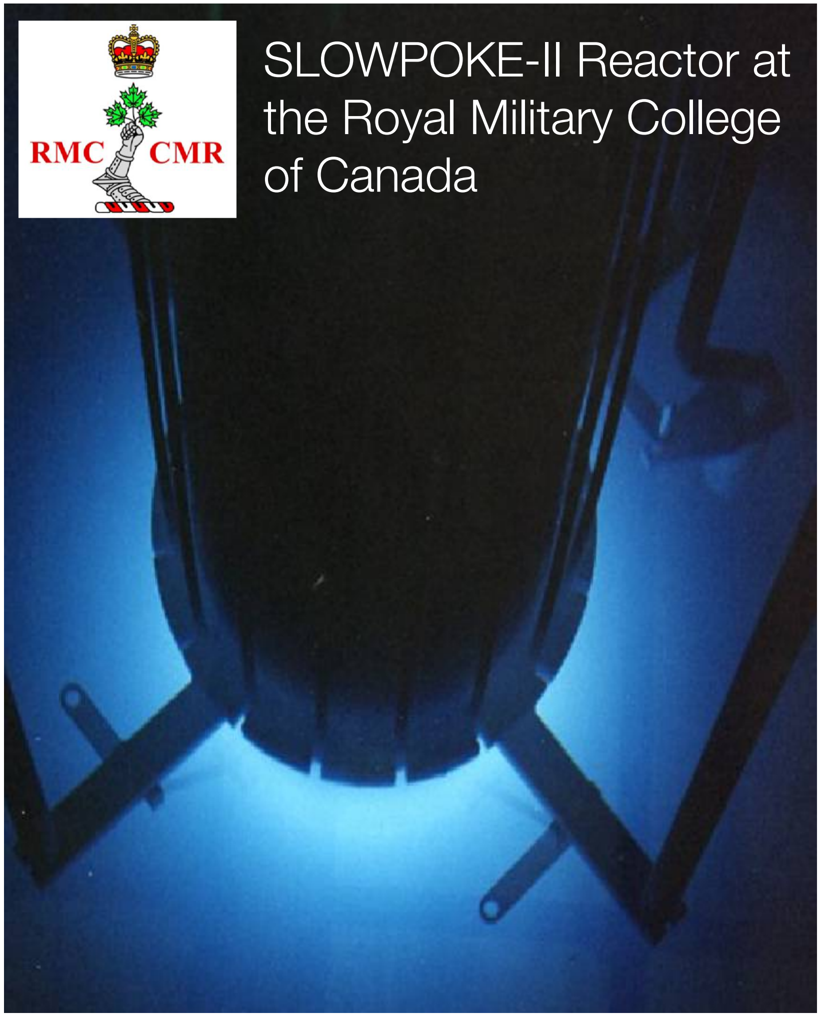

$^{40}Ca(n,\alpha)^{37}Ar$

Source produced in an oxygen-free environment

Counting of gaseous and solid by-products allows for indirect measurement of ^{37}Ar production

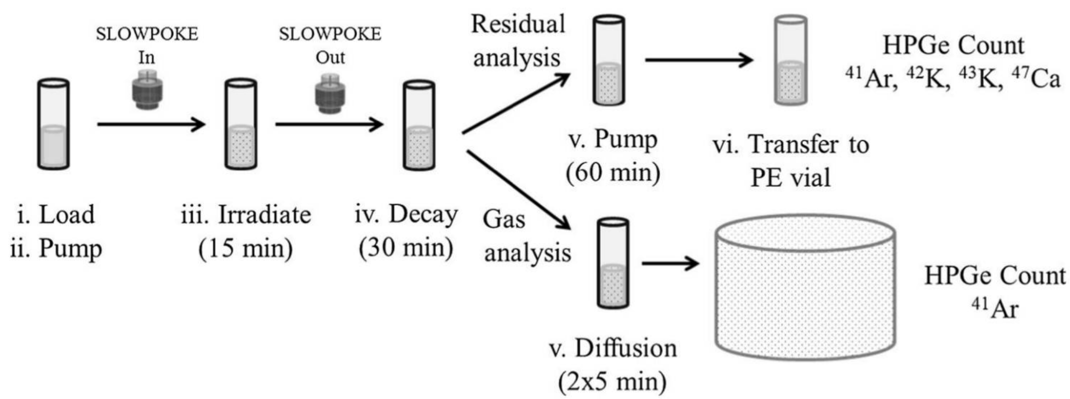

D.G. Kelly et al. Journal of Radioanalytical and Nuclear Chemistry 318(1), 279 (2018).